University of Alberta

Rheology of Sandy Polyacrylamide Gels: Application to Conformance

By

El sharif Bani

A thesis submitted to the Faculty of Graduate Studies and Research in partial fulfillment of the requirement for the degree of Master of Science

In

Petroleum Engineering

Department of Civil and Environmental Engineering

Edmonton, Alberta

Spring 2003

National Library of Canada
Acquisitions and Bibliographic Services
395 Wellington Street
Ottawa ON K1A 0N4
Canada

Bibliothèque nationale du Canada
Acquisitions et services bibliographiques
395, rue Wellington
Ottawa ON K1A 0N4
Canada

Your file Votre référence

Our file Notre référence

The author has granted a non-exclusive licence allowing the National Library of Canada to reproduce, loan, distribute or sell copies of this thesis in microform, paper or electronic formats.

L'auteur a accordé une licence non exclusive permettant à la Bibliothèque nationale du Canada de reproduire, prêter, distribuer ou vendre des copies de cette thèse sous la forme de microfiche/film, de reproduction sur papier ou sur format électronique.

The author retains ownership of the copyright in this thesis. Neither the thesis nor substantial extracts from it may be printed or otherwise reproduced without the author's permission.

L'auteur conserve la propriété du droit d'auteur qui protège cette thèse. Ni la thèse ni des extraits substantiels de celle-ci ne doivent être imprimés ou autrement reproduits sans son autorisation.

0-612-82246-X

Canada

University of Alberta

Library Release Form

Name of Author: ***El sharif Bani***

Title of Thesis: ***Rheology of Sandy Polyacrylamide Gels: Application to Conformance***

Degree: ***Master of Science***

Year this Degree Granted: ***2003***

Permission is hereby granted to the University of Alberta Library to reproduce single copies of this thesis and to lend or sell such copies for private, scholarly or scientific research purpose only.

The author reserves all other publication and other rights in association with the copyright in the thesis, and except as herein before provided, neither the thesis nor any substantial portion thereof may be printed or otherwise reproduced in any material form whatever without the author's prior written permission.

Signed Sharif

303 – 10610 – 108 Street
Edmonton, Alberta

Dated Jan. 27, 2003

University of Alberta

Faculty at Graduate Studies and Research

The undersigned certify that they have read, and recommended to the Faculty of Graduate Studies and Research, for acceptance, a thesis entitled "Rheology of Sandy Polyacrylamide Gels: Applications to Conformance", submitted by El-Sharif Bani in partial fulfillment of the requirements for the degree of Master of Science in Petroleum Engineering.

Dr. Marcel Polikar (Supervisor)

Dr. Bernard Tremblay (Co-supervisor)

Dr. Ergun Kuru

Dr. Ted Heidrick

Dated January 27/03

DEDICATION

This work is entirely dedicated to my brothers Omer AL Faroug, Dr. Ibrahim, Al Fatih, my beautiful wife Maria and the rest of my family.

My gratitude is immensely extended to my parents and friends. My dedication is also extended to all of my teachers and professors through out my education.

Abstract

Cold production is a primary non-thermal recovery method for heavy oil in unconsolidated formations. The oil is believed to be drained from the reservoir through highly permeable channels (wormholes), which often break into water zones leading to premature abandonment of many wells. An experimental set-up was designed to simulate the blocking of a wormhole in a formation using a 10 cm diameter, 1.2 meter long, screened pipe surrounded by a sand annulus.

The sandy polymer gel system developed for blocking a wormhole could resist a pressure gradient of at least 230 kPa/m. On a field perspective, the plug could block an aquifer pressure of 4 MPa over a length of 20 meters. The viscosity, settling and shear degradation of the sandy polyacrylamide slurries were measured at different sand concentrations in order to design gel treatments in the field.

ACKNOWLEDGEMENTS

The author expresses his sincere thanks and genuine gratitude to Professor Marcel Polikar and Dr. Bernard Tremblay for their great advices, guidance, understanding and encouragement throughout this project. The technical assistance, advice and support provided by Dr. Huang Haibo, Brian Wiwchar, Shauna Cameron and the scientific and technical staff of the heavy oil and oil sand division of the Alberta Research Council (ARC) are highly appreciated.

The technical assistance and discussions with Kaz Oldakowski are sincerely acknowledged.

The financial and technical support provided by the Alberta Research Council (ARC) are immensely acknowledged by the author.

TABLE OF CONTENTS

CHAPTER			PAGE
1	INTRODUCTION		1
	1.1	Introduction	1
	1.2	Statement of the problem	3
2	LITERATURE REVIEW		5
	2.1	Cold Production	5
		2.1.1 Characteristics of cold production	5
		2.1.2 Mechanisms of cold production	6
		2.1.3 Sand production	6
		2.1.4 Solution gas drive	8
		2.1.5 Viability of cold production	9
	2.2	Polymer Flooding	9
		2.2.1 Polyacrylamide gels	10
		2.2.2 Polymer degradation and stability	11
	2.3	Polymer rheology	13
		2.3.1 Rheology	13
		2.3.2 Rheological models	13
	2.4	Water shut-off	14
3	MATERIAL, APPARATUS AND PROCEDURE		25
	3.1	Experimental work	25
	3.2	Fluids	26
	3.3	Sands	27
		3.3.1 Grain size analysis	28
		3.3.2 Sand grain density measurement	29
		3.3.3 Maximum and minimum dry and wet density	29
	3.4	Water shut-off experiments	30
		3.4.1 First water shut-off experiment	30
		3.4.1.1 Packing	32

3.4.1.2 Annulus saturation 32
3.4.1.3 Sandy polymer slurry injection 32
3.4.1.4 Polymer squeeze 33
3.4.1.5 Polymer injection into annulus 33
3.4.1.6 Cell shut-in 33
3.4.2 Second water shut-off experiment 34
3.5 Rheological measurements 34
3.5.1 Sample preparation 35
3.5.2 Viscosity measurements 35
3.5.2.1 Measurement procedure 35
3.5.3 Settling tests 36
3.5.4 Gel strength screening test 37
3.5.5 Gel degradation tests 37
3.5.6 Capillary viscosity measurements 38
3.5.7 Yield stress measurements 38

4 RESULTS 44
4.1 Introduction 44
4.2 Mechanical and physical properties 44
4.2.1 Settling test 44
4.2.1.1 First settling test 45
4.2.1.2 Second settling tests 45
4.2.2 Gel strength screening test 45
4.2.3 Gel degradation test 45
4.3 Rheological properties 46
4.3.1 Injectivity of the slurry 46
4.3.2 Yield stress 47
4.3.3 Slippage effect 47
4.3.4 Rheology models 47
4.3.5 Relative viscosity 48
4.3.6 Rheology of 60% sandy polymer gel 49
4.4 Water Shut-off experiments 49
4.4.1 First water shut-off Experiment 49
4.4.1.1 First Part 49

4.4.1.2 Second Part....51
4.4.2 Second Water shut-off Experiment....53

5 DISCUSSION....81
5.1 Rheology, Settling and Degradation Tests....81
5.2 First Water Shut-off Experiment....83
5.3 Second Water Shut-off Experiment....85
5.4 Application of Results: Field Treatment....87

6 CONCLUSIONS AND RECOMMENDATIONS....96
6.1 Conclusions....96
6.2 Recommendations....97

REFERENCES....98
APPENDICES
Appendix A: Sand data....107
Appendix B: Calibration....109
Appendix C: Gel strength tests....110
Appendix D: Injectivity data....112
Appendix E: Degradation tests....116
Appendix F: Settling tests....118
Appendix G: Effect of geometry on slippage....138
Appendix H: Rheological models fitted....140
Appendix I: Viscosity of sandy polyacrylamide gel slurries....146
Appendix J: Relative viscosity of sandy polymer gel slurries....149
Appendix K: 60 wt% sandy polyacrylamide gel (rheological data)....152
Appendix L: First water shut-off experiment results and data....156
Appendix M: Second water shut-off experimental data....158

LIST OF TABLES

Table 2.1	Typical Canadian cold production reservoir characteristics.	18
Table 3.1	Sand equivalent diameters and coefficient of uniformity	39
Table 3.2	Wormhole (70/140) and annulus (F110) sand sieve analysis.	39
Table 3.3	Maximum and minimum density and porosity for sands	40
Table 3.4	Fluid, sand injection and leak-off	40
Table 3.5	Rheometer geometries description	40
Table 4.1	Final densities of settled sand (first settling test)	56
Table 4.2	Final densities of settled sand (second settling test)	56
Table 4.3	Weight/volume conversions for F 110 sand (wormhole sand)	56
Table 4.4	Viscosity measurements using the capillary viscometer (60 wt% sandy gel slurry).	57
Table 4.5	Yield stress for unsheared sand polymer slurries (shear rate = 2 sec^{-1}).	57
Table 4.6	Yield stress measurements for the crosslinked polymer (shear rate = 0.7 sec^{-1}) (time after blending).	57
Table 4.7	Yield stress measurements for the sandy polymer slurries (shear rate = 0.1 sec^{-1}).	58
Table 4.8	Power law fit for different sand concentrations.	58
Table 4.9	Slump test result (first water shut-off experiment (second phase)).	58
Table 4.10	Compaction of the sandy polymer gel plug along the wormhole (first water shut-off experiment second phase)).	59
Table 4.11	Compaction of the sandy polymer gel plug along the wormhole extended area (first water shut-off experiment (second phase)).	59
Table 4.12	Sandy gel plug displacement (first water shut-off experiment (second phase)).	59
Table 4.13	Slump test (second water shut-off experiment)	59

Table 4.14	Compaction of the sandy polymer gel plug along the wormhole (second water shut-off experiment).	60
Table 4.15	Compaction of the sandy polymer gel plug extracted from external pipe extensions at ends of screened tube (second water shut-off experiment).	60
Table 4.16	Sandy gel plug displacement (second water shut-off experiment)	60
Table 5.1	Parameters used in simulations	91
Table 5.2	Gel placement simulations	92
Table A.1	Sieve opening sizes	107
Table A.2	Permeability calculation for annulus (70/140) sand	107
Table A.3	Permeability calculation for wormhole (F 110) sand	108
Table A.4	Wormhole and annulus sand analysis (grain size distribution)	108
Table C.1	Gel strength rating and description	110
Table C.2	Gel strength rating equivalence scale	110
Table C.3	Gel strength screening test	111
Table D.1	Input data	112
Table D.2	Slurry densities	113
Table D.3	Final pressure drop versus flow rate	113
Table D.4	Power law index determination	114
Table D.5	Fann 35 viscosity measurements	114
Table D.6	Shear rate regime for the experiments	115
Table E .1	Degradation test	116
Table E .2	Residence time and displacement calculation	117
Table E .3	Degradation test shear rate calculation	117
Table F.1	First settling test	118
Table F.2	Second settling test	128
Table H.1	Carreau and Herschel-Bulkley (H-B) rheological models (sheared sandy polymer slurries).	141
Table H.2	Rheological models (sheared sandy polymer slurries)	141
Table H.3	Carreau and Herschel-Bulkley rheological models (unsheared sandy polymer).	142
Table H.4	Unsheared rheological models (sandy polymer slurries)	143
Table H.5	Rheological models fitted to the (crosslinked polymer, pure gel)	143

LIST OF FIGURES

Figure 1.1	Organization of the thesis	4
Figure 2.1	Map of heavy oil and bitumen deposits	19
Figure 2.2	Oil and sand production rates	19
Figure 2.3	Single well operation set-up in cold production.	20
Figure 2.4	Typical sand and gross fluid rates in a cold production cycle.	20
Figure 2.5	Longitudinal scan of wormhole development in sand pack	21
Figure 2.6	Normalized permeability increase versus porosity	22
Figure 2.7	Effect of drainage radius on fluid production rate	22
Figure 2.8	Effect of salt concentration on polymer gel viscosity.	23
Figure 2.9	Sensitivity of polyacrylamide gel to shear degradation.	23
Figure 2.10	Pressure gradient for extruding polymer gel through open fractures.	24
Figure 2.11	Yield stress for different fracture widths	24
Figure 3.1	Wormhole and annulus sand grain size distribution	41
Figure 3.2	Cell in the vertical position	41
Figure 3.3	Schematic diagram of apparatus.	42
Figure 3.4	Screened tube with pipe attachments at ends.	42
Figure 3.5	RT 20 ROTOVISCO shear rheometer	43
Figure 3.6	Fann 35 viscometer	43
Figure 4.1	Schematic of gel placement and settling	61
Figure 4.2	60 wt % sand polymer settling (first settling test)	62
Figure 4.3	Sand settling height percentage (second settling test)	62
Figure 4.4	Settling rate versus different sand concentrations (second settling test).	63
Figure 4.5	Porosity of settled sand layer for high sand concentrations (second settling test).	63
Figure 4.6	Porosity of settled sand layer for low sand concentrations (second settling test).	64
Figure 4.7	Gel strength screening test	64
Figure 4.8	Degradation test (60 wt% polyacrylamide slurry)	65
Figure 4.9	Effect of crosslinking on the gel viscosity no delay,	65

1.5 and 2.5 hours delay before testing.
Figure 4.10 Yield stress for sheared and unsheared sandy polymer gel..... 66
(shear rate = 2 sec^{-1})
Figure 4.11 Slip effect for the crosslinked pure polymer gel 66
(different geometries).
Figure 4.12 Slip effect on the 60 wt% sandy polymer gel (1.5 hour 67
delay, different geometries).
Figure 4.13 Viscosity versus shear rate for sandy polymer gels at high 67
sand concentrations (striated geometry, 1.5 hour delay)
(power law fit).
Figure 4.14 Viscosity versus shear rate for sandy polymer gels at low 68
sand concentrations (striated geometry, 1.5 hour delay)
(power law fit).
Figure 4.15 Shear stress versus shear rate for sandy polymer gels at high 68
sand concentrations (striated geometry, 1.5 hour delay)
(power law fit).
Figure 4.16 Shear stress versus shear rate for sandy polymer gels at low 69
sand concentrations (striated geometry, 1.5 hour delay)
(power law fit).
Figure 4.17 Viscosity for different sand concentrations (striated 69
geometry, no delay). Sandy polymer gel.
Figure 4.18 Relative viscosity versus sand concentration 70
(striated geometry, 1.5 hour delay, sheared sample).
Figure 4.19 Pressure inside wormhole during injection (first 70
water shut-off experiment (first part)).
Figure 4.20 Schematic diagram of the wormhole gel plug excavation 71
(first water shut-off experiment (second part)).
Figure 4.21 Water breakthrough test..... 72
Figure 4.22 Water breakthrough test (second part of the first 73
water shut-off experiment).
Figure 4.23 Wormhole gel plug excavation and sand concentration 74
(wt%) (first water shut-off experiment (second part)).
Figure 4.24 Slurry injection rate (water shut-off experiments)..... 75
Figure 4.25 Flow rate and pump pressure during slurry squeezing 75

(second water shut-off experiment).
Figure 4.26 Sand pack before excavation. 76
Figure 4.27 Cell in horizontal position during excavation 76
Figure 4.28 Layered screen removal for wormhole inspection..... 77
Figure 4.29 Water breakthrough test (second water shut-off experiment) 77
Figure 4.30 Wormhole gel plug excavation(second water 78
shut-off experiment).
Figure 4.31 Slumping of the sandy gel plug (second water shut-off..... 79
experiment).
Figure 4.32 Sandy polymer gel plug sectioned longitudinally 79
(second water shut-off experiment).
Figure 4.33 Wormhole gel plug excavation and sand concentration (wt%)..... 80
(second water shut-off experiment).
Figure 5.1 Thixotropy test (60 wt% sandy polymer gel) 93
Figure 5.2 Presence of air bubbles in high concentration 93
sandy polymer gels.
Figure 5.3 Presence of air bubbles in low concentration..... 94
sandy polymer gels.
Figure 5.4 Effect of leak-off on yield stress..... 94
Figure 5.5 Sandy gel plug yielding scenarios 1 to 3..... 95
Figure 5.6 Filter cake formation within channel wall 95
Figure B.1 Calibration of Moyno pump flow rate 109
Figure D.1 Pressure drop and flow rate using capillary viscometer..... 115
Figure F.1 Sandy polymer gel densities versus time for different 126
concentration (first settling test).
Figure F.2 60 wt% sandy polymer gel density and porosity versus time 126
(first settling test).
Figure F.3 Sandy polymer gel porosity versus time for different sand..... 127
concentrations (first settling test).
Figure F.4 Settling rate versus time for different sand concentrations.....127
(first settling test).
Figure F.5 Sandy polymer gel porosity versus time for different sand..... 136
concentrations (second settling test)
Figure F.6 60 wt% sandy polymer gel density and porosity versus time 136

(second settling test).
Figure F.7 Sandy polymer gel densities of settled sand layer for low sand concentrations (second settling test). 137
Figure F.8 Settling of sand in 60 wt% sand polymer gel in terms of height and volume percentage (second settling test). 137
Figure G.1 Slip effect (1.5 hour delay), pure gel (no sand) 138
Figure G.2 Slip effect (2.5 hour delay), pure gel (no sand) 138
Figure G.3 Slip effect for 60 wt% sandy polymer gel (no delay) 139
Figure H.1 Shear stress versus shear rate for different sand concentrations (data fitted with different models). 144
Figure H.2 Shear stress versus shear rate for 60 wt% sand polymer gel. slurry (data fitted to Carreau-Yasuda rheological model, no delay). 144
Figure H.3 Shear stress versus shear rate for 60 wt% sand polyacrylamide gel slurry (data fitted to Carreau-Yasuda rheological model, 1.5 hour delay). 145
Figure I.1 Viscosity versus sand concentrations (1.5 hour delay, striated geometry). 146
Figure I.2 Viscosity versus sand concentrations (2.5 hour delay, striated geometry). 146
Figure I.3 Viscosity versus shear rate(1.5 hour delay, striated geometry.). Sandy polymer slurries. 147
Figure I.4 Viscosity versus shear rate striated geometry (2.5 hour delay). Sandy polymer slurries. 147
Figure I.5 Viscosity versus shear rate for the 60 wt% sandy polymer gel (capillary tube viscometer). 148
Figure J.1 Relative viscosity versus sand concentration. (striated geometry, no delay, sheared samples). 149
Figure J.2 Relative viscosity versus sand concentration. (striated geometry, 1.5 hour delay, sheared samples). 149
Figure J.3 Relative viscosity versus sand concentration (striated geometry, 2.5 hour delay, presheared samples). 150
Figure J.4 Relative viscosity versus sand concentration (striated geometry, 1.5 hour delay, sheared samples). 150

Figure J.5 Relative viscosity versus sand concentration. 151
(striated geometry 2.5 hour delay, sheared samples).
Figure J.6 Relative viscosity versus sand concentration (striated 151
geometry 1.5 hour delay unsheared samples)
Figure K.1 60 wt% sandy polyacrylamide slurry viscosity (presheared,. 152
striated geometry).
Figure K.2 Preshear effect on 60 wt% sandy polyacrylamide slurry 152
viscosity (no delay, smooth geometry).
Figure K.3 Preshear effect on 60 wt% sandy polyacrylamide slurry.....153
(0.5 hour delay, smooth geometry).
Figure K.4 Preshear effect on 60 wt% sandy polyacrylamide 153
viscosity (2.5 hours delay, smooth geometry).
Figure K.5 Effect of delay time on 60 wt% sandy polyacrylamide slurry..... 154
(striated geometry).
Figure K.6 Effect of delay time on 60 wt% sandy polyacrylamide slurry..... 154
slurry (smooth geometry).
Figure K.7 Effect of delay time on 60 wt% sandy polyacrylamide 155
slurry relative viscosity (smooth geometry).
Figure K.8 Effect of delay time on 60 wt% sandy polyacrylamide 155
slurry relative viscosity (striated geometry).
Figure L.1 Injection and squeezing pressures (first water 156
shut-off experiment (first part)).
Figure L.2 Pressure versus time during crosslinked polymer squeezing 156
into annulus (first water shut-off experiment (first part)).
Figure L.3 Water breakthrough test (first water shut-off..... 157
experiment (first part)).
Figure M.1 Pressure inside wormhole during slurry injection 158
(second water shut-off experiment).
Figure M.2 Flow rate and injection pressure during slurry injection 158
(second water shut-off experiment).
Figure M.3 Pressure inside wormhole during polymer gel squeeze..... 159
into the annulus (second water shut-off experiment).
Figure M.4 Polymer gel flooding rate and injection pressure(second..... 159
water shut-off experiment).

Figure M.5 Flow rate during squeezing of gel for first and second water shut-off experiments. 160

Figure M.6 Polymer gel flooding rate. Comparison for first and second water shut-off experiments. 160

LIST OF NOMENCLATURE

A	Flow area (m^2)
a	Carreau-Yasuda model coefficient
dp	Pressure drop (kPa)
$\frac{dp}{dl}$	Pressure gradient (kPa/m)
D	Rheometer cup diameter
k	Power law constant (Pa)
k^1	Power law model coefficient (Pa)
K_o	Effective permeability to oil (Darcy or m^2)
K_p	Permeability of the sand – fluid mixture (Darcy or m^2)
K_w	Effective permeability to water (Darcy or m^2)
L	Length of capillary tube (m)
M	Mobility ratio (dimensionless)
M_s	Mass of the sand (g)
n	Power law index (dimensionless)
p_R	Reservoir pressure (MPa)
Q	Volumetric flow rate (m^3/hr)
R	Rheometer cup radius
T	Temperature of the rheometer (^{0}C)
U_m	Average velocity across section (m/s)
v_f	Fluid velocity (m/s)
w_f	Fracture width (cm)

LIST OF SYMBOLS

Δp	Pressure drop (Pa)
λ	Carreau-Yasuda model time constant (dimensionless)
λ_w	Water phase mobility (m^2/Pa/s)
λ_o	Oil phase mobility (m^2/Pa/s)
μ	Fluid viscosity (Pa.s)
μ_o	Oil viscosity (Pa.s)
μ_w	Water viscosity (Pa.s)
γ	Shear rate (sec^{-1})
γ_b	Characteristic shear rate for Cross model (sec^{-1})
γ_{corr}	Corrected shear rate (sec^{-1})
γ_{app}	Apparent shear rate (sec^{-1})
τ	Shear stress (Pa)
τ_o	Yield stress (Pa)
η	Fluid viscosity (Pa.s)
η_o	Zero shear rate viscosity (Pa.s)
η_∞	Infinite shear rate viscosity (Pa.s)
ρ_s	Sand density (g/cm^3)
ϕ	Porosity of the medium

CHAPTER 1

1.1 Introduction

Cold production of heavy oil in unconsolidated formations is a non-thermal process in which sand and oil are produced simultaneously. This process has been applied successfully in several oil fields in Alberta and Saskatchewan, Canada [1]. Sand production, under certain reservoir conditions, leads to the formation of highly permeable channels referred to as "wormholes", which grow out into the formation starting at the wellbore, and lead to a greater access of the reservoir. Sand production and the subsequent formation of wormholes are believed to be responsible, in part, for the higher flow rates observed in cold production. The high viscosity of the heavy oil also leads to more efficient solution-gas drive since the gas dispersion within the oil is more stable. Therefore, gas breakthrough, leading to a reduction in drive, occurs at a higher critical gas saturation than for conventional oil. In Canada, heavy oil and tar sand deposits exceed 300×10^9 m^3 total oil in place [2]. Depletion of the conventional oil reserves makes the exploitation of these huge deposits of heavy oil through cold production of increasing importance.

The cold production process is faced with two major technical problems among others. Firstly, high water cuts result in many oil wells being prematurely abandoned. Due to the mobility difference, wormholes often break into water zones leading to water cuts as high as 99% within a short period of time. In Alberta, 4.6×10^8 m^3 of water were produced in 1996 [3]. Secondly, disposal of large quantities of co-produced sand increases operational costs. In the Lloydminister area (Canada), the cost of sand disposal is approximately \$100/m^3.

Most of the work done on water shut-off and reservoir conformance control treatments using polymer gel was conducted in porous media with varying degrees of success [4-6]. Given the larger diameter of wormholes compared to

the dimensions of pore bodies in a porous medium, polymer gels, without reinforcing agents form a weak gel plug. Zhou et al. [7] more recently developed a clay gel method for blocking highly permeable channels and fractures. In spite of the encouraging laboratory results, field trials were not as successful as expected. The clay gel was likely not strong enough to withstand the aquifer pressure. In addition, the clay gel method is limited by the formation salinity.

An efficient gel system for blocking wormholes and highly conductive channels should have the following characteristics:

1. gel material should be placed at the proper location in the reservoir.
2. gelation should take place under the formation conditions.
3. gel should be strong enough to withstand the formation water pressure.
4. system should be economical with minimum environmental impact.

From rheological tests and sand settling measurements, a 60 wt% sand polyacrylamide gel slurry was selected for injection into the screened pipe. The slurry inside the open channel was squeezed, resulting in a significant leak-off of the polymer gel from the open channel into the surrounding annulus. The leak-off of the polymer gel increased the sand concentration inside the open channel to more than 85 wt%. After shutting in the experimental cell for 3 to 5 days to allow gelation, the polymer gel plug was tested in a water breakthrough test to determine its yield stress. The water breakthrough occurred at a pressure gradient varying between 230 and 340 kPa/m. The corresponding average yield stress of the sandy gel plug varied between 6 and 9 kPa. In comparison, the yield stress of the clay gel used by Zhou [9] was only 1 kPa

The addition of sand to the polyacrylamide gel resulted in significant gel strength increase. It was also found that the higher the polymer concentration, the stronger the gel plug. A thick filter cake was observed along the gel plug, which effectively strengthened the plug.

The rheological and settling tests performed showed that these materials are strongly shear thinning and that the sand within the slurry would not settle significantly during the gelation period within the wormhole at 60 wt% sand concentration. The measured yield stress of the polymer gel plug would suggest that water production through wormholes in cold production could effectively be blocked under field conditions. In field terms, the sandy gel plug could resist a pressure of approximately 4 MPa over a distance of 20 meters. These results indicated that the sandy polymer gel system is a viable candidate for conformance control treatments. Figure 1.1 shows the linkage between the different components of the thesis. The data obtained in the top three boxes in this figure comprises the bulk of the thesis. These data are being used in gel placement evaluations for water shut-off treatments in the field.

1.2 Statement of the problem

In 1997, more than three billion barrels of water were produced leading to a water to oil ratio of 6:1 in western Canada [8]. Different methods of controlling excessive water production in the oil industry have been employed in different reservoir formations with varying degrees of success. Chemical and clay gels were employed selectively in the oil industry. The application of these treatments was mainly to mature reservoirs with abandoned wells or in enhanced (secondary) oil recovery where an oil depleted flow path exists between injectors and producers. These methods involve injection of a gel system that would effectively plug the water sources or decrease the permeability in water producing zones.

Most methods involved injection of polymer gels. Despite their apparent success in porous media and waterfloods, these gels were not able to withstand the water encroachment pressure in certain cold production reservoirs [9]. Clay gel, which seemingly provides a gel plug of sufficient strength for fractures [7], cannot block larger channel such as wormholes. In addition, the salinity of the formation must

be below 3% for the clay slurry to gel. An urgent need still exists in cold production operations for an effective, viable and economical technology to prevent and control excessive water co-production.

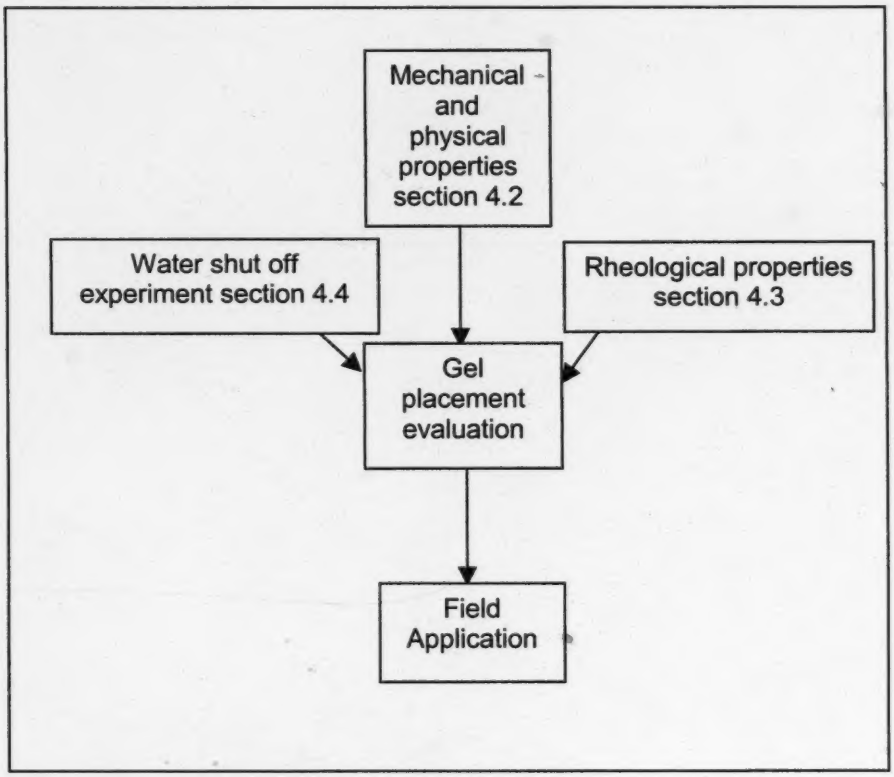
Mechanical and physical properties section 4.2
Water shut off experiment section 4.4
Rheological properties section 4.3
Gel placement evaluation
Field Application

Figure 1.1 Organization of the thesis.

CHAPTER 2
LITERATURE REVIEW

2.1 Cold Production

Cold production has been applied successfully in several unconsolidated heavy oil fields in Alberta and Saskatchewan, Canada (Cold Lake, Lindbergh and Lloydminister Figure 2.1) [1] The production rate for cold production wells (Figure 2.2) is much higher (10 to 50 times) than that predicted using a reservoir simulator assuming no sand production [1]. Similar increases in oil production rate with sand production are predicted from Darcy's radial flow equation, conventional well testing and material balance equations [2,12-23]. Advances in progressive cavity pump design and operation have allowed sand to be transported more easily up vertical wells. A typical cold production well is shown in Figure 2.3. Typical Canadian cold production reservoir characteristics are given in Table 2.1 (live oil is defined as an oil that contains some gas in solution).

2.1.1 Characteristics of Cold Production

The viability of the cold production process is essentially associated with solution gas drive as well as with the initiation and maintenance of sand production [24-26]. The initial volumetric sand cut, which was found to vary from 10% to 50% [26-30], was observed to stabilize within approximately six months to one year to lower values from 0.1% to 2% [30-32] (Figure 2.4). The initiation of the production of such large volumes of sand requires the adoption and implementation of aggressive perforation strategies. A novel workover technique to re-initiate and encourage sanding at later stages in the producing well's life can possibly help [24,30]. With the introduction of large capacity progressive cavity pumps, cold production wells may produce as much as 30 m^3/d of oil at peak production [2,24,25,31]. Oil production rates in a typical cold production well slowly increase to the peak rate then gradually decline [24]. Implementation of cold production techniques revealed that there is no apparent large free gas

zones developed even after years of production [24]. Cold production techniques may render 5 – 15% of the original oil in place (OOIP) recoverable [2,32]. Some cold production wells water-out within months [10,24].

2.1.2 Mechanisms of Cold Production

Field and laboratory observations suggest that the main drive mechanisms leading to the unexpectedly high primary oil recovery achieved from heavy oil reservoirs can be grouped mainly into two groups; mechanisms associated with sand production (sand erosion and geomechanical effects) [1,18,19,33,34] and mechanisms associated with solution gas drive (foamy oil) [1,15,35,36].

2.1.3 Sand Production

There are three scenarios generally believed to be responsible for sand production:

1. wormholes formed by erosion with some yielding around the wormholes.
2. yielding around well with wormholes growing outwards from the yielding zone.
3. yielding only around the well growing radially outwards with time.

Sand production is greater in formations with uncemented sands, high oil viscosity and high pressure drawdown rates [37-39].

Tremblay et al [1] believe, based on laboratory experiments (Figure 2.5) [27], numerical calculations of wormhole growth, tracer tests in the field [10] and cement loss during drilling [37], in the first scenario postulating that the creation of wormholes is the main reason for sand production and subsequent reservoir access. Wang and Dusseault [13,16,21,24,25] believe, based on analytical and numerical calculations, in the second scenario (sand yielding with wormholes growing radially outwards). In this scenario the combined effects of the drag force on the sand grains, due to the flow, the yielding of the sand, due to the overburden stress, and at later stages, the scouring (transport) of sand within the wormholes, are responsible for sand production. Dusseault et al. [24], on the

other hand, adopt the third scenario based on analytical calculations. They believe that the formation around a vertical well yields due the shear failure. The failed sand would then be transported radially toward a vertical well by the drag force on the sand grains [19]. The production of the sand within the dilated zone with the oil into the wellbore, would tend to reduce resistance to fluid flow since the relative velocity between the oil and the sand would decrease. In this scenario, the theoretical analysis suggests this process can perhaps double the liquid rate at the well [24].

In the second and third scenarios, the continuous production of sand as a consequence of the formation failure and drag force on the sand grains causes the formation porosity to increase around the wellbore. This increase in porosity increases the fluid effective permeability with respect to the reservoir matrix material as shown in Figure 2.6 [13,27,31,34,36]. It is important to note, however, that the Kozeny-Carmen equation (Figure 2.6), derived for a porous medium, should not be used for "porosities" above approximately 55% for most sand produced by cold production. Above this "porosity" the sand and oil mixture is no longer a porous medium. According to Dusseault et al. [19,32,40], the continuous process of formation failure and removal of sand from the near wellbore region enhances the drainage radius (Figure 2.7), and would provide continuous pore deblocking near the wellbore due to fines and gas bubble blockage and asphaltene precipitation. However, asphaltene precipitation has not been observed in laboratory experiments during primary production [45]. Sand production can also lead, in rare cases, to cap rock subsidence, which induces higher formation stresses around the dilated sand region. These higher stresses would induce higher pore pressure, which is believed could support the pressure drive mechanism sustaining longer production periods. This is referred to as compaction drive [36]. Compaction drive has not been observed in Alberta during cold production, which could be attributed to the over-consolidated (compaction) nature of western Canadian reservoir formations as opposed to some

Venezuelan formations. In cold production, open channel forms within sand filled wormholes by erosion.

2.1.4 Solution-Gas Drive (Foamy Oil)

Smith [34] was one of the first to note the importance of the foamy oil mechanism in analyzing cold production. He suggested that the evolved gas below the bubble point formed microbubbles smaller than the pore throat size, which were carried with the flowing oil phase. The presence of these microbubbles would increase the compressibility of the system and maintain a higher reservoir pressure leading to greater recovery. Huerta et al. [41], Ehlig-Economides et al. [17], postulated that the presence of entrained gas in the oil phase results in significant increases of the oil phase compressibility near the well bore. This increase in the compressibility would result in an increased productivity [17]. Metwally et al. [36] claimed that the presence of microbubbles results in a destabilization of the sand, causing it to flow. This destabilization reduces locally the in situ stresses within the sand, which leads to the growth of the disturbed zone into channels (wormholes) of high permeability. The presence of microbubbles as a discontinuous phase would result in a very effective solution gas drive. The high viscosity of heavy oil is believed to enable the sand to be suspended and carried to the surface more easily during the cold production process [30]. The viscosity of foamy oil was postulated by some researchers to be reduced due to asphaltene precipitation [35,43,44]. This postulated reduction in viscosity would enhance the oil mobility. Maini et al. [45] disproved this theory by showing experimentally that the presence of freshly nucleated gas bubbles in fact decreases the oil mobility. Poon et al. [46] believe that Non-Newtonian flow behavior of the gas dispersion enhances the production rate. Pooladi-Darvish and Firoozabadi [47] attributed the high recovery in heavy oil to the low gas mobility during the solution gas drive process. Maini. et al. [48] suggested that the in–situ formation of foamy leads to a natural pressure maintenance mechanism. Bora et al. [49] found that the presence of asphaltenes appeared to hinder the coalescence of gas bubbles as well as to increase the degree of

supersaturation needed to initiate gas bubble nucleation. The authors suggested that other mechanisms such as wormhole growth, sand production and viscous coupling effects might also contribute to higher recovery in heavy oil.

2.1.5 Viability of Cold Production

In cold production, typical vertical or inclined wells can maintain a rate of 5 – 15 m^3/d, often for many years. In addition, the payback period is relatively short. Despite these advantages, there are two major concerns:

- disposal of produced sand containing residual hydrocarbons, which can pose an environmental hazard. [13,16,18].
- early water break-through, which renders many cold production heavy oil wells uneconomical. [9,10,24].

2.2 Polymer Flooding

Polyacrylamide solution being a non-Newtonian fluid, a proper knowledge of its rheological behavior is important in the design of a successful water shut-off treatment in the field. In the following section, a brief introduction to some basic polymer rheology, as well as previous work done on both polymer rheological measurements and water shut-off treatments, are presented.

Polymers were first recommended for application in the oil industry in the early 1960s to remedy the inefficiency of waterflooding by lowering the mobility ratio between the injected water and the oil in the reservoir [50]. Polymer solutions, with the addition of appropriate chemicals, will gel when injected into the reservoir. When these gels are injected into a porous medium, a semi-permanent decrease in permeability of the watered-out region of the reservoir results. Therefore, more oil can be swept from the reservoir. [50,51]. The mobility ratio (M) is defined as the ratio of the mobility of the displacing fluid to the mobility of the displaced fluid as shown in the following equation:

$$M = \frac{\lambda_w}{\lambda_o} \qquad (2.1)$$

The water and oil mobilities, λ_w and λ_o, respectively are given by:

$$\lambda_w = \frac{K_w}{\mu_w} \qquad (2.2)$$

and

$$\lambda_o = \frac{K_o}{\mu_o} \qquad (2\text{-}3)$$

A favorable mobility ratio for water flooding occurs when the ratio is less than or equal to one. A high mobility ratio results in water fingering through the oil phase [52]. In order to achieve a favorable mobility ratio, it is necessary to increase greatly the viscous – to – capillary force balance between the water and the oil phases in the displacement process [50-52]. Some of the polymers used for conformance control are synthetic, such as high molecular weight partially hydrolyzed polyacrylamides (average molecular weight in the range of 2 to 20× 10^6) and biopolymers. These high molecular weight biopolymers are obtained from the fermentation of natural substances rich in glucides [50,51].

2.2.1 Polyacrylamide Gels

Polyacrylamide, in its partially hydrolyzed form (HPAM), is a synthetic straight-chain polymer of acrylamide monomers, some of which have been hydrolyzed. The degree of hydrolysis, defined as the solubility of the polymer in water, may be important in certain physical properties such as polymer adsorption on sand, shear stability and thermal stability [51]. HPAM is a polyelectrolyte which will react quite strongly with ions in solution. From the laboratory and fieldwork conducted on polyacrylamide, it has been observed that polyacrylamides have the following limitations for conformance control: 1) polyacrylamide molecules tend to ball up in saline water at excessive salt concentration, and 2) the polymer degrades through the breaking of the molecules by mechanical actions [50,51].

The viscosity of polymers in solution results from molecular interaction. A long polymer chain has many modes of motion, which may interact along its entire length with solvent molecules leading to energy dissipation. The deformation of high molecular weight polymer dissipates more energy than for low molecular weight polymers in solutions. Figure 2.8 shows the relative viscosity plotted against various salt concentrations of 15%, 25% and 34% hydrolyzed HPAM and unhydrolyzed PAM (same molecular weight for the polyacrylamide) in sodium chloride brine for a polymer concentration of 600 mg/litre at a temperature of 25^0C and shear rate of 7.3 sec^{-1}.

Previous work by Wiwchar et al. [53] on the effects of water salinity on the mechanical properties of sandy polymer gels showed that within the range investigated, salt concentration did not appear to have any significant effect on the strength of the sandy polyacrylamide gel. The sandy polyacrylamide slurries were tolerant to a wide range of salt concentration as verified by Wiwchar et al. In the water shut-off experiments described in Chapter 4, the polyacrylamide solutions were prepared in 5 wt% NaCL and 0.25 wt% $CaCL_2$ solutions. The salinity of the polyacrylamide was the same as in the formation. Therefore, problems with salinity are not anticipated in the field

2.2.2 Polymer degradation and stability

Polymer degradation refers to any process that will break down the molecular structure of the macromolecules or disrupt the crosslinking between the molecules. Polymer degradation can be divided into three main categories:

1. chemical degradation, which refers to the break down of the molecules, either through short term attack by contaminants, additives and any component present in the injected fluid (oxygen, iron, etc), or long term attack through hydrolysis.
2. mechanical or shear degradation which refers to the break down of the molecules or of the crosslinks in a high shear region as a result of high mechanical stresses.

3. biological degradation, which refers to the microbial break down of macromolecules by bacteria during storage or in the reservoir [50,51].

In field operations, polymer formulations are subjected to significant shearing as they flow from the mixing pumps through the lines into the wellbore and finally into the desired location in the reservoir. In addition, these polymer solutions are in contact with contaminants, such as iron in the flow equipment, which can affect crosslinking of the gel. At reservoir conditions other than cold production, these formulations may be exposed to high formation temperature and/or to bacterial attack, which could also affect their efficiency. Mechanical degradation due to shear stress also occurs when the polymer gel flows through the porous medium.

Polymer shear degradation and stability are evaluated in terms of polymer viscosity retention. Mechanical degradation of the polymer solution is tested by pushing the material through a porous material at field injection rates. The mechanical degradation effect is evaluated by measuring the decrease in viscosity as quantified by the screen factor. This factor is defined as the ratio of the flow time for the injection of a specified volume of polymer solution through a screen to the flow time for the injection of the same volume of the solvent, used in preparing the polymer solution, through the same screen at a constant injection pressure.

Polyacrylamides can be sensitive to shear stress induced degradation, as illustrated in Figure 2.9. In this case, the viscosity decreased with increased preshearing through a consolidated sandstone core. The earlier work of Hill et al. [54] and Martin [55] showed the vulnerability of polyacrylamide to shear degradation and elongation, which was attributed to the flexible chain molecular structure. The elongational stresses experienced by the viscoelastic polymer solution flowing through the constricted pore throat also would lead to mechanical degradation. Shear degradation has also been observed in the experiments described in this thesis. Polymer degradation is more severe at high flow rates (Figure 2.9), longer flow times and for higher salinity brines. The

degradation process involves the breaking down of the higher molecular weight species into lower molecular weight fragments [56]. Martin [57], in his quest for improving the stress stability of HPAM, adopted an approach to stiffen the backbone of the HPAM but was unsuccessful. Akistinat [58] observed that the stress stability of HPAM was affected by the degree of hydrolysis. HPAM, with values of hydrolysis above 20%, were shown to be more stable to stress.

2.3 Polymer Rheology

2.3.1 Rheology

Rheology is the study of the relationship between the applied stresses and the deformation of a body. Bodies in this context can be solids, liquids, or gases. The most general form of the relationship between the applied stress and the resulting deformation for an inelastic fluid under shear, is the rheological equation of state:

$$\tau = -\eta(\gamma)\gamma \tag{2.4}$$

If the viscosity of a fluid is independent of the applied shear rate, then it is called a Newtonian fluid. Most polymer solutions are non-Newtonian fluids (viscosity does not remain constant at different rates of deformation), and can also exhibit visco-elastic behavior associated with the viscous (dissipative) and elastic (storage) responses.

2.3.2 Rheological Models

Numerous empirical equations (models) are available to characterize the Newtonian and non – Newtonian fluid behavior of slurries The Carreau-Yasuda, Herschel – Bulkley and power law models [59] were found to fit adequately the rheological measurements obtained in this study. The viscosity for some of these models was calculated from the following equations:

Carreau Yasuda model

$$\eta = \eta_\infty + (\eta_o - \eta_\infty)/(1 + (\lambda\gamma)^a)^{(1-n)/a} \quad (2.5)$$

Power Law Model

$$\eta = k\gamma^{n-1} \quad (2.6)$$

Herschel-Bulkley Model

$$\eta = \tau_o/\gamma + k(\gamma)^{(n-1)} \quad (2.7)$$

2.4 Water shut-off

Most of the work done on water shut-off treatments using polymer gel was conducted in porous media with varying degrees of success [4-6]. This review will concentrate on treatments for fractured reservoirs since they are closer to wormholes in terms of conductivity than a porous medium.

O'Brien et al. [60] designed polymer gel treatments in horizontal wells of the Idd Elsharigi North Dome Shuaiba reservoir in Qatar. A high molecular weight, partially hydrolyzed polyacrylamide, crosslinked with chromium (III) acetate was injected to plug the conductive faults in contact with the injector. The treatment was successful but the pumping of a very large volume (3,790 bbls) was required. The authors concluded that deep penetration of polymer gel did not necessarily improve oil recovery relative to shallower treatments.

Zhou et al. [7] developed a water shut-off method for high permeability channels such as fractures and wormholes using swelling clays. In this process, the swelling clays are mixed with an aqueous KCL solution, which inhibits swelling and the slurry is then injected into the open channels. The swelling clays will gel once in contact with formation water through cation exchange between the (Potassium, K^+ cations) in the solution and the (Sodium, Na^+ cations) in the formation. Zhou et al. conducted a series of laboratory experiments, using a sand

pack with an open channel at the centre, to test this process. With the addition of small amounts of dispersant into a KCL solution, up to 40 wt% bentonite slurry was made to flow. A range of yield stresses for different clay gel concentrations was measured. The yield stress ranged between 0.6 to 1.2 kPa for the sand-free clay gel as measured in a 2.54 cm diameter channel Calculations based on tracer tests [10] and calculations of the erosion rate within wormholes [11] suggest that the open channels in the field can reach 10 cm in diameter. Clay gel within an open channel of 10 cm could resist a pressure gradient between 24 and 48 kPa/m [53]. From a field perspective, a 150 meter length of a blocked channel would be required to resist a typical aquifer pressure of 3.6 to 7.2 MPa. The field-testing of the method showed that this method was able to reduce the water cut to 60% for the first three weeks [9,11]. However, the water increased back to 85% afterwards. The failure of the treatment could be attributed to the low yield stress of the clay gel and to fingering of the fresh water during the post-flush treatment.

Seright [61] conducted a series of experiments to investigate how Cr(III)-acetate crosslinked HPAM gels propagate and dehydrate during extrusion through fractures. In these experiments, the pressure gradient required to extrude gel through fractures was relatively insensitive to the applied injection rate. The rate of gel front propagation in the fractures significantly increased with increased injection rate. He recommended that in field applications, the highest practical injection rate should be used. For the sandy polyacrylamide gel however, high flow rates can lead to preferential caking at the inlet of open channels because of the high pressure at that location, which means the sandy gel cannot penetrate as far into the wormhole.

Seright [62] observed that gel dehydration effects became less pronounced as the fracture width increased. He also noticed that a minimum pressure gradient was required to extrude gels through fractures. Once this minimum pressure gradient was exceeded, gel extrusion was insensitive to the flow rate. This

pressure gradient can be estimated using the relationship: $dp/dl = 0.02(w_f)^{-2}$ (Figure 2.10), where w_f is the fracture width in inches and the pressure gradient (dp/dl) is in psi/in. This behavior was attributed to a strong slip effect shown by the gel [63]. The yield stress calculated for the data obtained from Seright [62] for different fracture widths along with the yield stress measured in the water shut-off experiments for the sandy polymer gel are displayed in Figure 2.11 The yield stress of the sandy polymer gel used to block a 10 cm diameter channel was approximately 10 to 1000 fold higher than that of the pure polyacrylamide gel used in blocking the fractures. In their experiments, the polyacrylamide concentration was 0.5 wt% with crosslinker concentration of 0.0417 wt%. The molecular weight of the polymer was approximately 5×10^6. The polyacrylamide concentration for the sandy polymer gel (1.2 wt%) was higher leading to a stronger gel.

Seright [64] conducted experimental investigations to probe the mechanism responsible for the propagation of Cr(III)-acetate crosslinked HPAM gel through fractured sandstone core. The author found that a continuous increase in pressure gradient was not observed during gel extrusion, indicating progressive plugging due to dehydration did not occur. He observed that the composition of the gel propagating through the fracture was similar to that of the injected gel. The gel that dehydrated in the fracture ceased to propagate and formed a filter cake of dehydrated gel on the fracture faces. Dehydration is not an issue in the placement of the sandy polymer gel into a watered-out wormhole since the flow rate (leak-off) of the gel is much lower. The gel treatment also lasts for a shorter period of time (less than 1 hour) than for the treatment referred to by Seright [64] therefore less dehydration occurs. The size of the wormhole (diameter) is also larger than the fractures, therefore, less dispersion of the polyacrylamide molecules to the walls of the channel can occur for a wormhole.

Liu et al. [65] measured the rheology of Cr(III)-acetate crosslinked HPAM gel. They observed that during gel extrusion through a fracture, a minimum pressure

gradient must be applied for the gel to flow. Liu et al. employed the yield stress, τ_y, which was measured independently, to calculate the minimum pressure gradient:

$$dp/dl = 2\tau_y / w_o \qquad (2.8)$$

where w_o = fracture width

Liu et al. [65] found that the shear stress on the wall of the fracture was fairly insensitive to the applied shear rate. This observation is consistent with other observations [63,66].

Broseta et al. [67] studied the influence of shearing sequences, representative of field conditions, for a high molecular weight polyacrylamide to be used for plugging fractures and for a low molecular weight polyacrylamide to be used for plugging porous media. They measured the viscosity, storage modulus, yield stress and gelation time of the gelling solution. Broseta et al. found that the effect of pre-shearing of the solution is to limit the gelation or viscosity rise of the gel due to the formation of aggregates of crosslinked polymers. They found that the gelation time increased with shear rate for high molecular weight formulations but was unaffected by shear for low molecular weight. They demonstrated that the gels recovered to approximately the same yield stress after being sheared and subjected to a sufficiently long period of rest. The same was observed for the sandy polymer gel. The sandy polymer gel regained almost all its full strength after being sheared for a period of time and being allowed to rest for 4 to 5 days. The measured yield stresses were in the same range as those observed for samples left under quiescent conditions right from the start.

Lai et al. [68] developed a method of blocking, fractures, channels, cavities around wells, with neutrally buoyant solid plastic pellets suspended in crosslinked polymer, which gels within the cavities or voids. The method emphasized the use of solid particles of density essentially equal to the carrier fluid density. The solid particles concentration was limited to 50 wt% of the mixture compared to 60 wt%

sand of the mixture in the sandy polymer gel system. Assuming that 7,500 kg of solid filler is required for a field treatment, Lai et al's method would cost about C$ 12,375 just for the pellets (polyethylene) at a cost of C$ 1.65 per kg. This type of pellet is one of the least expensive available. In contrast, the sandy polymer gel system would cost about C$ 1,050 for the solid filler (sand) at a price of C$ 0.14 per kg for the sand. These cost estimates do not include transportation costs. The use of sand produced during cold production would reduce sand disposal costs. The sand would not need to be transported to the field location. In addition, less polymer gel would be required for the treatment leading to a lower operational cost.

Most of the work with polymer gels for water shut off treatment was done on porous media. However, some was done on fractures but non was conducted on an open large channels.

Table 2.1 Typical Canadian cold production reservoir characteristics [1]

Reservoir characteristic	
Reservoir Sand	Unconsolidated
Porosity, %	29 – 35
Thickness, m	3 – 10
Oil gravity, °API	< 20
GOR, m^3/m^3	5 – 15
Average Produced Sand D_{50}, mm	0.1 – 0.3
Viscosity, cP (live)	1,000 – 20,000
Bubble Point Pressure, MPa	2 – 5
Reservoir Temperature, $°C$	15 - 20
Depth, m	400 – 800
Reservoir Pressure, MPa	3 – 6
Reservoir Permeability, D	0.5 – 10
Oil Saturation, %	65 – 85

Figure 2.1 Map of heavy oil and bitumen deposits.
Courtesy Alberta Department of Energy.

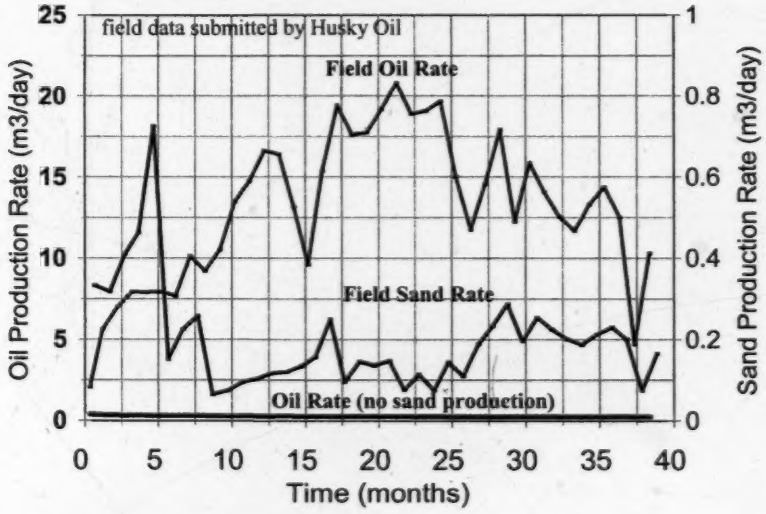

Figure 2.2 Oil and sand production rates.
Courtesy Tremblay et al. [1].

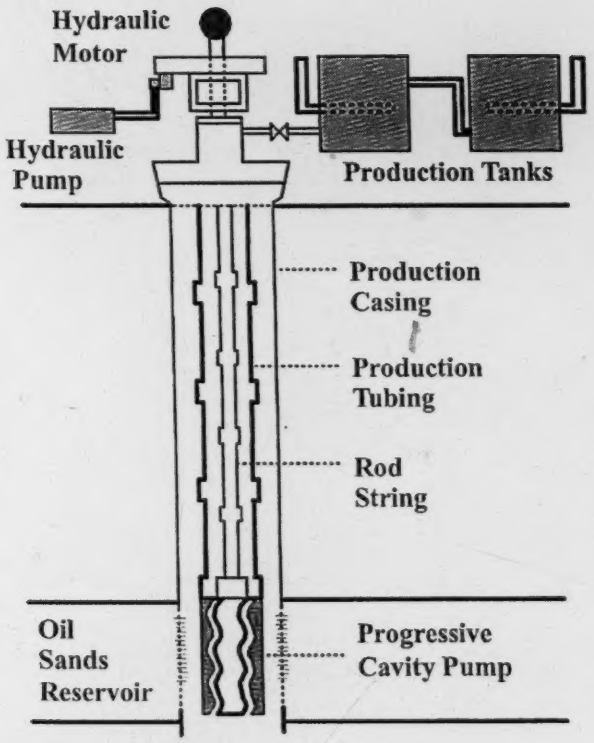

Figure 2.3 Single well operation set-up in cold production.
Courtesy Yeung [30].

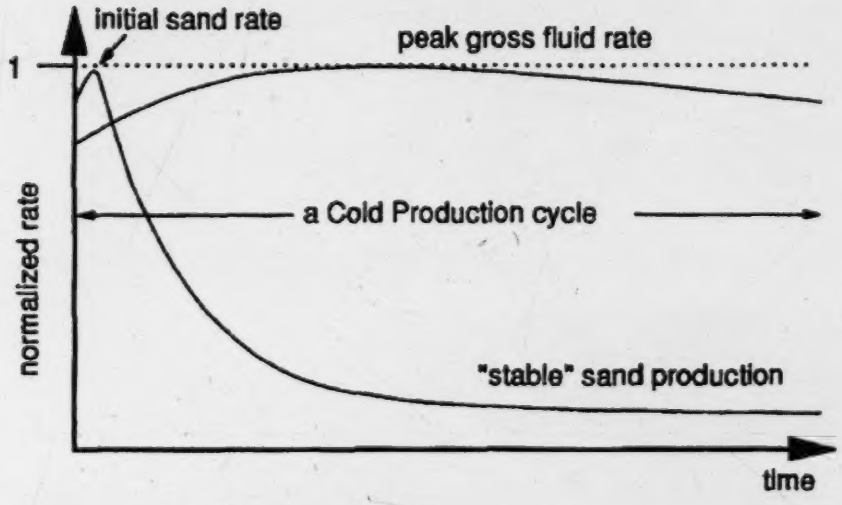

Figure 2.4 Typical sand and gross fluid rates in a cold production cycle.
Courtesy Dusseault et al. [32]

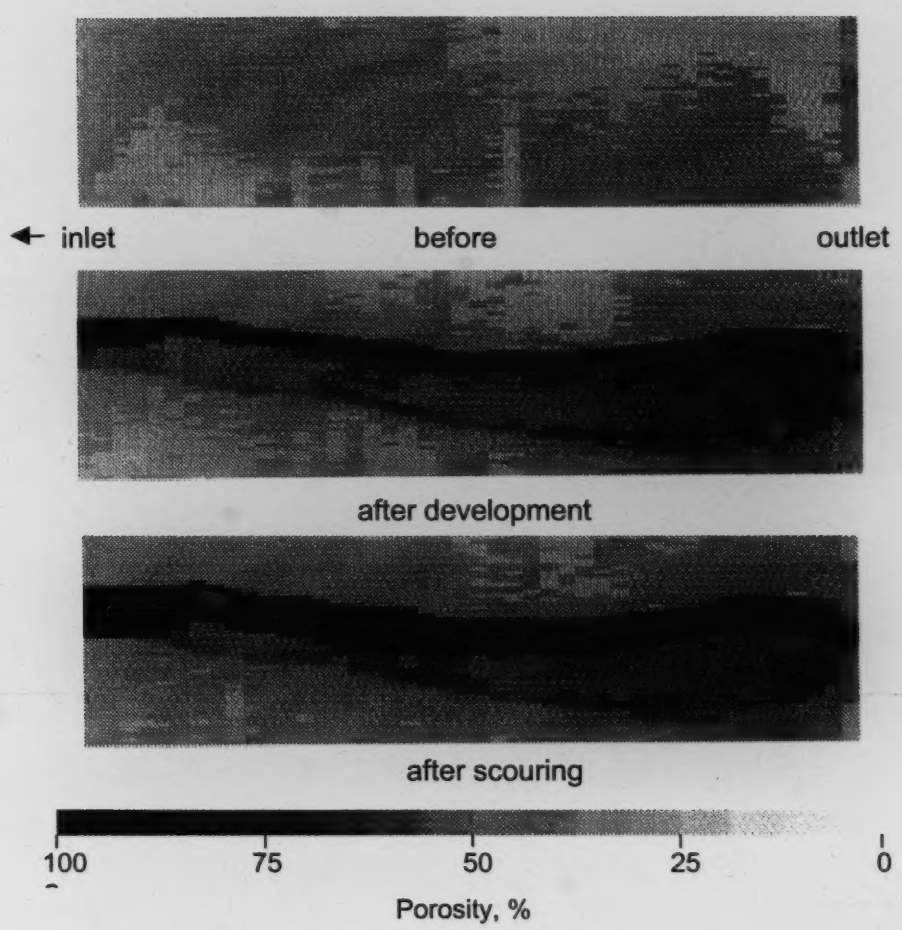

Figure 2.5 Longitudinal scan of wormhole development in sand pack
Courtesy Tremblay et al. [27].

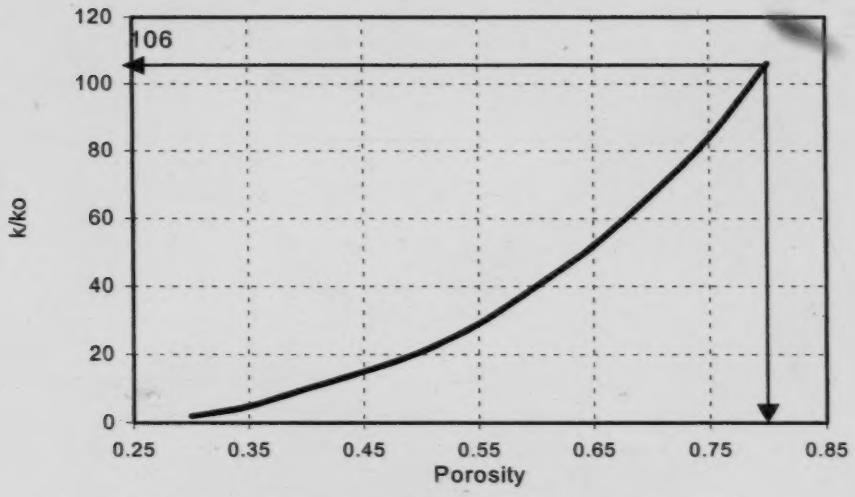

Figure 2.6 Normalized permeability increase versus porosity.
Courtesy Metwally et al. [36].

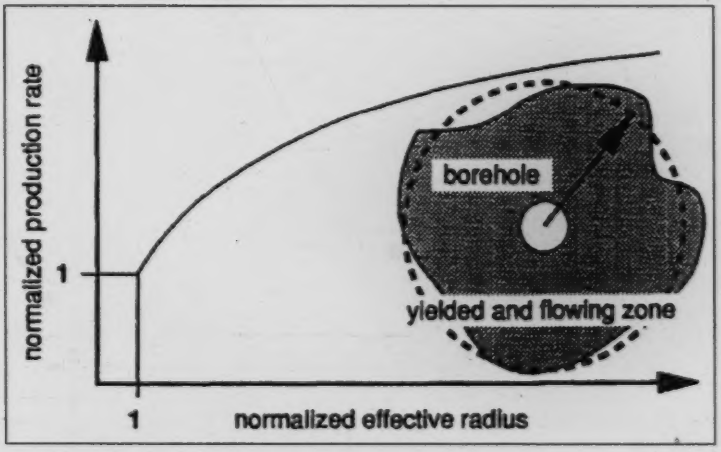

Figure 2.7 Effect of increasing drainage radius on fluid production rate.
Courtesy Dusseault et al. [32].

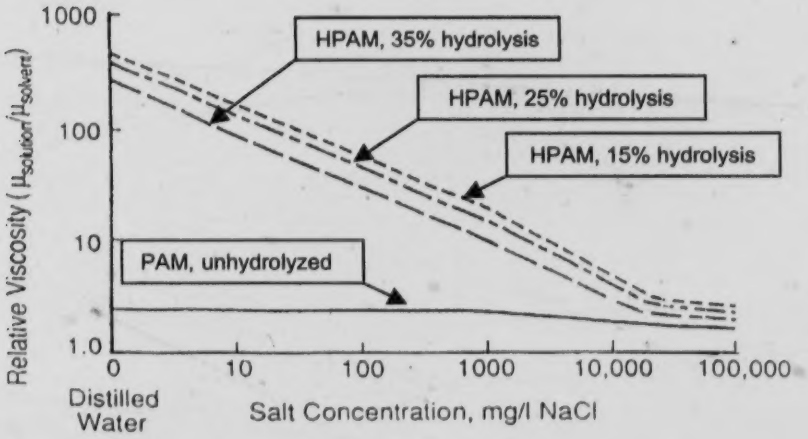

Figure 2.8 Effect of salt concentration on polyacrylamide gel viscosity. Courtesy Sorbie [51].

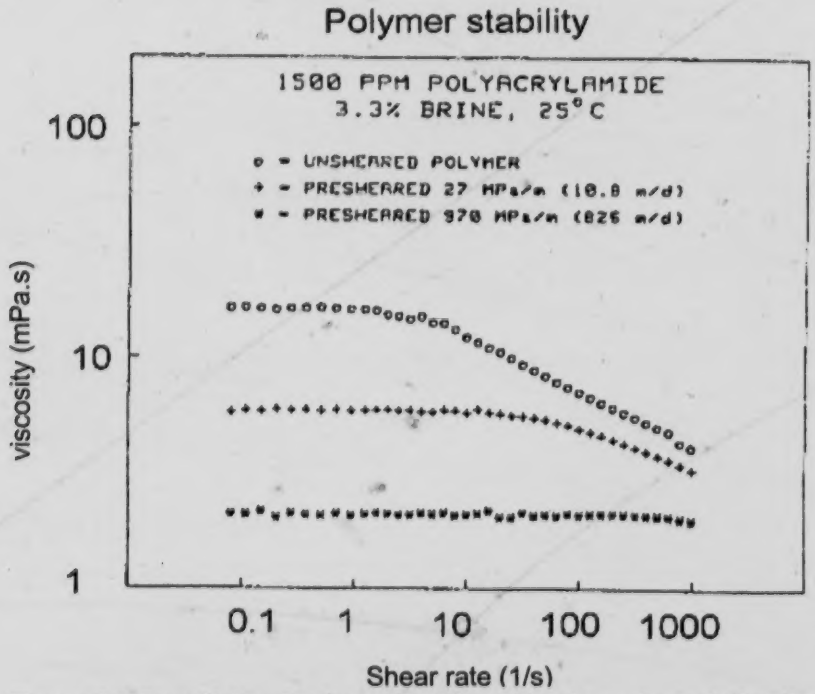

Figure 2.9 Sensitivity of polyacrylamide gel to shear degradation through a sand stone core. Courtesy Sorbie [51].

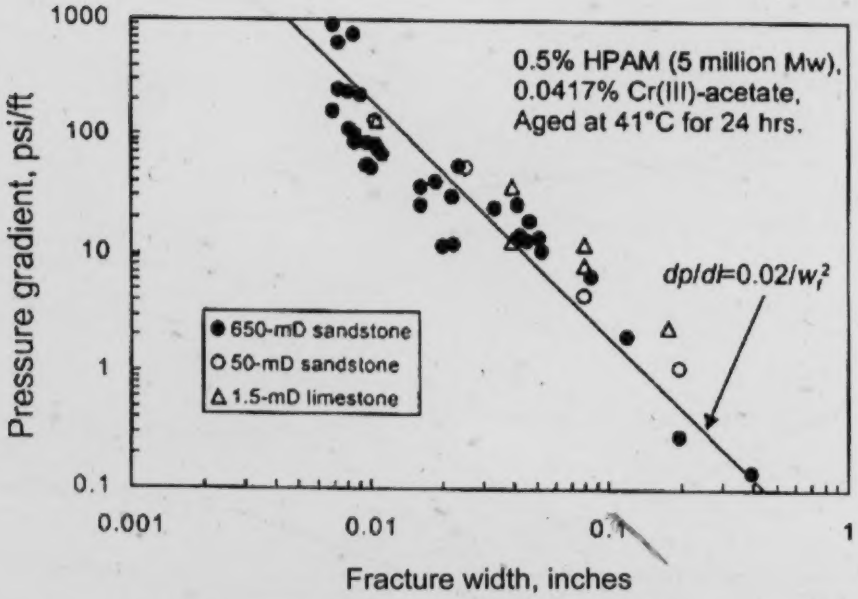

Figure 2.10 Pressure gradient for extruding polymer gel through open fractures. Courtesy Seright [64].

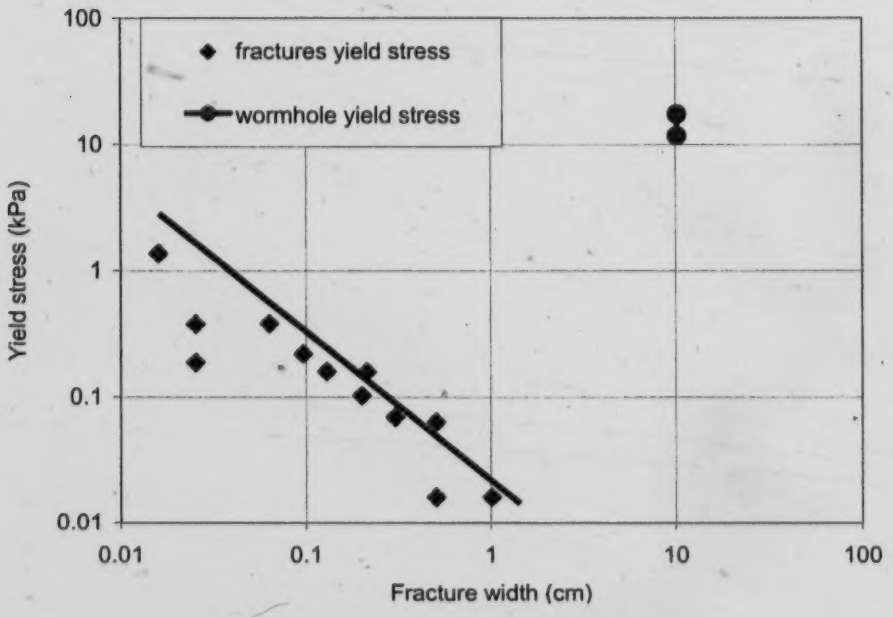

Figure 2.11 Yield stress for different fracture widths
Data obtained from Seright [62]

CHAPTER 3

MATERIAL, APPARATUS AND PROCEDURE

A new sandy polymer gel system for blocking wormholes and highly conductive fractures was developed. An experimental set up was designed to simulate the blocking of an open channel within a wormhole. The apparatus consisted of a screened pipe, 10 cm in diameter by 1.2 meter in length, surrounded by an annular sand pack. The diameter of the screened pipe was estimated, based on previous inter-well tracer tests [10] and erosion calculations within wormholes [11], to be similar to the diameter of an open channel within a wormhole in the field. Two water shut off experiments were conducted. In the first water shut off experiment, only the strength the sandy gel system was investigated while the placement and strength of the sandy gel system were investigated in the second water shut off experiment.

The data and knowledge obtained in this thesis are being applied to design water shut-off treatments for cold production wells. The main concerns in designing a water shut-off treatment are:

1. the strength of the sandy polymer gel
2. the injectivity of the slurry
3. the placement of the gel
4. the cost of the treatment

These concerns were taken into account in selecting a sand concentration of 60 wt% and a polyacrylamide concentration of 12,000 ppm.

3.1 Experimental Work

The experimental work is divided into two parts:

In the first part of this work, rheological measurements and tests were conducted to determine the viscosity and yield stress of crosslinked polyacrylamide sand slurries of different sand concentrations. These measurements were used in

calculating the injectivity of the sandy polymer gels in wormhole blocking treatments. Settling tests were also performed to determine how much settling would occur within a wormhole in the field since the sand-free gel above the settled sand layer, is weaker. This weaker gel layer was taken into account in calculating the blocking capability of a sandy polymer gel in the field.

In the second part of this work, water shut-off experiments were conducted with the prime objective of forming a plug of sandy polymer gel of sufficiently high strength to withstand the highest pressure gradient representative of field conditions. Tests to investigate the effect of iron contamination and shearing on the gel strength while pumping were also performed. Maximum and minimum density tests were performed to calculate the density and porosity ranges for the sand packs that were prepared in the experiment. Slumping tests in which the relative shrinkage in the longitudinal direction of the gel plug after being placed vertically in a bucket were performed to determine qualitatively the strength of the crosslinked polymer sand slurry.

The materials used along with their properties, the equipment used for running water shut-off experiments and the rheological measurements are described in the following sections.

3.2 Fluids

The Hi Vis 350 polymer used in this work, is a high molecular weight, anionic copolymer of acrylamide. Polymer concentrations of 8,000 ppm and 10,000 ppm were used in preparing the polymer gel in the first experiment. A concentration of 12,000 ppm was used for the second experiment as well as for the rheological measurements. A polyacrylamide solution was first prepared by dissolving the polyacrylamide into a solution of 5 wt% NaCl and 0.25 wt% $CaCl_2$. Chromium acetate ($CrAc_3$) was used as the crosslinking agent. Polymer to crosslinker ratios

of 10:1 and 40:1 were used for the first and the second experiments, respectively.

The Hi Vis 350 polymer solution was prepared in batches of one liter by adding the granular polymer at concentrations of 8,000 ppm, 10,000 ppm or 12,000 ppm to a brine solution. The mixing was performed in two stages at high blender speed for a duration of 6 minutes. A rest period of 2 minutes was allowed between the two stages in order for the granular polymer to hydrate. The polymer solution was further mixed with a magnetic stirrer for 36 hours at room temperature to ensure complete dissolution of the polymer.

In the first experiment, the crosslinker was added to the polymer solution and stirred for one hour until completely mixed, as indicated by a uniform bluish coloration. An electric sigma blade mixer was used to blend the crosslinked polymer solution and sand at the desired weight ratio. The mixing was performed in batches of three liters each. Each batch was mixed for 20 minutes.

In the second experiment, due to the high concentration of the polymer, as well as the high polymer to crosslinker ratio, the strategy for mixing of the crosslinked polymer and the sand was changed to allow for a more uniform mixture. The crosslinker agent was added in two stages. In the first stage, one quarter of the crosslinker was added to the polymer solution prior to the addition of the sand. Sand was then added, and the mixture was blended for 15 minutes in the sigma blade mixer. In the second stage, the reminder of the crosslinker agent was then added, and the entire mixture was blended for an additional 15 minutes.

3.3 Sands

The 70/140 sand used for packing the annulus was obtained from the Badger Mining Co. An F 110 sand, obtained from U. S. Silica Company, was used in preparing the crosslinked polymer sand slurry to be injected into the wormhole.

The permeability of the 70/140 sand and F 110 sand was 10 Darcy and 5 Darcy respectively as measured in separate experiments (Appendix A). The porosity of the 70/140 sand packs varied between 34% and 37% while the porosity of the F 110 sand packs ranged from 36% to 41%. The porosity was calculated from the maximum density tests (Appendix A).

3.3.1 Grain Size Analysis

The particle size distribution and average grain size of the two previous sands was measured. The ASTM method (D 422 – 63) [70], was followed in performing the grain size analysis for each of the samples tested. In this method, particles are separated into different groups by sieving 100 g of a given sample through a set of standard sieves and weighing the sand material retained at each sieve size. The weight percentage of each fraction was calculated. The sieve sizes used in measuring the particle size distribution of the sands were 45, 60, 80, 100, 120, 140, 170, 200, 230, 325 and 400 U.S mesh.

The coefficient of uniformity C_u, is defined as:

$$C_u = D_{60}/D_{10} \qquad (3.1)$$

where D_{60} and D_{10} are the sieve sizes, which allow 60% and 10% by weight respectively, of the sand to pass through. This coefficient gives an indication of the sorting of the sand. The average grain size of each sample was taken as the D_{50}. These coefficients are given in Table 3.1. Wormhole and annulus sands sieve analysis data are shown in Table 3.2.

Sands having a wide range of grain sizes are said to be poorly sorted. Sands with a narrow range of grain sizes are considered to be well sorted. From the grain size analysis, the F 110 was classified as a very fine, well-sorted sand having a rounded shape with a D_{50} of 0.1 mm (Figure 3.1). The specific gravity of the F 110 sand was about 2.65 g/cm^3 as determined by the "Standard Test Method for Rubber Chemicals-Density". Designation: D 1817-96 [71]. The

average absolute permeability of a separate sand pack prepared using this sand at a porosity of 33.8% was calculated using Darcy's law to be 5.4 Darcies (Appendix A).

The 70/140 sand was a fine, very well sorted sand with a D_{50} of 0.175 mm (Figure 3.1). This sand is relatively coarse in comparison to the F 110 sand. The average absolute permeability of a separate sand pack prepared using a 70/140 sand at a porosity of 36 % was calculated using Darcy's law to be 10.5 Darcies. The specific gravity was approximately 2.65 g/cm^3 as determined by the "Standard Test Method for Rubber Chemicals-Density". Designation: D 1817-96 [71].

3.3.2 Sand Grain Density Measurement

The density of the sand grains was measured using the ASTM (1817-96) method [71]. Both water and methanol were used as solvents. Use of methanol results in less trapped air and less potential residual oil. Standard tables were used to obtain the density of the methanol. Three measurements were taken for each sample. The average values of these measurements were taken as the density for each tested sample.

3.3.3 Maximum and Minimum Dry and Wet Density

The purpose of these tests was to compare the porosities of the sands within the annulus and within the wormhole, after the injection of the slurry, to the maximum and minimum porosities which can be achieved by packing the given sands. The ASTM methods (D 4253-93) [72] and (D 4254-91) [73] were followed in determining the range of porosities and densities for both samples.

There are two kinds of tests to determine the maximum and minimum density of the sand: dry and wet. In the dry test, a dry sample of the sand is tested; whereas in the wet test, a fully water saturated sample of sand is tested. Four

measurements of the F 110 sand were taken and averaged for all dry and wet maximum and minimum densities. Five measurements of both of the maximum and minimum densities of the dry 70/140 sand were averaged. Dry and wet samples of the F 110 sand were used to measure the densities while only a dry sample was tested for the 70/140 sand. The maximum and minimum porosities of the sand were calculated from the minimum and maximum densities and the volume of the cell. Results are displayed in Table 3.3.

3.4 Water Shut-off Experiments

Two water shut-off experiments were performed. The first water shut-off experiment was divided into two parts. The equipment and procedure for the water shut-off experiments will be described in the following sections.

3.4.1 First Water Shut-off Experiment

The primary objective of this experiment was to determine the sandy polymer gel strength in the "wormhole", evaluate the injectivity of the sandy polymer gel and evaluate the extent of sand compaction along the length of the wormhole as polymer "leaked-off" into the annulus sand formation. In the first part of the first experiment, polyacrylamide concentrations of 8,000 ppm and 12,000 ppm were used for preparing the crosslinked polymer gel injected into the annulus. A concentration of 10,000 ppm polyacrylamide was used for preparing the crosslinked polymer sand slurry injected into the wormhole. A polymer to crosslinker ratio of 10:1 was used for gels in the first part. A sand concentration of 60 wt% was utilized in preparing the sandy polymer slurry. Brine water was prepared using 5 wt% NaCl and 0.25 wt% $CaCl_2$ in deionized water to represent formation water.

The apparatus used for conducting this experiment is shown in Figures 3.2.and 3.3. The physical model consisted of a flanged connected pipe 1.2 m long with an inner diameter of approximately 20 cm and a concentric screened pipe 1.2 m

long by 10 cm in diameter. The screened pipe had three concentric layers of mesh screen (400, 250 and 32 mesh) sized to give rigidity and to prevent sand movement. This pipe simulated an open channel (wormhole) (Figure 3.4). The pipe extended 46 cm outward from both ends of the annular sand pack. The annulus sand around the screened pipe simulated the surrounding formation.

Four pressure transducers, equally spaced along the pack, were installed through the annulus sand pack down to the axis of the screened pipe to monitor the pressure behavior within the wormhole. A pair of couplings was attached at either end of the extended pipe section of the wormhole to inject the fluid and slurry, and to produce the effluent. The cell was placed on a steel stand and pivoted to the ceiling by a rope to change its orientation. A three-way ball valve and a straight ball valve were attached to the cell inlet and outlet, respectively (Figure 3.3). The three-way valve at the cell inlet was connected through two hydraulic hoses to a progressive cavity pump (PCP type CDF 6P3) to allow slurry flow into the wormhole. The hoses were approximately 4 cm in diameter (ID) and had a pressure rating of 1.7 MPa. The second bypass hose was used to divert the slurry flow into a vessel if the pressure build up inside the wormhole would not allow any further injection.

A pressure transducer attached to the end of the pump was connected to a data acquisition system. The pump was controlled by the same data acquisition system and would shut-off whenever the injection pressure exceeded 1.5 MPa. A ball valve was located at the end of the Moyno pump to control the slurry and crosslinked polymer solution flow through the pump. The outlet end of the screened tube was connected through a 0.4 cm inner diameter tube to a vessel placed on an electronic balance. Twelve drains were distributed throughout the circumference and length of the cell to allow polymer solution leak-off from the wormhole (screened tube) into the annulus, and outward to the effluent-collecting vessel (Figure 3.3).

3.4.1.1 Packing

The cell was positioned vertically upward. A high frequency vibration was applied using a vibrator connected to the bottom of the cell in order to obtain a uniform sand distribution. The vibrator pressure was set at 200 kPa. The 70/140 sand was poured freely through a 32-mesh screen. A low frequency vibration was applied intermittently using a hammer to increase the packing density. The cell top was then closed by using a hydraulic wrench.

3.4.1.2 Annulus Saturation

A vacuum was applied at the top of the sand pack to remove entrapped air. Deionized water was used to saturate the cell. The water was raised in a pail to a higher elevation and allowed to flow under gravity through a tap into a hose connected to the top of the cell. After the water level stabilized, a one-liter capacity pump was used to inject additional water in order to displace the remaining trapped air. The cell was inclined at 45^0 and put under vacuum at the top of the cell to ensure that any trapped air was sucked out. The cell saturation was inferred from the high-pressure build up during pressurization. Pressure was built-up to 3.4 MPa in the cell to check for water leakage.

3.4.1.3 Sandy Polymer Slurry Injection

The Moyno pump was cleaned and flushed with water. The slurry was prepared as stated in section 3.2. Twenty liters of slurry were injected into the wormhole. The cell was inclined at 45^0 during the slurry injection. The slurry was re-circulated through the bypass hose connected to the three-way valve before injecting it into the screened tube (wormhole channel) (Figure 3.4). The wormhole inlet valve was opened for injecting the slurry into the wormhole at 0.025 m^3/hr to 0.05 m^3/hr while carefully observing the effluent produced into the collecting vessel. The injection was stopped regularly to empty the effluent-collecting vessel. At first, only water was produced. Once the slurry started to be

produced, the slurry injection was stopped and the wormhole outlet valve was closed.

3.4.1.4 Polymer Squeeze

The drains at the outer circumference of the sand pack were opened. The slurry was then injected initially into the wormhole at 0.05 m^3/hr while the injection pressure was below 1.5 MPa. Injection continued intermittently until no further injection was possible. The weight of effluent leaking-off was recorded. Data for the first test are given in Table 3.4. Five liters of crosslinked polymer sand slurry were injected during the leak-off.

3.4.1.5 Polymer Injection into Annulus

The pump was thoroughly cleaned. Crosslinked polymer prepared as stated in (section 3.2) was injected into one end of the annulus. At first, only water was produced out of the opposite end of the annulus. The injection continued until the crosslinked polymer was produced as a pure effluent. In the second part of the first water shut-off experiment, a crosslinked polymer with an increased polymer to crosslinker ratio of 40:1 and a polymer concentration of 12,000 ppm was injected.

3.4.1.6 Cell Shut-in

The wormhole inlet and outlet valves were closed. The cell was shut in for three days for gelation of the slurry at 45^0 inclination during the first part of the first water shut-off experiment, and five days in the horizontal position during the second part of the experiment. The results of the first water shut-off experiment are given in Chapter 4.

3.4.2 Second Water Shut-off Experiment

The objective of this experiment was to improve on the gel plug strength obtained in the first experiment. In this experiment, the polymer concentration of the crosslinked polymer gel injected into the annulus and of the crosslinked polymer gel in the sandy slurry injected into the wormhole was 12,000 ppm. A polymer to crosslinker ratio of 40:1 was used. A sand concentration of 60 wt% was utilized in preparing the polymer sand slurry. The injection rate varied between 0.05 and 0.1 m^3/hour. In the second experiment, the slurry was injected while the sand pack was in the horizontal position. In the first experiment, the slurry was injected from the bottom with the sand pack in the vertical position. Therefore, the injection strategy in the second experiment was closer to the field conditions. The apparatus and physical model used for conducting the experiment were the same as in the first experiment. The experimental steps utilized in the first experiment were followed with some modifications. The addition of the crosslinker was performed in two stages. These changes in the preparation strategy were adopted to prevent a rise in slurry viscosity during mixing due to gelation and to allow a better dispersion of the sand. The crosslinked polymer slurry was prepared in two batches of 10 liters each. Injection started immediately after the first batch was prepared. The second batch preparation started midway after injecting the first batch. The shut-in period was increased to 5 days with the cell positioned in the horizontal position simulating more closely field conditions. Data on fluid and sand injection and gel leak-off by weight for the second experiment are given in Table 3.4.

3.5 Rheological Measurements

The objectives of these measurements were to determine the slurry viscosity, strength and gelation time in order to help in designing a system with an appropriate injectivity and optimized sand concentration. A Rotovisco RT 20 shear Rheometer and a Fann 35 viscometer, shown in Figure 3.5 and 3.6 respectively were used. Different sand concentrations, ranging from 20 to 75

wt%, were used in preparing the crosslinked polymer sand slurry. Visual gel strength screening tests were performed. The effect of iron and shear on the gelation strength build-up of the slurries was also evaluated.

3.5.1 Sample Preparation

The brine was prepared following the same procedure as in the water shut-off tests. Chromium acetate ($CrAc_3$) was used as the crosslinking agent. A polymer to crosslinker ratio of 40:1 (weight ratio) was used. The crosslinker was added and mixed thoroughly until a uniform colorization was observed. The desired weight of sand was added to the crosslinked polymer solution, which was thoroughly mixed in a 500 mL beaker. A one-liter capacity laboratory blender was used to preshear the slurry prior to conducting viscosity and yield stress measurements or gel strength screening and settling tests. Some rheological measurements were performed immediately after preparation of the gel slurries whereas different gelation times were allowed for other tests.

3.5.2 Viscosity Measurements

Viscosity measurements for the crosslinked polymer solution as well as for the crosslinked polymer sand slurry of different sand concentrations were performed both with or without preshear. Slurries with sand concentrations of 20, 30, 40, 50, 60, 65, 70 and 75 wt% were prepared. Three sets of measurements, at different delay times of zero, one hour and 2.5 hours. Different geometries with different gap size and roughness were utilized to test for wall slippage effects. The fluids were tested after different gelation times to determine the viscosity and gel strength build-up with time. Two different bob geometries were utilized (Table 3.5).

3.5.2.1 Measurement Procedure

The Rotovisco RT20 is a controlled rate/stress rheometer manufactured by HAAKE. The Rheo Win Pro software package was provided with the rheometer for data acquisition and analysis. The Fann 35 viscometer, which is more

portable, was used for measuring the initial slurry viscosity during the water shut off experiment.

The cooling bath was set at the desired temperature. A pre-shear period of 4 minutes was set for each measurement at a controlled shear rate of 0.7 sec^{-1}. Two shear rate sweeps were set for each measurement cycle; one sweep in which the shear rate increased in twenty steps to the maximum rate, followed by a sweep in which the shear rate was decreased in twenty equal steps back to zero. All the shear rate sweeps were set within a range of 0 to 450 sec^{-1}. Each time step lasted 2 minutes. A fresh sample was added for each measurement. All measurement samples were prepared as stated in section 3.5.1. The samples were poured into the measurement cup and placed onto the cup holder. The sample cup was automatically lifted to the rotor and the measurement was performed.

3.5.3 Settling Tests

These tests were conducted to determine the effect of sand concentration on the degree of sand settling in the slurry and the magnitude of the settling of the sand within the slurry as a function of time in order to determine how much sand-free gel would remain in a wormhole in the field. The sand concentrations were: 20, 30, 40, 50, 60, 65, 70 and 75 wt%. The sand settling rate will be used as an input parameter in the numerical simulation for sandy gel placement within wormholes.

Graduated cylinders, each having a volume of 100 cm^3, were used. The polyacrylamide solution was prepared as described in section 3.5.1. Sand at the desired concentration was added to the crosslinked polyacrylamide gel and properly mixed until a uniform, homogenous mixture was observed. One hundred grams of the crosslinked polyacrylamide sand slurry was poured into the cylindrical tube using a funnel. These cylindrical tubes were monitored for sand settling for a duration of 5 days.

Two series of tests were performed to check for repeatability. The results of these tests were very similar. In the first series of tests, sand settling readings with time were recorded every 15 minutes for the first 12 hours then every 12 hours for the reminder of the 5-day duration. In the second test, readings were recorded every 5 minutes for the first 12 hours then every 15 minutes for the next 12 hours. On the second and third days, readings were taken every 3 and 6 hours, respectively, and then every 10 to 12 hours for the rest of the time duration.

3.5.4 Gel Strength Screening Test

The objective of this test was to evaluate the time the crosslinked polymer sand slurry would take to reach the maximum attainable gel strength. Gel strength for different sand concentrations (20 to 75 wt%) was evaluated with time. In this test, the crosslinked polymer solutions and sand were mixed in a beaker till a uniform homogenous mixture was observed. The homogenous mixture was then poured, using a funnel, into 30 mL disposable centrifuge tubes with screw caps. These tubes were kept at room temperature (21^0C), and visually observed for 3 weeks. In the UNOCAL method used [69], gel strength is rated from fluid (code 1) to ringing rigid gel (code 6) (Appendix C)

3.5.5 Gel Degradation Tests

Under field conditions, the injected gel solution is exposed to iron in the tanks and through the tubing. In addition, the gel undergoes appreciable amounts of shear. These factors may potentially have adverse effects on the strength of the final gel plug [51]. The objective of the degradation test was to determine the effect of iron and shear on the gelation strength build-up of the crosslinked polymer sand slurries in terms of their residence time through a Moyno pump.

In this test, a 60 wt% sand crosslinked polyacrylamide slurry was re-circulated though the Moyno pump at different flow rates. The residence time was calculated by dividing the pump volume by the flow rate. Effluent was collected

after each flow rate and tested for its gel strength. The gelation strength was estimated following the UNOCAL method described in Dovan et al. [69] (Appendix E). Five liters of crosslinked polymer solution (12,000 ppm Hi Vis 350, 5 wt% NaCl, 0.25 wt% $CaCl_2$, 264 ppm $CrAc_3$) were used. The experimental procedure consisted of the following steps: the Moyno pump was cleaned and flushed with deionized water; the crosslinked polymer was re-circulated through the Moyno pump; effluent samples were taken at regular intervals at different flow rates; four samples were re-circulated at pump rates of 0.025 m^3/hr, 0.050 m^3/hr, 0.075 m^3/hr and 0.1 m^3/hr for 5-minute at each flow rate. The last sample was re-circulated at the maximum pump rate of 0.1 m^3/hr for a 70-minute interval.

3.5.6 Capillary Viscosity Test

In this test, viscosity measurements on a polyacrylamide sand slurry were conducted using a capillary viscometer in order to go to higher shear rates. The capillary rheometer consisted of stainless steel tubing, 457 cm long and having an inner diameter of 0.4 cm. Pressure taps were located at either end. Four differential pressure transmitters, with different pressure ranges were used to measure the pressure drop over a wide range of flow rates. The viscometer was calibrated with water. The calibration data is given in Appendix D. The crosslinked polymer sand slurry was prepared following the procedure used in the second water shut off experiment. The crosslinked polymer sand slurry was injected through the capillary rheometer using the Moyno pump. Slurry flow could not be achieved at sand concentrations of 75 wt% of sand.

3.5.7 Yield Stress Measurements

The yield stress is defined as the amount of stress the sandy gel could withstand before it yields. Yield stress measurements for different crosslinked polymer sand slurries with sand concentrations of 20, 30, 40, 50, 60, 65, 70 and 75% were performed for sheared and unsheared samples. The yield stress was measured using the RT 20 Rotovisco shear rheometer. A controlled shear rate sweep was used for each measurement. At the start of the measurement, the shear stress

increased linearly with time since the material deformed elastically. The shear stress at which there was a sudden decrease in the shear stress magnitude was defined as the yield stress.

Table 3.1 Sand equivalent diameters and coefficient of uniformity

Sand	D_{90}(mm)	D_{60}(mm)	D_{50}(mm)	D_{10}(mm)	C_u(mm)
Annulus	0.200	0.180	0.170	0.110	1.636
Wormhole	0.160	0.103	0.100	0.068	1.515

Table 3.2 Wormhole (F110) and annulus (70/140) sand sieve analysis data

Sieve #	Size (mm)	Finer than (%) (wormhole sand)	Finer than (%) (annulus sand)
45	0.355	100.00	100.00
60	0.250	99.85	99.95
80	0.180	98.49	83.85
100	0.150	90.44	37.97
120	0.125	80.19	21.35
140	0.106	63.41	6.32
170	0.090	36.75	1.10
200	0.075	17.57	0.32
230	0.063	6.31	0.00
325	0.045	1.75	0.00
400	0.038	0.05	0.00

Table 3.3 Maximum and minimum density and porosity for sands used in this study

Sand sample	Avg. max. density (kg/m^3)	Avg. min. density (kg/m^3)	Avg. max. porosity (%)	Avg. min. porosity (%)	Avg. max. void ratio	Avg. min. void ratio
wormhole dry	1,582.97	1,517.36	42	39	0.72	0.65
wormhole wet	1,671.30	1,530.50	41	36	0.70	0.56
annulus dry	1,688.79	1,632.40	37	35	0.60	0.54

Table 3.4 Fluid, sand injection and leak-off

SPS = sandy polymer slurry

Tests	(Sand) annulus packing (g)	Water injected (cell saturation) (g)	Fluid leaked -off (g)	SPS injected (g)	SPS volume injected (liters)	Cross-linked polymer injected into annulus (g)
First experiment	47,505.9	39,981.4	4,300.0	18,500.0	11,515.4	5,000.0
Second experiment	46,979.6	39,671.4	5.866.0	19,000.0	11,826.6	5,000.0

Table 3.5 Rheometer geometries description

Terms	Rotor type	Gap size (mm)	Cup internal dia. (mm)	Spindle (bob) dia (mm)
Striated	Z-38 (grooved)	3.15	44.38	38.08
Smooth	Z-41	1.50	44.38	41.45

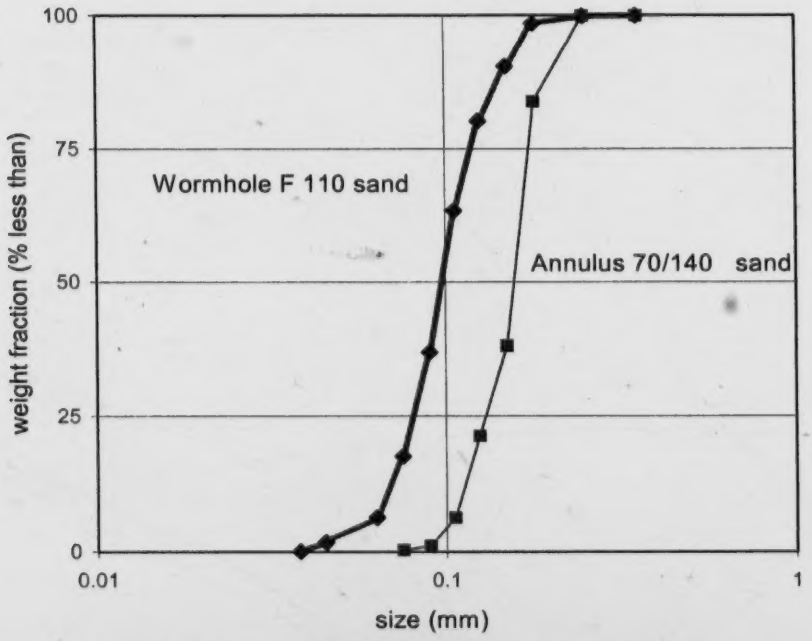

Figure 3.1 Wormhole and annulus sand grain size distribution

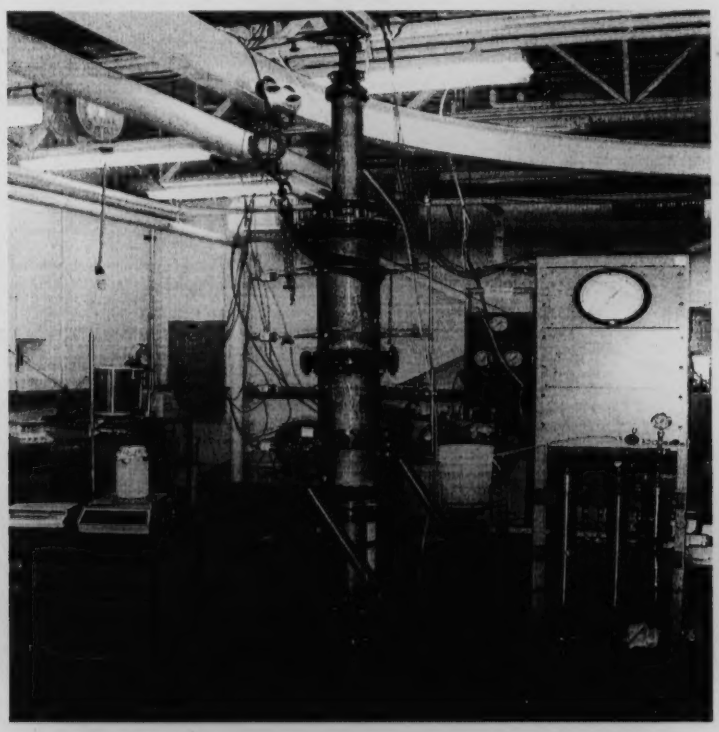

Figure 3.2 Cell in the vertical position

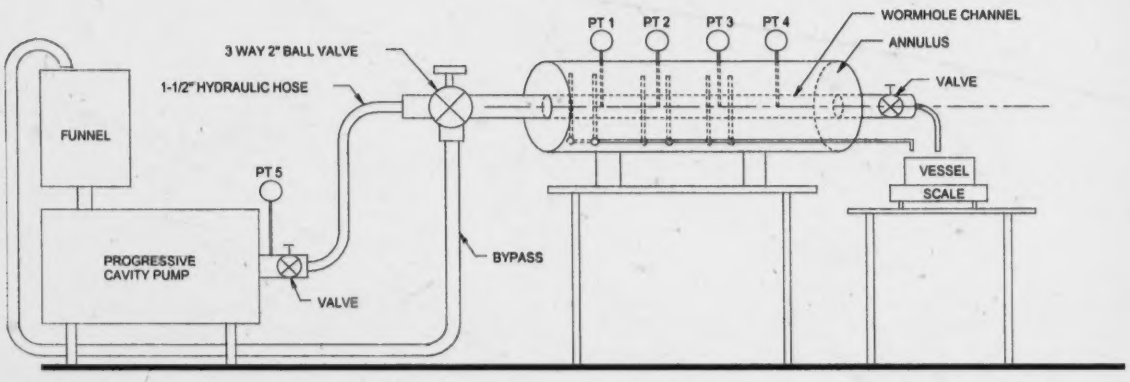

Figure 3.3 Schematic diagram of the apparatus.

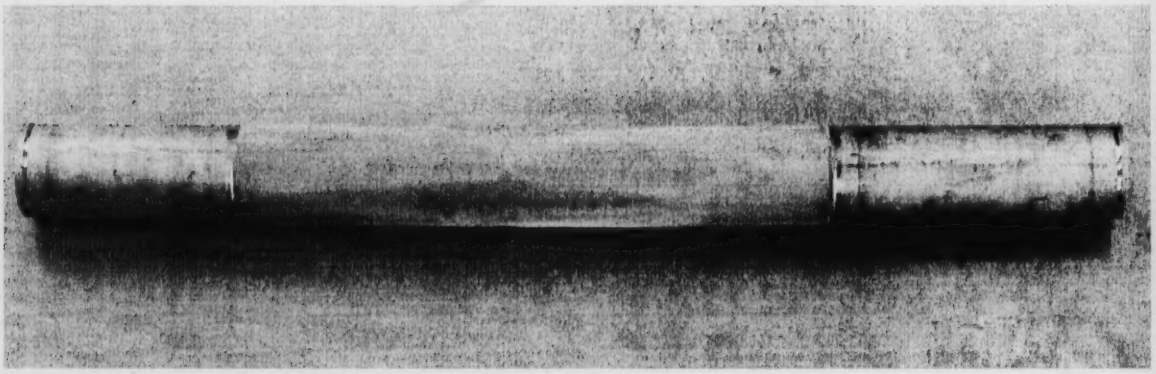

Figure 3.4 Screened tube with pipe attachments at ends.

Figure 3.5 RT 20 ROTOVISCO shear rheometer.

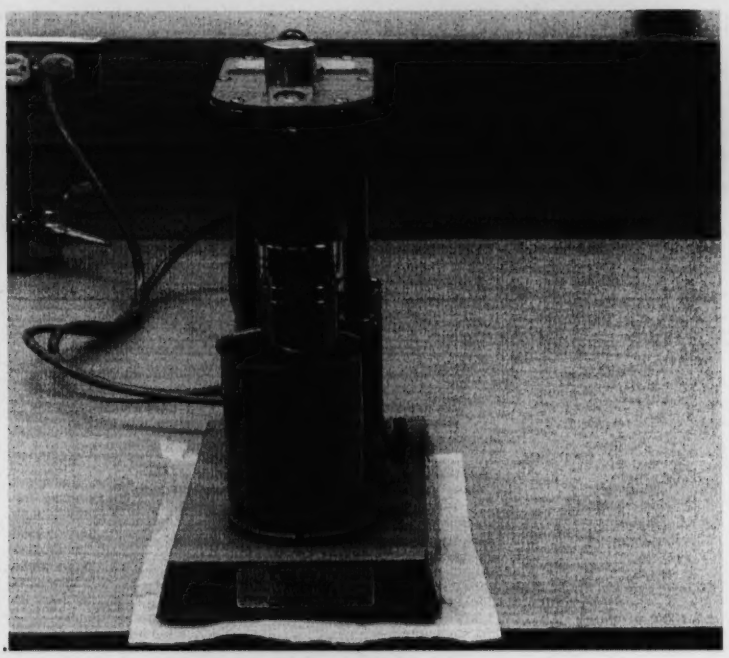

Figure 3.6 Fann 35 viscometer.

CHAPTER 4

Results

4.1 Introduction

The presentation of the experimental results is divided into three parts: the mechanical and physical properties of the materials used, the rheological properties of the crosslinked polymer and sandy gel slurries, and the water shut-off experiments.

The results and knowledge gained from the mechanical, physical and rheological properties were used in the design and conduct of the first water shut-off experiment. The second water shut-off experiment improved on the main experimental parameters, which were: the polymer concentration, polymer to crosslinker ratio, sand concentration and gelation time.

4.2 Mechanical and Physical Properties

4.2.1 Settling Tests

The objectives of these tests were to obtain information leading to the selection of the optimum gel system for water shut off treatment. The measured parameters were:

1. the height of the sand-free polymer gel after the sand settled within the slurry.
2. the effect of sand concentration on the settling rate.
3. the concentration of the settled sand.

As will be shown in a further section, when a sandy polymer gel is injected into a channel, the gel will leak-off into the surrounding formation leading to the build-up of a filter cake. A central core of sandy polymer gel is left at the channel center, however, as shown in Figure 4.1a. When the sand within the caked channel settles, it will leave a layer of pure gel as in Figure 4.1b. This layer of the pure gel is weaker than the sandy polymer gel and can yield more easily.

4.2.1.1 First Settling Test

The results of these tests are shown in Table 4.1 and in Appendix F. These results illustrate that, for the 60 wt% formulation, up to 167% of the minimum standard porosity of the F 110 sand (36%) can be achieved by the settled sand. The degree of settling, in terms of both height and height percentage of the decanted (sand-free) gel layer is shown in Figure 4.2 for the 60 wt% sandy polymer gel.

4.2.1.2 Second Settling Test

The second settling test was conducted to confirm the results of the first settling test. In this test, the settling was observed at shorter time intervals. The results are shown in Table 4.2 and in Appendix F. Figures 4.2 to 4.6 illustrate the decrease in porosity and the increase in settling with time for different sandy polymer gels. These results are almost identical to the results obtained in the first test. Table 4.3 converts sand weights to volumes that were used in the calculations assuming a sand density of 2.65 g/cm^3.

4.2.2 Gel Strength Screening Test

Figure 4.7 illustrates that all these slurries reached their maximum strength within 3 to 6 days. The addition of sand to the crosslinked polymer increased the gel strength significantly. The gel strength test was not conducted for sand concentrations greater than 75 wt% since the sand slurry at those concentrations, could not likely be injected into the reservoir as suggested by observations of sand bridging in tubing in the laboratory. Detailed test data on the gel strength measurement, are presented in Appendix C.

4.2.3 Gel Degradation Test

In the preparation of the water shut-off experiments, concern was expressed about possible gel degradation due to iron contamination and high shear stresses. In certain gel treatments, severe degradation, in terms of viscosity

reduction was observed due to the contact of the polyacrylamide gel with steel piping [74]. The 60 wt% sandy polymer slurry, used in the water shut-off experiments, was tested for these effects. The test procedure was described in section 3.5.5. The results of this test are displayed in Figure 4.8 and Appendix E. These results show that, shear degradation and contact with iron were not a major concern in terms of the final gel strength for the 60 wt% sandy polymer slurry in the water shut-off experiments. The gel reached the same strength in 6 to 9 days, except for the 130 minutes case where the shear degradation effect was evident.

4.3 Rheological Properties

4.3.1 Injectivity of the Slurry

The capillary viscometer was used to measure the viscosity of sandy gel slurries at high shear rates. The pressure drop and flow rate were accurately measured and used to calculate the viscosity and power law index. Viscosity measurements were taken for a range of sand concentrations for different geometries, shear rates or shear stresses. Figure 4.17 shows that the sandy polymer gel slurries flow behavior is strongly shear thinning. Shear thinning is a non-Newtonian flow behavior in liquids where the viscosity of the material decreases with increasing shear rate. Shear thinning often occurs as a consequence of high molecular weight molecules being oriented by the shear stress. The shear rate at the wall of the capillary tube was corrected for shear thinning using the power law index shown in Table 4.4. The sandy polymer slurry and the crosslinked polymer were injected at rates of 15 to 30 liters/hour.

Figure 4.9 shows that the addition of the crosslinking agent ($CrAc_3$) to the polymer solution resulted in a more viscous solution.

4.3.2 Yield Stress

The sandy polymer slurry and the crosslinked polymer exhibited an apparent yield stress that was proportional to their aging period after blending and to the sand, crosslinker and polymer concentrations. The time and shear history dependency of the yield stress are shown in Figure 4.10 and Tables 4.5 through 4.7. The samples (without preshear) displayed higher yield stress than the sheared samples (tested after preshearing), which reaffirms the sensitivity of the polyacrylamide gel to shear stress [74].

The increase in yield stress must be taken into account in gel placement treatments since the gel is often batch mixed and can be stored in tanks before being injected into the formation. The yield stress of the presheared sample tested after a 2 hour delay was significantly higher as displayed in Table 4.7

4.3.3 Slippage Effect

Polymer solutions and suspensions with high volume fractions of dispersed solid phase are known to be susceptible to slip at the measuring instrument walls as well as at the solid boundaries during shear flow. Slip can lead to a distorted velocity profile, resulting in an apparent shear thinning increase. One method of verifying for slip is to measure the viscosity of the material using concentric cylinder geometries with different gap sizes. If slip exists it will lead to differences in viscosity. Two different gaps sizes, described in Table 3.5, were used for the viscosity measurements. Figures 4.11 and 4.12 illustrate that the wall slip effect on the crosslinked polymer and the sandy polymer gel is of no major concern since the viscosity did not depend on the gap size. Therefore, no further corrections were made.

4.3.4 Rheology Models

The rheological measurements for sandy polymer gels were conducted for different aging periods, geometries and sand concentrations. These

measurements were fitted to some well-known rheological models for future gel placement calculations. These models are shown in Appendix H. Some of these models seem to characterize the flow behavior at low shear rates while others work better at high shear rates. The volume fraction of the dispersed solid phase was a significant factor in the characterization of the material response. The Carreau - Yasuda model was quite adequate in characterizing the sandy polymer gellant behavior over a wide range of shear rates (Appendix H). Figures 4.13, 4.14 and 4.17 show viscosity fits for different sand concentrations using the power law model. The power law model proved useful in filter cake and gel placement for field treatment calculations. Table 4.8 displays power law fits for different sand concentrations at low and high shear rate regimes. The transition shear rate separating the two regimes is also shown in the Table.

4.3.5 Relative Viscosity

The relative viscosity is defined as the ratio of the viscosity of the sandy polymer slurry to the viscosity of the polymer. This parameter is independent of the liquid phase viscosity and shear rate for Newtonian fluids and is an important factor in modeling flow through pipes. For non-Newtonian fluids, such as the sandy polymer slurries, the relative viscosity also depends on the shear rate. The relative viscosity was calculated for:

- different delay times after initial mixing
- different measurement geometries
- different shear rates
- different sand concentrations

The relative viscosity increased with increasing sand concentration, at a given shear rate (Appendix J), and decreased with increasing shear rate, at a given sand concentration (Figure 4.18 and Appendix J).

4.3.6 Rheology of 60 wt% Sandy Polymer Gel

A 60 wt% sandy polyacrylamide gel was used throughout the water shut-off experiments. This sand concentration was approximately the highest at which the sandy polymer gel could be injected in the experiments. The effects of shear history, measurement time delay and geometry on the viscosity were investigated. Detailed results of these measurements are displayed in Appendix K.

The high viscosities at low shear rate imply that less settling of the 60 wt% sandy polymer gel would occur within the wormhole when the injection is stopped. The significant shear-thinning of the sandy polymer gel allows it to be injected at a reasonable pressure. More details on the viscosity measurements are given in Appendix K.

4.4 Water Shut-off Experiments

4.4.1 First Water Shut-off Experiment

The first water shut-off experiment was conducted in two parts. In the first part, the gel plug failed immediately at the start of the experiment. It was thought that the water might have fingered through the annulus. Therefore, fifteen liters of polymer solution of higher polymer and crosslinker concentrations were injected into the annulus sand pack resulting in a stronger gel. In addition, the gel was allowed to set for a longer time (three days).

4.4.1.1 First Part

The pore volume of the annulus and wormhole was 10 liters. In the first part of the first water shut-off experiment, the sandy polymer gel slurry was injected into the wormhole with relative ease. The injection pressure at the pump and inside the wormhole was very low, indicating insignificant pressure drop along the wormhole (Figure 4.19). The sandy polymer gel slurry injection was continued

until the slurry was produced at the effluent-collecting vessel as indicated by the sudden pressure increase inside the wormhole resulting from the pressure build-up in the tubing connecting the pump to the wormhole. After injecting 27 liters of slurry into the wormhole, the effluent valve was closed and the sandy polymer gel injection was continued. The squeezing of the polymer gel into the annulus (formation) continued until no further sandy polymer gel slurry could be injected into the wormhole without reaching the maximum pressure (1.5 MPa). These high pressures were caused by the build-up of the sand at the entrance to the wormhole. A total polymer gel volume of approximately 4.3 liters was squeezed into the annulus. One additional pore volume (10 liters) of crosslinked polymer was then injected into the annulus at one end of the sand pack. The concentric cell was closed for three days to allow the gelation of the injected sandy polymer slurry inside the wormhole, as well as the gelation of the polymer solution injected into the annulus.

The strength of the sandy polymer gel was measured in terms of its ability to withstand an applied pressure at one end of the screened tube. The pressure was applied in increasing steps until the sandy gel plug yielded. Each step would last for as much as three hours. In order to simulate the direction of the plug failure under field conditions relative to the slurry injection direction, the pressure was applied through the outlet end of the wormhole. The outlet and the inlet ends, as described in the following tests, are relative to the slurry injection direction during the filling of the wormhole. The experimental procedure followed in these tests after the complete gelation of the sandy polymer gel plug, was as follows:

1. The pipe couplings were removed from both ends of the pipe.
2. Sandy gel from both ends was excavated to a distance of 13 cm.
3. The collected sandy gel was weighed, oven dried and re-weighed to measure the sand concentration.
4. The pipe couplings were reinstalled.
5. The excavated volumes at both ends were filled with deionized water.

6. A one-liter accumulator was connected to the wormhole outlet in order to pressurize the plug simulating the aquifer pressure.
7. The wormhole inlet was connected through a 0.43 cm I.D tube to an effluent-collecting vessel placed on an electronic scale.
8. The wormhole inlet valve was closed.
9. The wormhole outlet valve was opened as the accumulator was pressurized.
10. The wormhole inlet valve was then opened. The effluent weight was always closely observed, as any sudden increase in the effluent weight would indicate the gel plug had failed.
11. The pressure was increased gradually until failure was reached. Figure 4.21 is a schematic of the water breakthrough test.

The sandy polymer gel plug failed 3.5 minutes after the start of the water breakthrough test at a very low pressure of approximately 20 kPa corresponding to a pressure gradient of approximately 16 kPa/m The shear strength of the sandy polymer gel plug at the wall of the screened pipe was calculated to be approximately 0.4 kPa using equation D.2 in Appendix D.

4.4.1.2 Second Part

In the second part of the first water shut-off experiment, an additional 1.5 pore volume (15 liters) of crosslinked polymer gellant, with a higher polymer concentration of 12,000 ppm and higher polymer to cross-linker ratio of 40:1, was injected into the annulus. An accumulator connected to a constant displacement pump was used to reduce any potential shear degradation due to the pumping of the slurry. The cell was vertically oriented to fill uniformly the screened tube and was then shut-in for 3 days for gelation. The same gel strength test preparations were followed as discussed for the first part of the first water shut-off experiment. The sandy polymer gel plug failed at a pressure of approximately 263 kPa (equivalent pressure gradient of approximately 216 kPa/m) as shown in Figure 4.22. The shear strength of the sandy polymer gel plug at the wall of the

screened pipe was calculated to be approximately 5 kPa using equation D.2 in Appendix D.

The cell was dismantled at the end of the test to physically measure and evaluate the compaction and propagation of the sandy polymer gel plug (Figures 4.20 and 4.23). The excavation showed that an appreciable degree of settling of the sand particles had occurred along sections of the plug resulting from the inability of the crosslinked polymer in the slurry to hold the sand particles in suspension following the injection and the squeezing processes.

Slumping tests were performed to provide a qualitative measure of the yield strength of the gel plug. Slumping is defined as the relative shrinkage in the longitudinal direction of the gel plug after it is placed vertically. The sandy polymer gel inside the screened pipe was cut in six lengths immediately after dismantling the concentric cell. The lengths of sandy gel were placed vertically to measure decrease in length, due to gravity relative to their initial length. The ratio of the final length to the initial length was defined as the degree of slumping. These sections were positioned in a bucket with the longitudinal axis in the vertical position. Seventy-two hours later, the sections were re-measured. The results of the slumping after 72 hours are presented in Table 4.9 for the first experiment.

The sand compaction along the wormhole and the extended areas is displayed in Tables 4.10 and 4.11. The sandy polymer gel plug compaction (sand concentration) varied from 72% at the wormhole inlet to 79% at the wormhole outlet as illustrated in Figure 4.23. The sandy polymer gel plug slid approximately 13 cm and 6 cm along the wormhole (in the same direction) at the inlet and outlet, respectively as shown in Table 4.12. A relatively poor gelation of the crosslinked polymer in the annulus formation was observed.

4.4.2 Second Water Shut-off Experiment

The objective of this experiment was to improve upon the results obtained in the first water shut-off experiment by using a stronger gel within the sandy polymer gel slurry. The polymer concentration of the gel injected into the annulus and of the gel within the injected sandy gel slurry injected into the simulated wormhole was increased to 12,000 ppm. The injection rate varied between 0.05 m^3/hour and 0.1 m^3/hour. The pressure inside the screened tube during the filling process was low as shown in Figure 4.19. The preparations for gel strength testing were the same as described for the first water shut-off experiment.

The adjustment made to improve the second water shut-off test resulted in a shorter injection period as shown in Figure 4.24. A high pressure build-up in the tubing connecting the pump to the wormhole signalled the end of the squeezing process as well as the start of sand compaction at the inlet to and inside the wormhole as shown in Figure 4.25. The wormhole gel plug excavation for the second water shut-off experiment is shown in Figures 4.26 to 4.28.

The measurement of the strength of the sandy polymer plug was conducted in stepwise pressure increases at the wormhole outlet until yielding occurred (after 29 hours). The sandy polymer gel plug yielded when the pressure was increased from 274 kPa to 415 kPa (Figure 4.29). This pressure range corresponds to a range in pressure gradient of approximately 225 kPa/m to 340 kPa/m. The shear strength (yield stress) of the plug at the wall of the screened pipe was calculated to range between 6 and 9 kPa. Equation D.2 in Appendix D was used to calculate the shear strength.

The fittings at both ends of the pipe were dismantled. Water was removed from both ends of the extended pipes (Figure 4.30). The flanges at either end of the annular pack were removed and approximately three quarters of the annulus sand was removed. The two halves of the flanged connected pipe were separated enough to allow the cutting of the screened pipe (wormhole) using a

metal saw. The two parts of the wormhole were pulled out from either end of the cell (Figure 4.26). The screened pipe was laid down and cut lengthwise with shears. Figure 4.28 shows the removal of the layered screen for inspection of the sandy polymer gel plug. The cell was disassembled and the gel plug was pulled out and sectioned to evaluate the compaction process (Figures 4.30, 4.31 and 4.32).

Slumping tests were performed as described previously. Considerably less slumping occurred than in the first water shut-off experiment The sandy polymer gel at the interface with the water at the injection end may have had a tendency to slump more in the first water shut-off experiment leaving a channel at the top for the water to flow. Figure 4.31 shows the slumping of the gel plug for the second experiment. The sandy polymer gel plug was sectioned into five parts to be inspected individually. The slumping results are shown in Table 4.13. As mentioned less slumping was recorded in the second water shut-off experiment as compared with the first water shut-off experiment (Table 4.9).

The sandy polymer gel plug slid approximately 6 cm and 2 cm along the wormhole at the inlet and outlet respectively after yielding. Figures 4.31, 4.32 and Tables 4.14 to 4.16 revealed that a high degree of compaction, gelation uniformity and continuous propagation of the sandy polymer gel were achieved in this second water shut-off experiment. Strong gelation of the crosslinked polymer was observed in the annulus

A thicker filter cake was formed within the screened tube simulating the wormhole. A small sand-free layer of polymer was formed at the center of the sandy gel polymer as shown in Figure 4.32. The sandy polymer gel within the black line in Figure 4.32 was much softer than the region outside the black lines. A sand compaction of more than 80% (porosity of 38%) was measured in this later region while a compaction of 69% (porosity of 53%) was measured within the black line excluding the pure gel region as shown in Figure 4.33. The

relatively high degree of compaction observed relative to that in the first water shut-off experiment led to a stronger sandy polymer gel in the wormhole.

Table 4.1 Final porosities of settled sandy gel (first settling test)

Sand concentration (wt%)	Final porosity (%)	Final porosity increase (% of minimum)	Density of the sandy gel (kg/m^3)	Sand-free height (cm)	Settling height (%)
75	44	22	1,910	0.66	3.53
70	51	42	1,809	0.80	4.26
65	55	53	1,737	1.40	7.37
60	60	67	1,656	1.50	8.06
50	67	86	1,547	3.00	16.04
40	63	75	1,613	8.40	45.41
30	53	47	1,776	12.60	70.00
20	51	42	1,801	15.40	82.35

Table 4.2 Final porosities of settled sandy gel (second settling test)

Sand concentration (wt%)	Final porosity (%)	Final porosity increase (% of minimum)	Density of the sandy gel (kg/m^3)	Sand-free height (cm)	Settling height (%)
75	44	22	1,915	0.80	4.23
70	50	39	1,818	0.90	4.81
65	56	56	1,729	1.10	5.91
60	61	69	1,649	1.40	7.37
50	65	81	1,574	3.90	21.79
40	67	86	1,545	7.60	92.00
30	51	42	1,802	14.30	77.30
20	51	42	1,801	15.90	84.13

Table 4.3 Weight/volume conversion for F 110 sand (wormhole sand)

Sand concentration (wt %)	Sand concentration (vol. %)
80	60.4
75	53.4
70	47.1
65	41.5
60	36.4
50	27.6
40	20.3
30	14.1
20	8.7

Table 4.4 Viscosity measurements using the capillary viscometer (60 wt% sandy gel slurry)

Rate (cc/sec)	DP (kPa)	Shear stress (Pa)	Corrected shear rate (1/s)	Viscosity (Pa.s)	k	n
1.13	155	35.10	195.93	0.18	0.30	0.55
3.02	270	61.15	521.52	0.12	0.30	0.55
4.95	345	78.13	855.76	0.09	0.30	0.55
6.87	422	95.57	1187.11	0.08	0.30	0.55

Table 4.5 Yield stress for unsheared sand polymer slurries (no preshear). (shear rate = 2 sec^{-1}).

Sand concentration (wt %)	Yield stress (Pa)
30	88
40	132
50	200
60	325
65	340
70	620
75	670

Table 4.6 Yield stress measurements for the crosslinked polymer (pure gel) (shear rate = 0.7 sec^{-1}). Subscript: time delay before testing

Geometry	$\tau_{0.5hour}(Pa)$	$\tau_{1hour}(Pa)$	$\tau_{2hours}(Pa)$
striated	0.52	0.55	0.58
smooth	0.50	0.52	0.54

Table 4.7 Yield stress measurements for the sandy polymer slurries (shear rate = 0.1 sec^{-1}). Subscript: time delay before testing.

Sand concentration (wt%)	$\tau_{0.5hour}(Pa)$	$\tau_{1hour}(Pa)$	$\tau_{2hours}(Pa)$
20	2.1	3.2	45
30	2.6	4.4	55
40	3.0	4.8	> 800
50	4.0	6.0	> 800
60	7.6	10	> 800
65	14	60	> 800
70	36	> 800	> 800
75	212	> 800	> 800

Table 4.8 Power law fit for different sand concentrations

Sand concentration (wt%)	Low shear rate		High shear rate		Transition shear rate (sec^{-1})
	k	n	k	n	
0	0.1459	0.9369	0.4946	0.6388	63.23
20	0.7043	0.783	0.5709	0.7658	55.00
40	0.8638	0.8007	1.5011	0.6282	63.21
50	2.1156	0.6784	3.8489	0.5183	63.21
60	8.9056	0.4396	7.4121	0.4893	63.21
65	18.825	0.3531	15.953	0.3842	63.21
70	28.174	0.4024	45.138	0.2926	63.21
75	227.74	0.1677	174.14	0.265	63.21

Table 4.9 Slump test result (first water shut-off experiment (second part))

Section #	Slump (% of initial length)
Inlet (1)	36.5
Inlet (2)	38.5
Outlet (2) and (1)	29.2
Extended area outlet (2)	27.8

Table 4.10 Porosity and compaction of the sandy polymer gel plug along the wormhole (first water shut-off experiment (second part))

Section #	Sand concentration (wt%)	Density of sandy gel (kg/m^3)	Porosity (%)
Inlet (1)	72.9	1,330	48
Inlet (2)	72.9	1,330	48
Outlet (1)	78.4	1,527	40
Outlet (2)	77.1	1,477	42

Table 4.11 Porosity and compaction of the sandy polymer gel plug along the wormhole extended area (first water shut-off experiment (second part))

Section	Sand concentration (wt%)	Density of sandy gel (kg/m^3)	Porosity (%)
Inlet	79.0	1,548	40
Outlet	72.1	1,303	49

Table 4.12 Sandy gel plug excavation (first water shut-off experiment (second part))

Distance excavated from the **inlet** end	38 cm
Distance excavated from the **outlet** end	39 cm
Distance from the **inlet** end to the gel plug	25 cm
Distance from the **outlet** end to the gel plug	46 cm
Displacement at **inlet**	13 cm
Displacement at **outlet**	6 cm

Table 4.13 Slump test result (second water shut-off experiment)

Section #	Slump (% of initial length)
Ext.area inlet (2)	13.8
Inlet (1)	13.6
Inlet (2)	6.8
Outlet (2)	8.7
Outlet (1)	5.4
Ext.area outlet (2)	15.4

Table 4.14 Porosity and compaction of the sandy polymer gel plug along the wormhole (second water shut-off experiment)

Section #	Sand concentration (wt%)	Density of sandy gel (kg/m^3)	Porosity (%)
Inlet gel plug(1)	84.8	1,790	30
Inlet gel plug(2)	78.1	1,483	41
Inlet gel plug(3)	79.4	1,509	38
Outlet gel plug(2)	82.6	1,694	32
Outlet gel plug(1)	82.3	1,683	33

Table 4.15 Porosity and compaction of the sandy polymer gel plug extracted from external pipe extensions at ends of screened tube (second water shut-off experiment)

Section #	Sand concentration	Density of sandy gel (kg/m^3)	Porosity (%)
Ext.area inlet(1) before water breakthrough test	69.0	1,206	52
Ext.area inlet(2) after water breakthrough test	81.9	1,664	35
Ext. area outlet(1) before water breakthrough test	67.3	1,154	54
Ext.area outlet(2) after water break through test	78.4	1,526	40
Sand free polymer layer	68.5	1,192	53

Table 4.16 Sandy gel plug displacement (second water shut-off experiment)

Distance excavated from the **inlet** end	36 cm
Distance excavated from the **outlet** end	48 cm
Distance from the **inlet** end to the gel plug in the wormhole after the test	31 cm
Distance from the **outlet** end to the gel plug in the wormhole after the test	50 cm
Inlet displacement	6 cm
Outlet displacement	2 cm

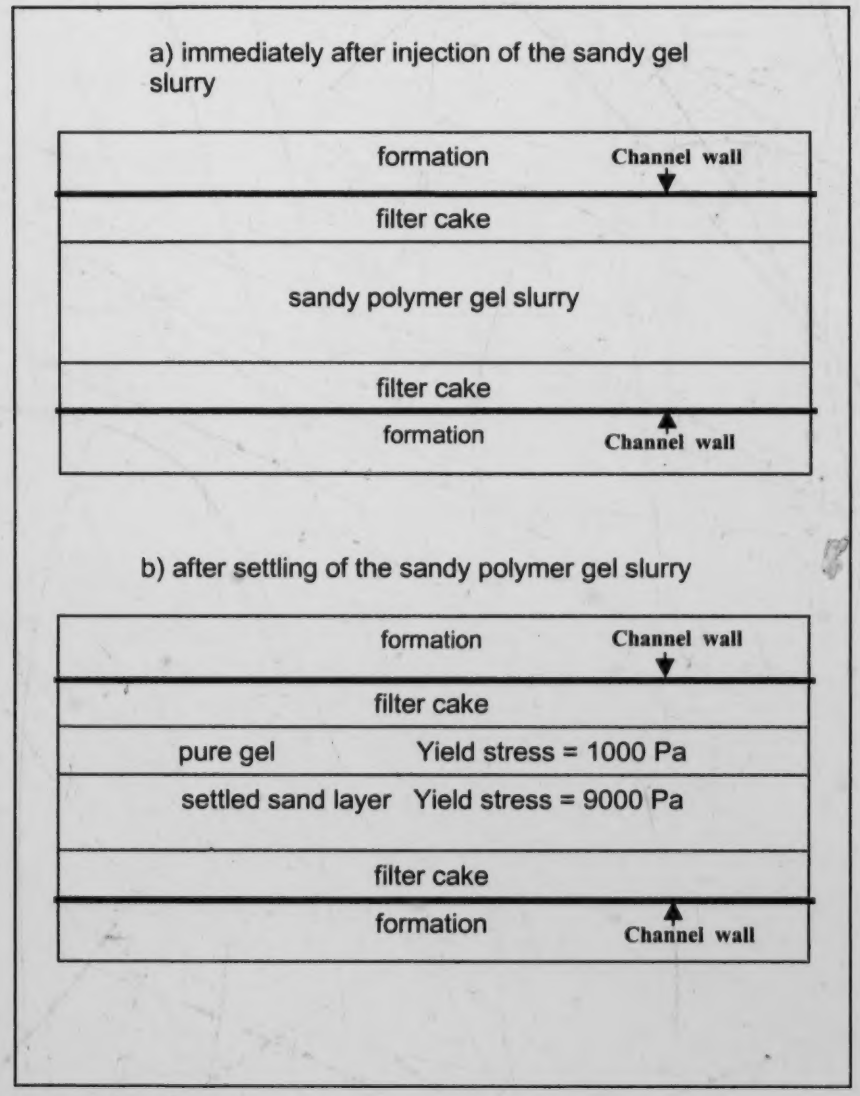

Figure 4.1 Schematic of gel placement and settling.

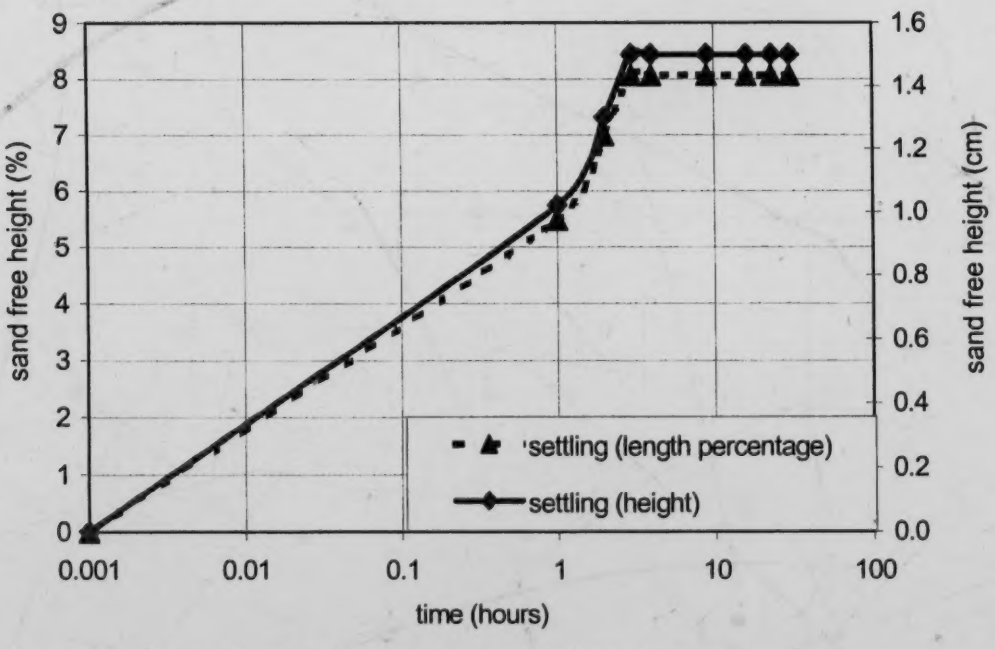

Figure 4.2 60 wt% sand polymer settling (first settling test).

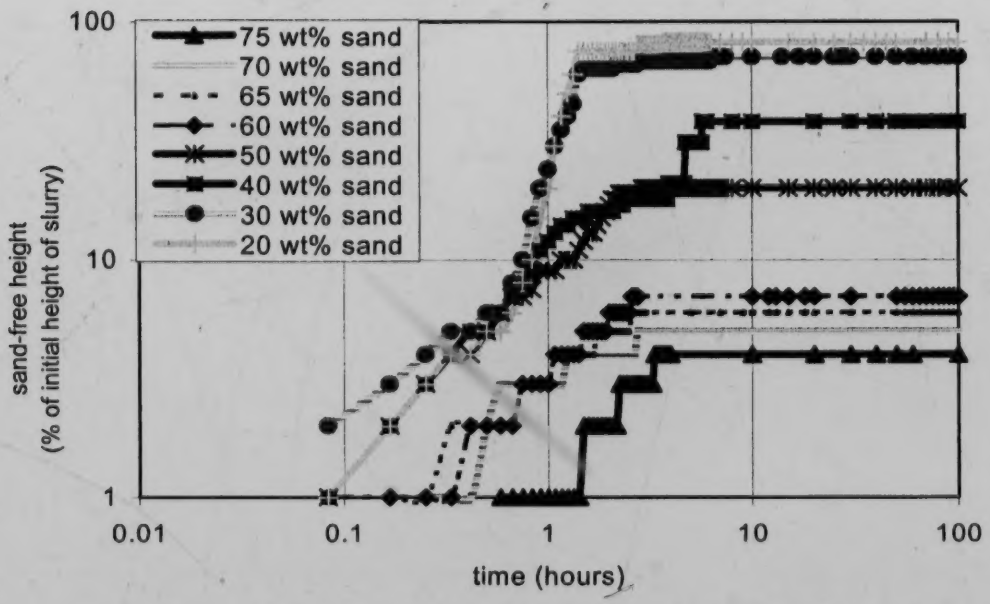

Figure 4.3 Sand settling height percentage (second settling test).

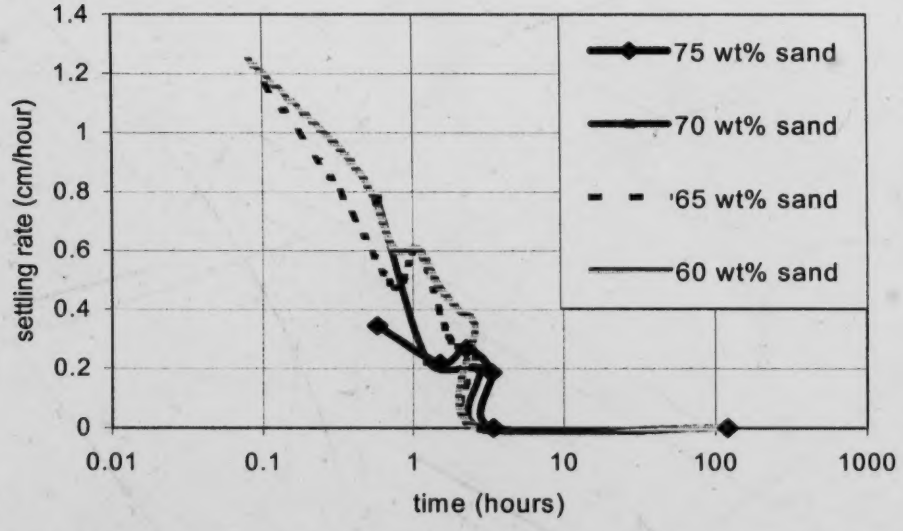

Figure 4.4 Settling rate versus different sand concentrations (second settling test).

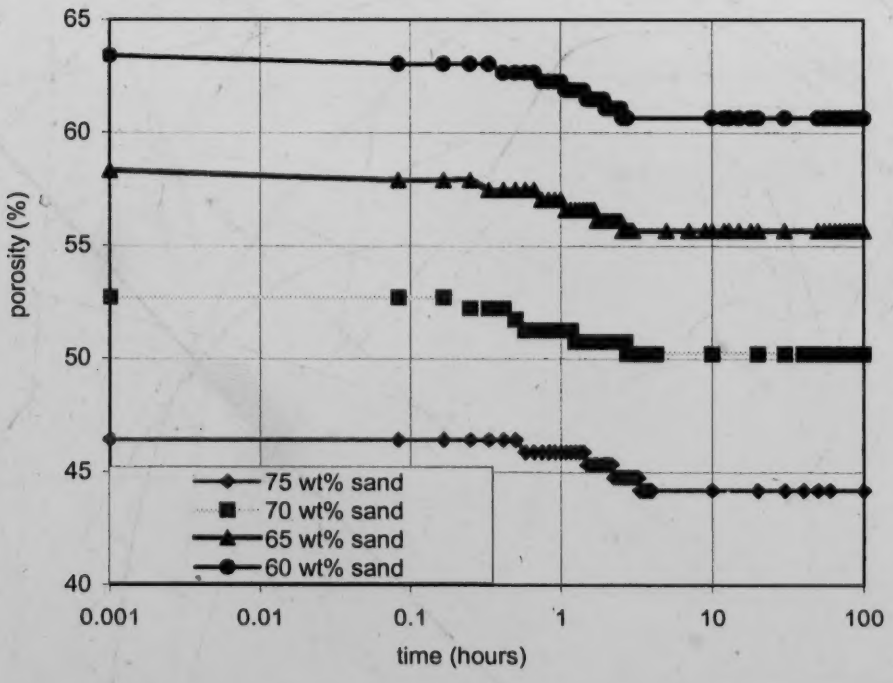

Figure 4.5 Porosity of settled sand layer for high sand concentrations (second settling test).

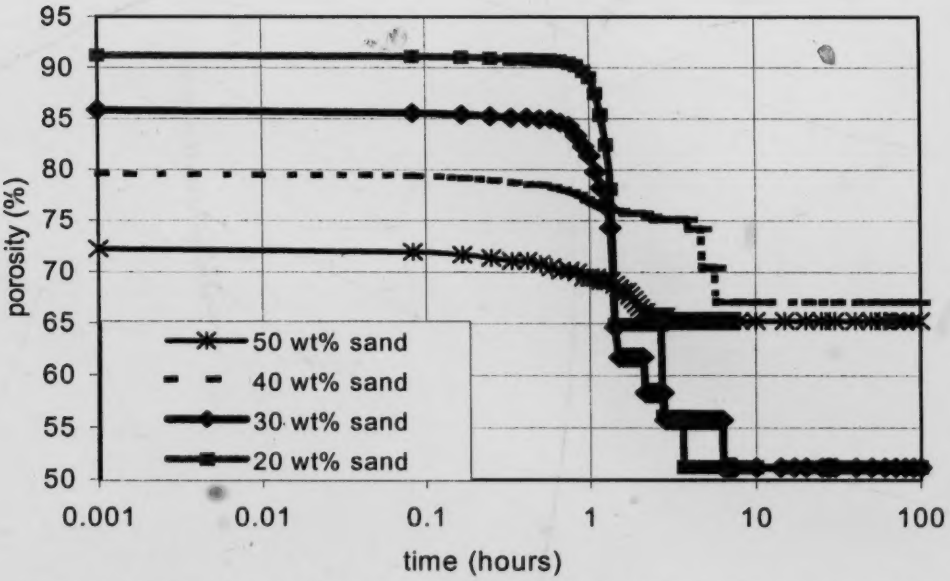

Figure 4.6 Porosity of settled sand layer for low sand concentrations (second settling test).

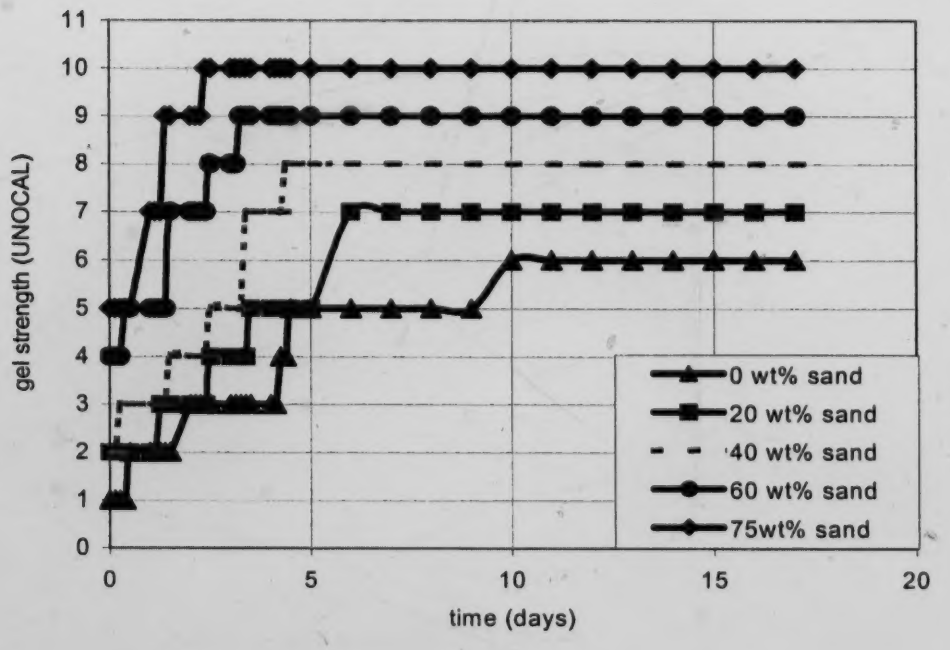

Figure 4.7 Gel strength screening test.

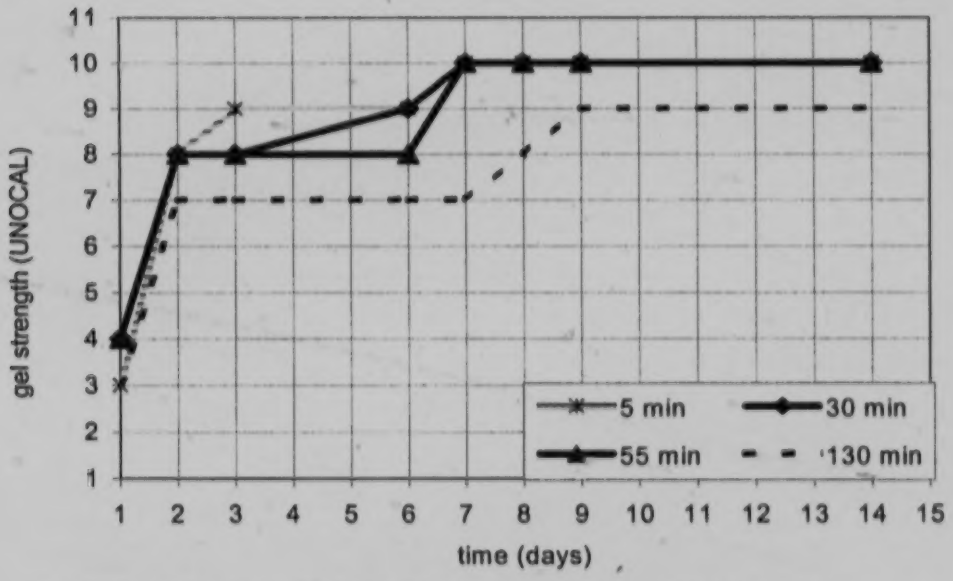

Figure 4.8 Degradation test (60 wt% sandy polyacrylamide slurry).

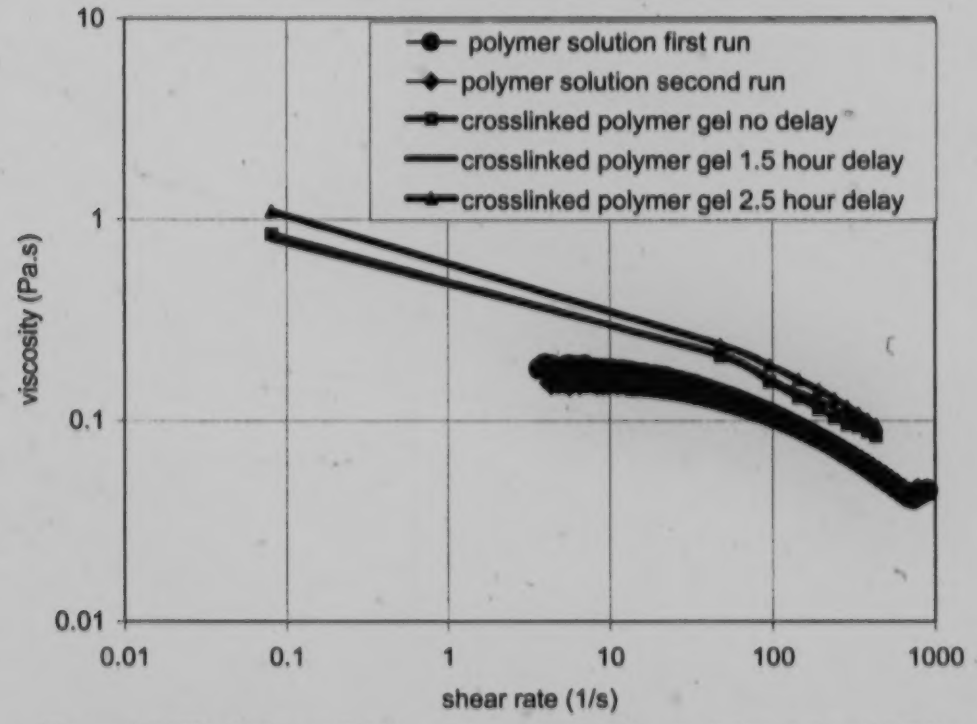
polymer solution first run
polymer solution second run
crosslinked polymer gel no delay
crosslinked polymer gel 1.5 hour delay
crosslinked polymer gel 2.5 hour delay
viscosity (Pa.s)
shear rate (1/s)

Figure 4.9 Effect of crosslinking on the gel viscosity, no delay, 1.5 and 2.5 hour delay before testing.

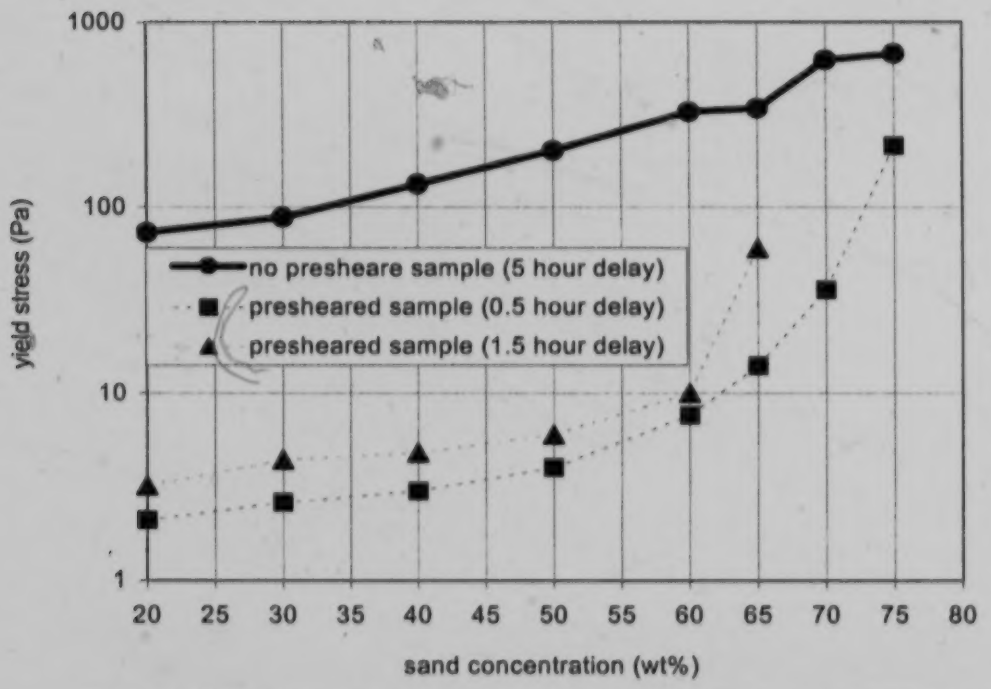

Figure 4.10 Yield stress for sheared and unsheared sandy polymer gel (shear rate = 2 sec^{-1}).

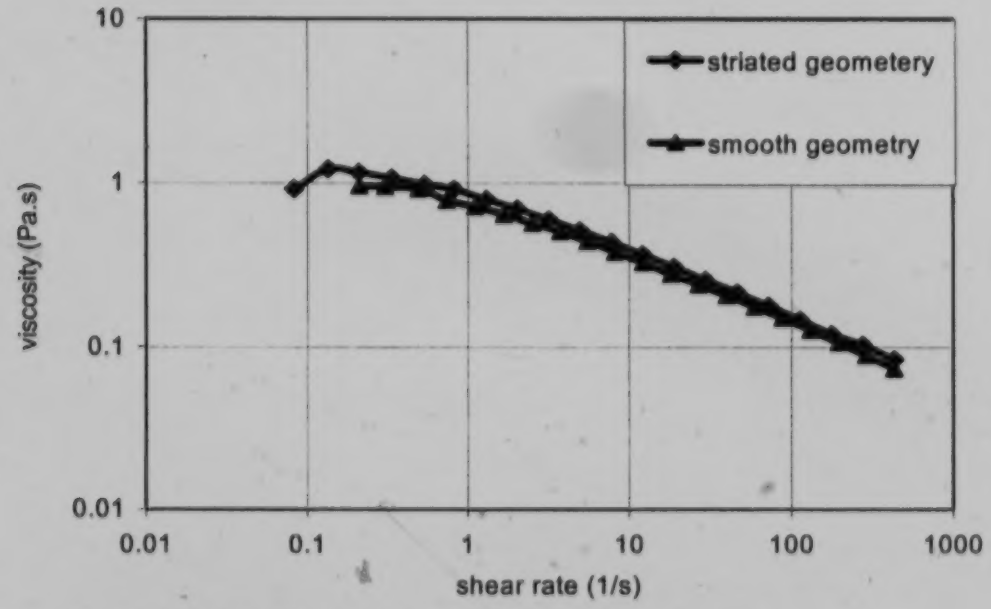

Figure 4.11 Slip effect for the crosslinked pure polymer gel (different geometries).

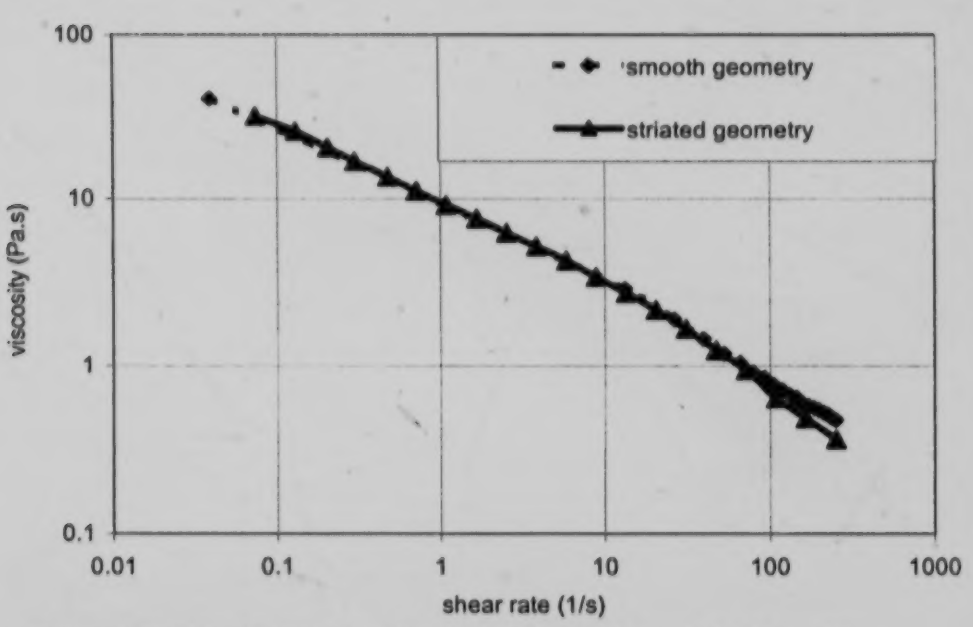

Figure 4.12 Slip effect on the 60 wt% sandy polymer gel (1.5 hour delay, different geometries).

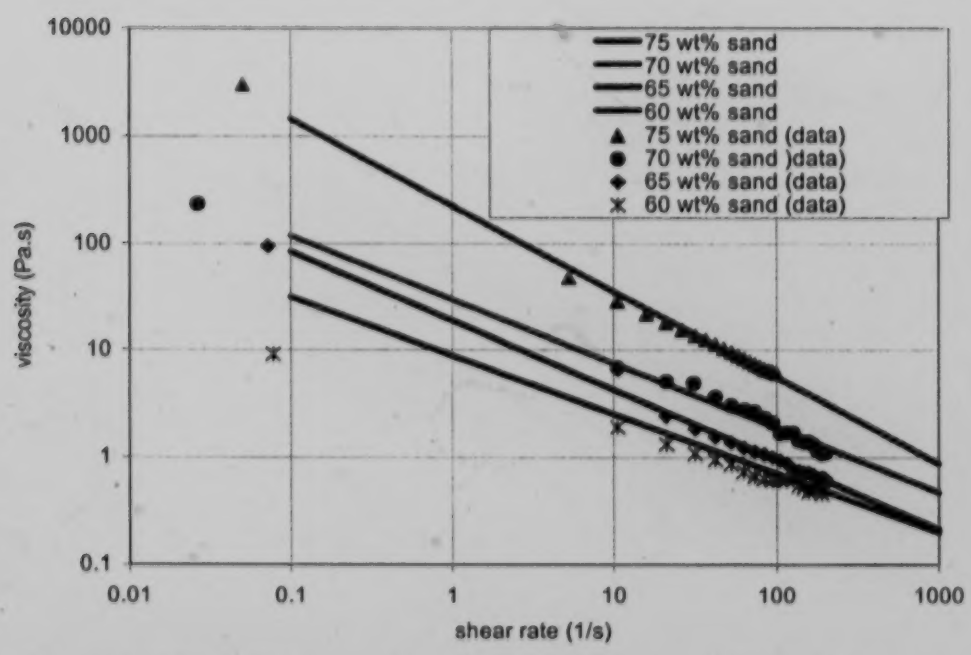

Figure 4.13 Viscosity versus shear rate for sandy polymer gels at high sand concentrations (striated geometry, 1.5 hour delay) (power law fit).

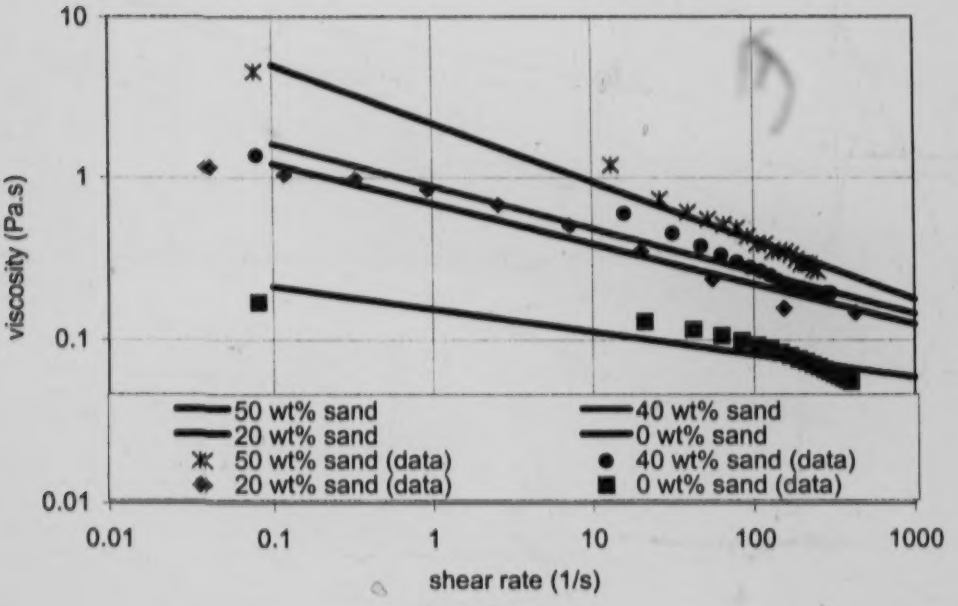

Figure 4.14 Viscosity versus shear rate for sandy polymer gels at low sand concentrations (striated geometry, 1.5 hour delay) (power law fit).

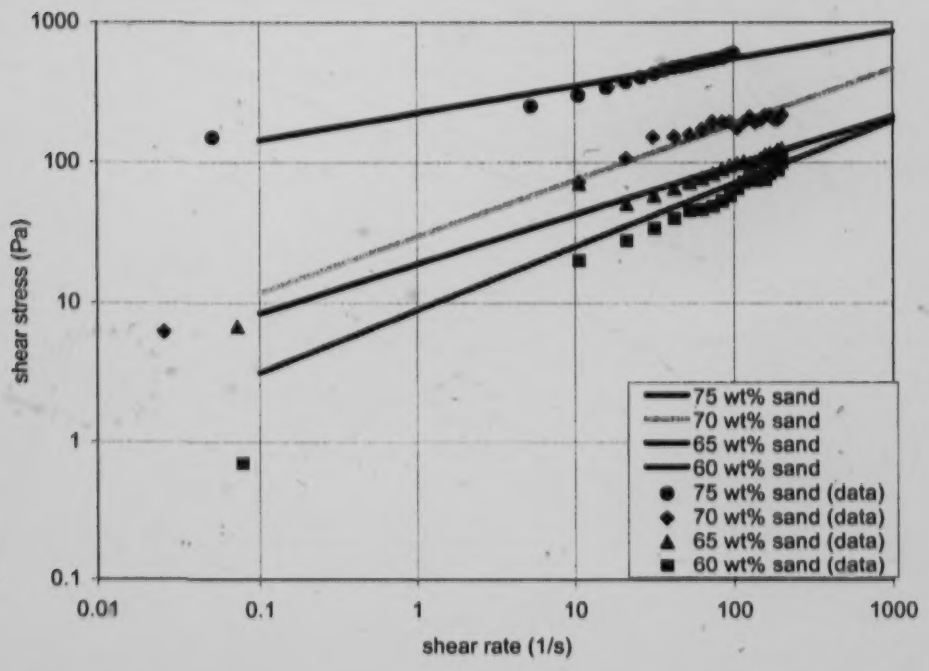

Figure 4.15 Shear stress versus shear rate for sandy polymer gels at high sand concentrations (striated geometry, 1.5 hour delay) (power law fit).

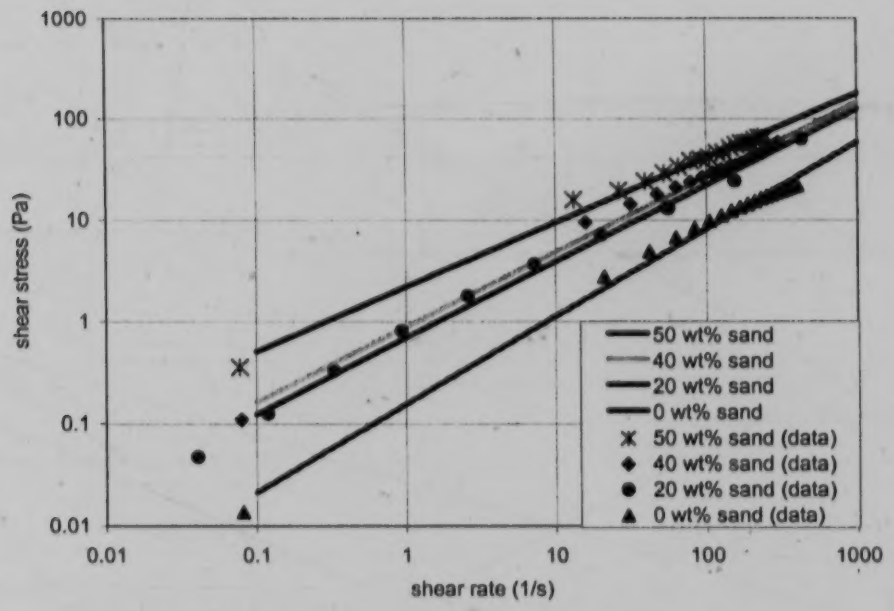

Figure 4.16 Shear stress versus shear rate for sandy polymer gels at low sand concentrations (striated geometry 1.5 hour delay) (power law fit).

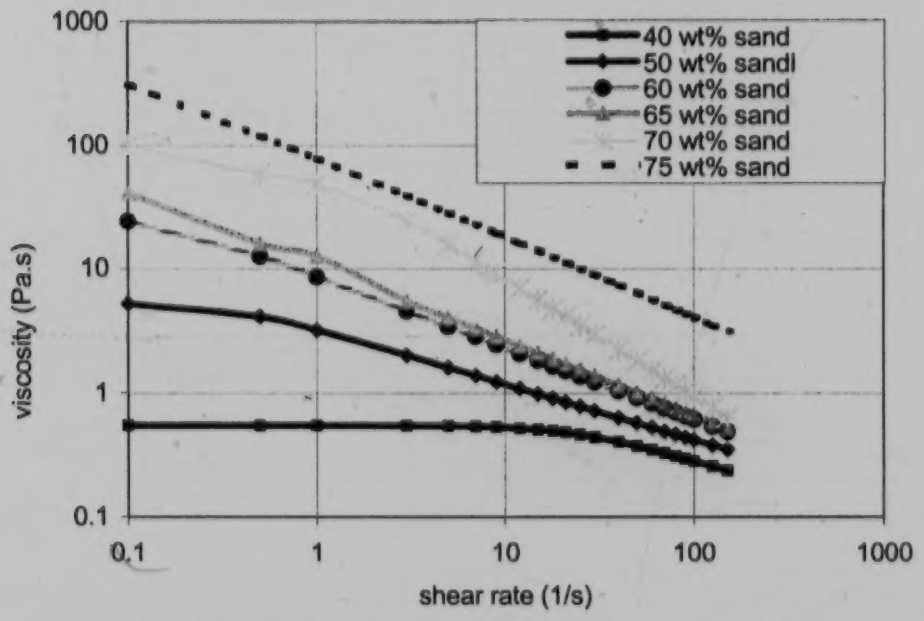

Figure 4.17 Viscosity for different sand concentrations (striated geometry, no delay) sandy polymer gels.

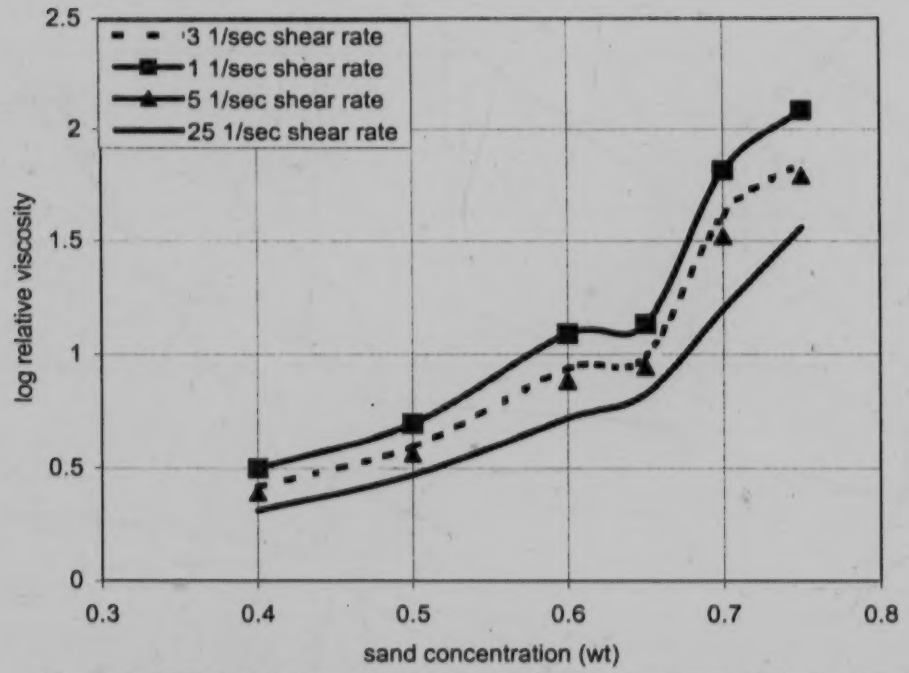

Figure 4.18 Relative viscosity versus sand concentration (striated geometry, 1.5 hour delay, sheared sample).

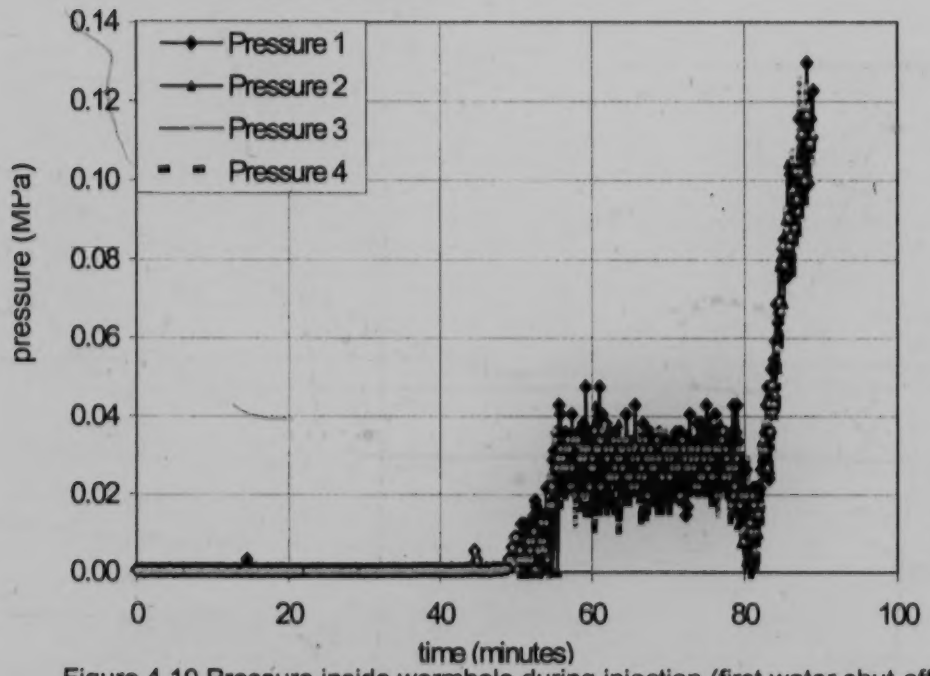

Figure 4.19 Pressure inside wormhole during injection (first water shut-off experiment (first part)). See Figure 3.3 for pressure port locations.

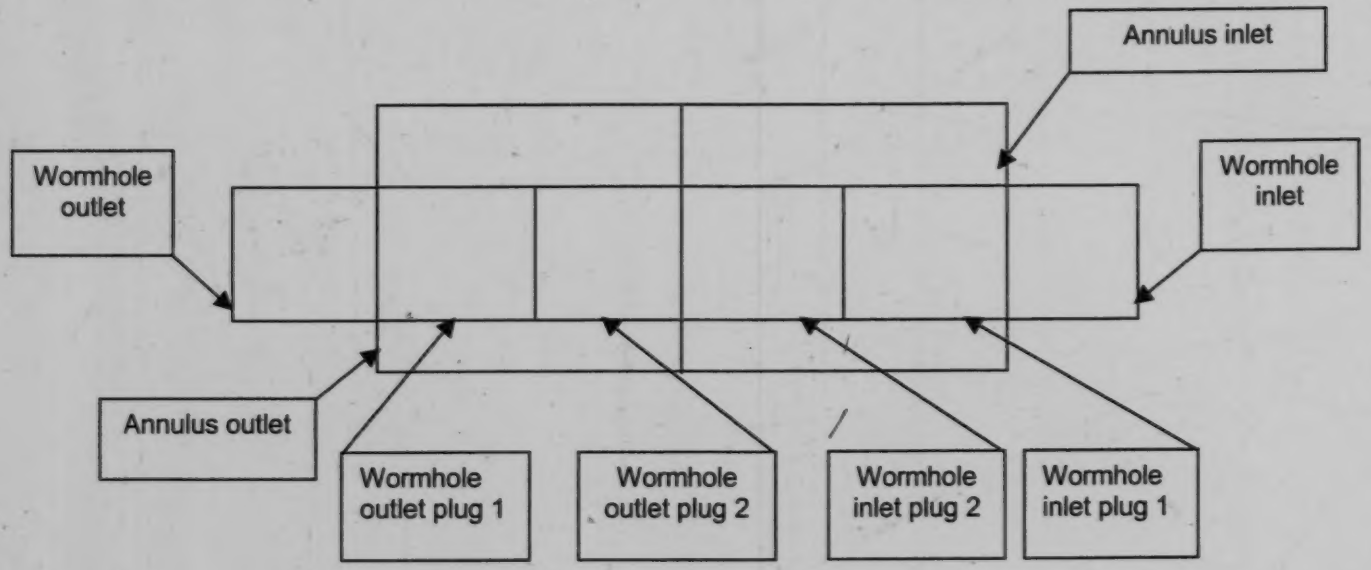

Figure 4.20 Schematic diagram of the wormhole gel plug excavation (first water shut-off experiment (second part)).

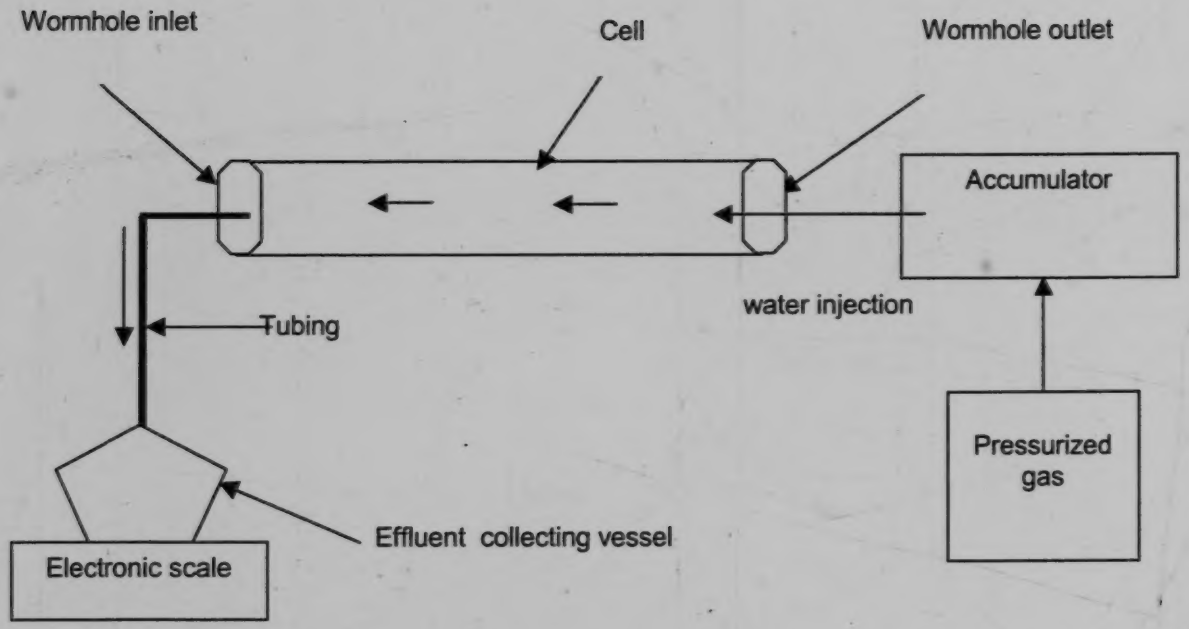

Figure 4.21 Water breakthrough test.

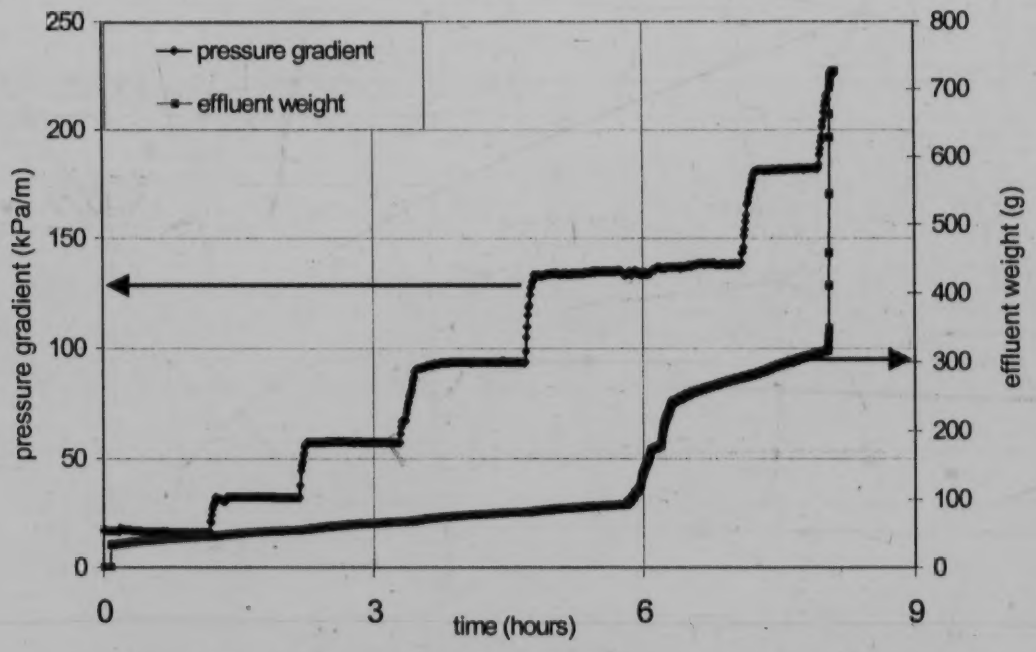

Figure 4.22 Water breakthrough test (second part of the first water shut-off experiment).

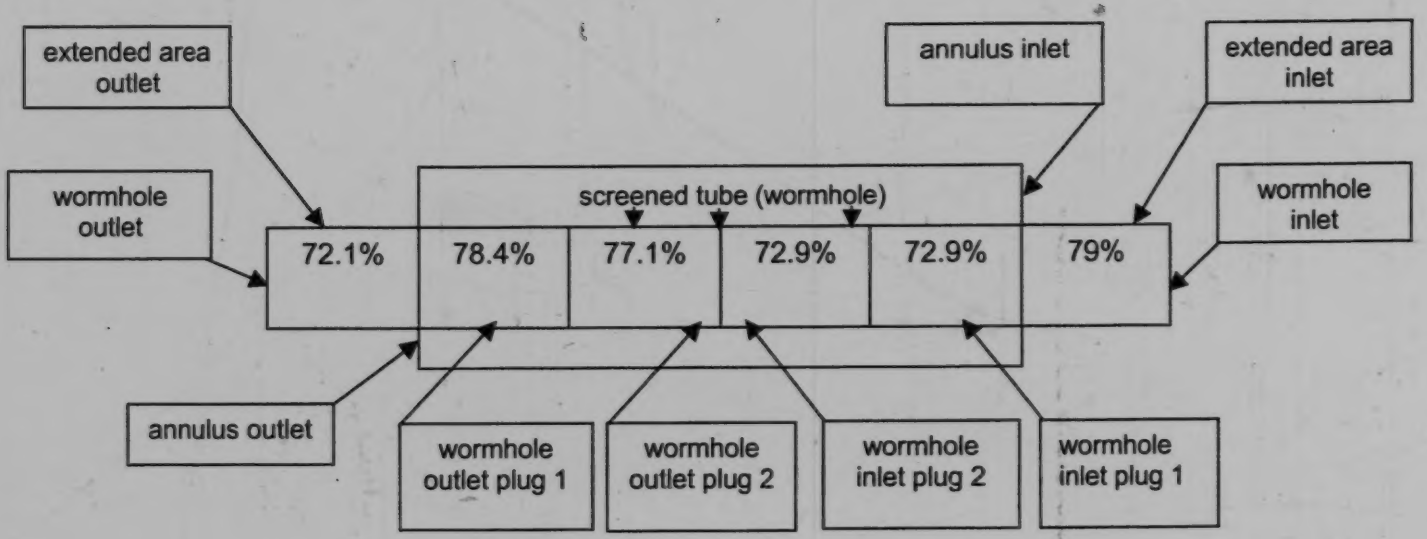

Figure 4.23 Wormhole gel plug excavation and sand concentration (wt%) (first water shut-off experiment (second part)).

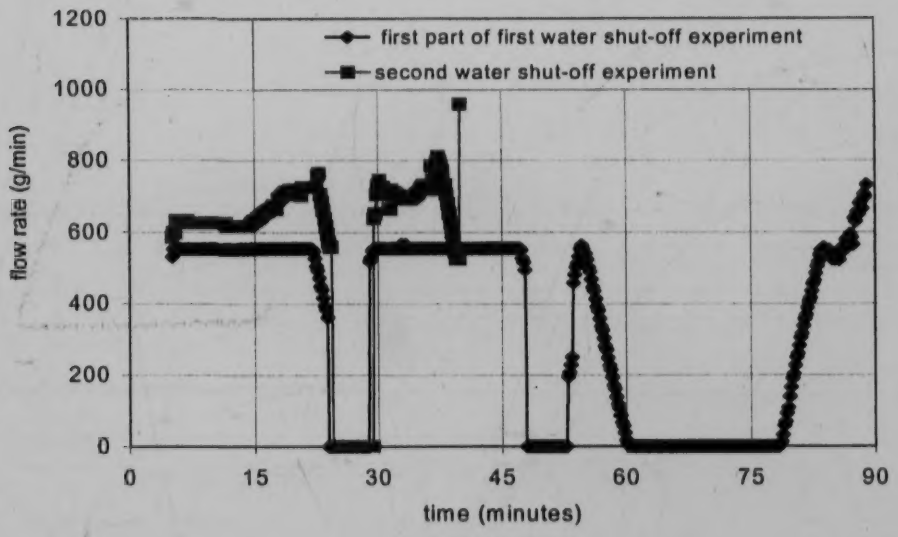

Figure 4.24 Slurry injection rate (water shut-off experiments).

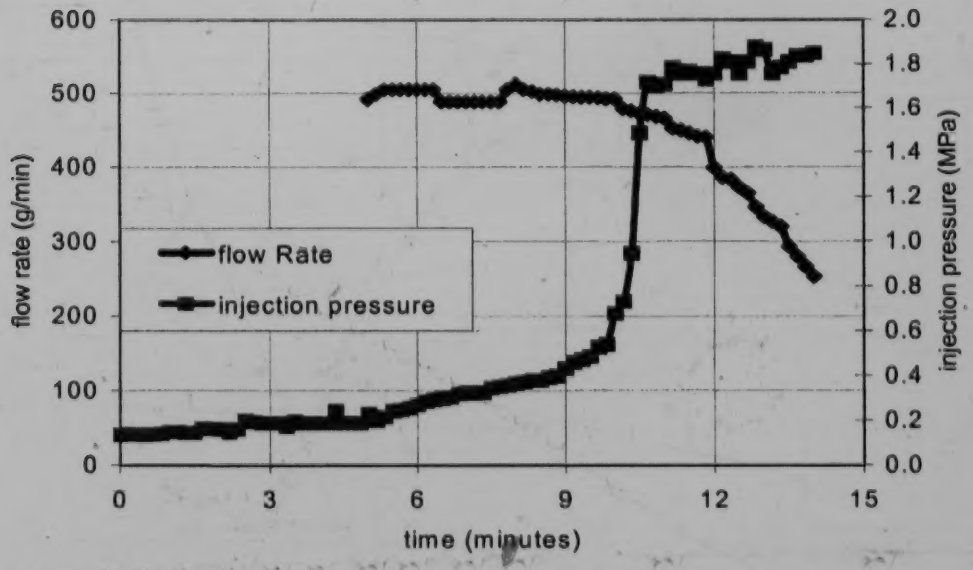

Figure 4.25 Flow rate and pump pressure during slurry squeezing (second water shut-off experiment).

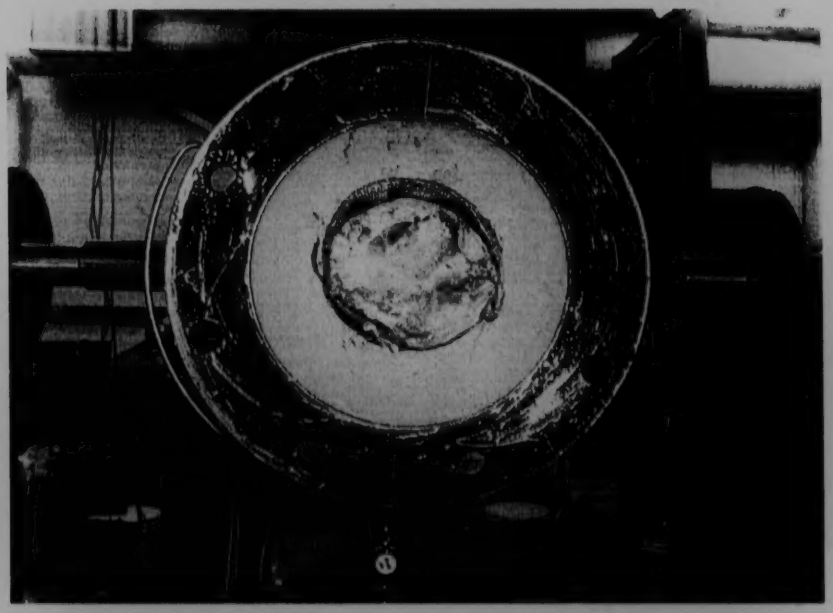

Figure 4.26 Sand pack before excavation.

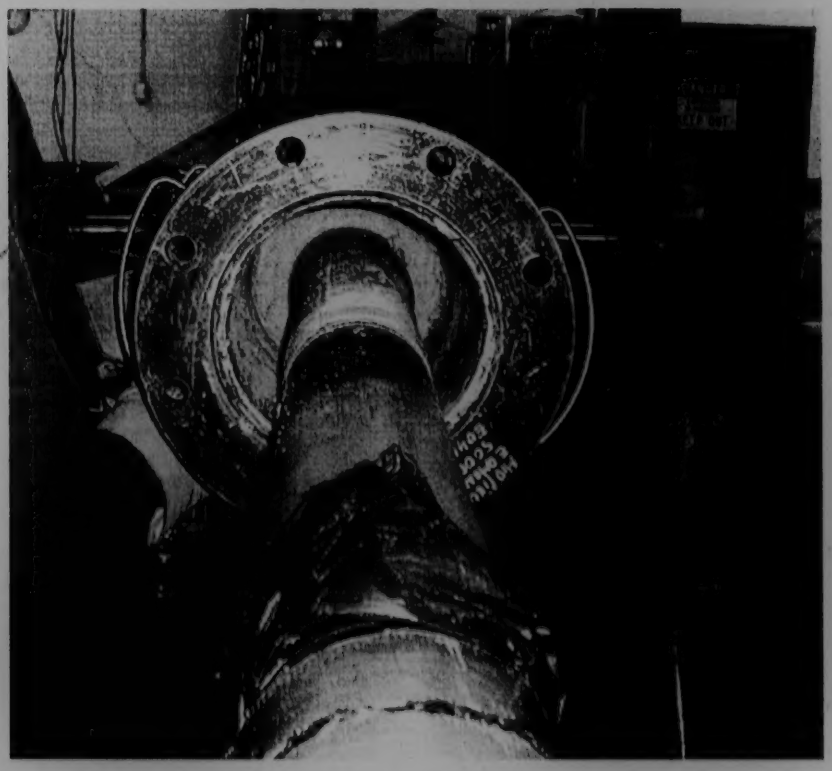

Figure 4.27 Cell in horizontal position during excavation.

Figure 4.28 Layered screen removal for wormhole inspection.

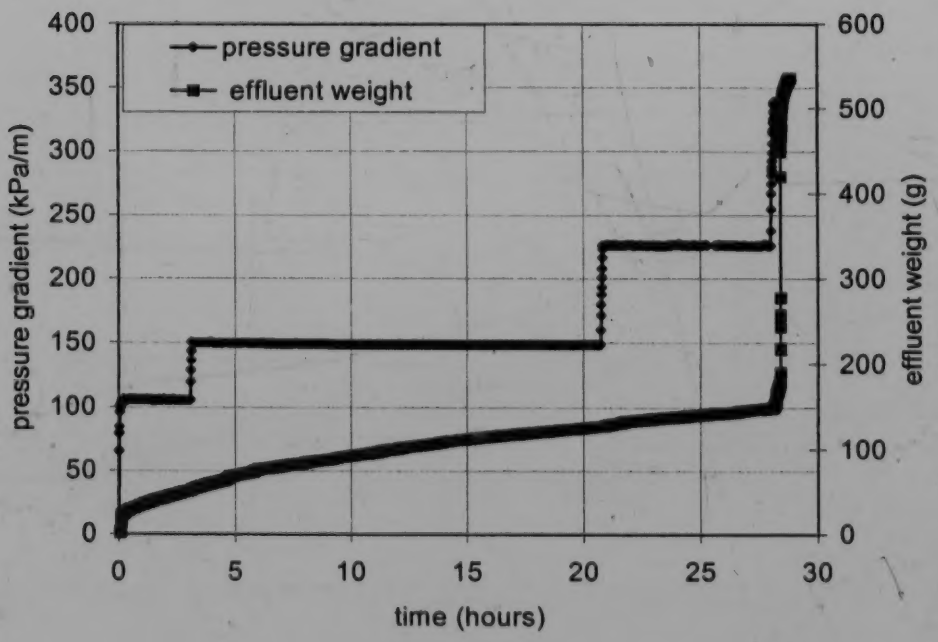

Figure 4.29 Water breakthrough test (second water shut-off experiment).

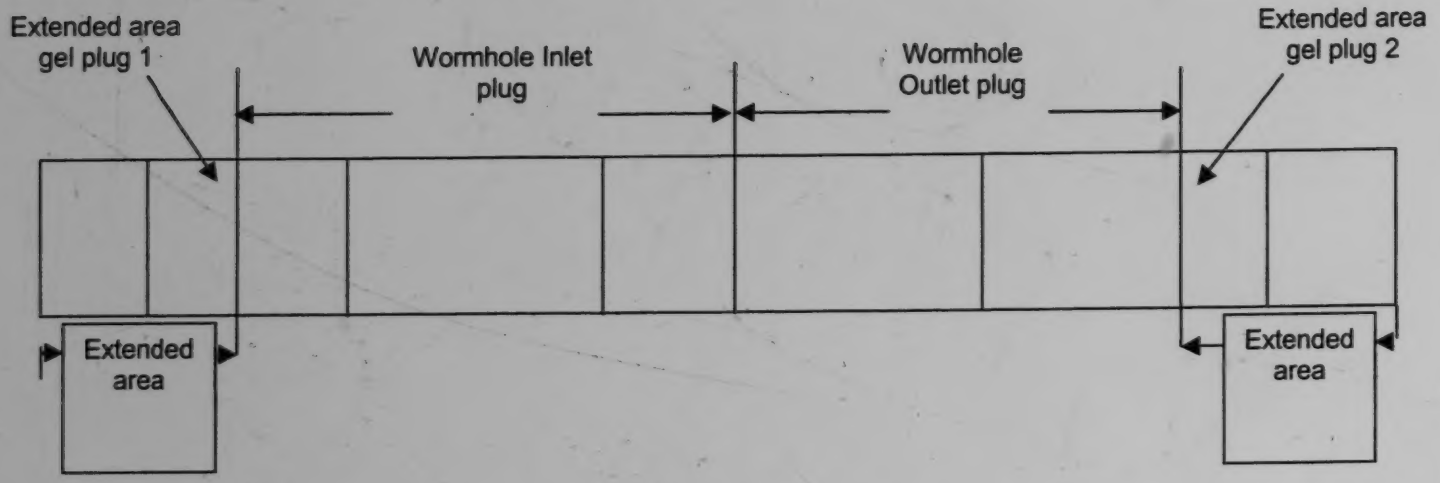

Figure 4.30 Wormhole gel plug excavation (second water shut-off test).

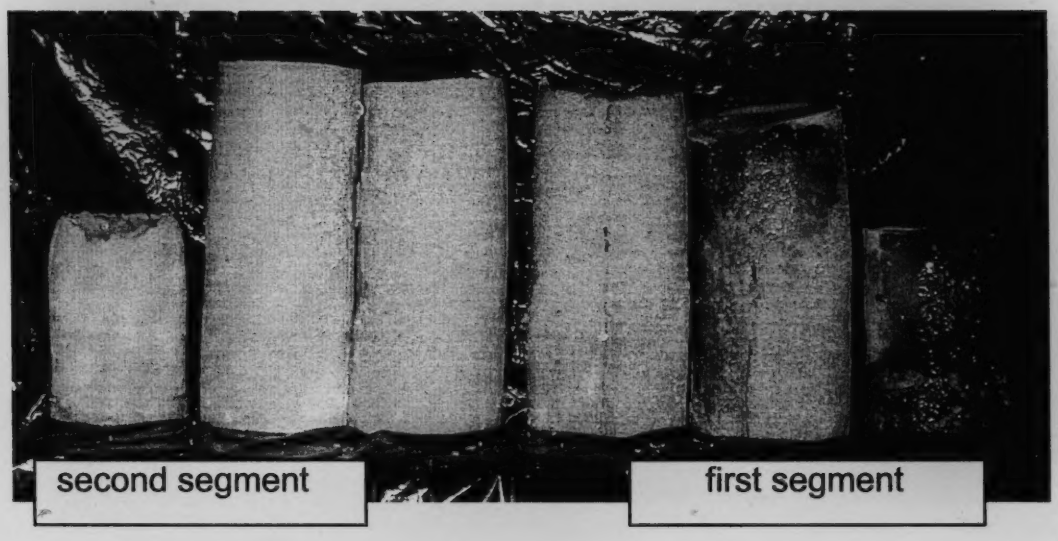

Figure 4.31 Slumping of the sandy gel plug.

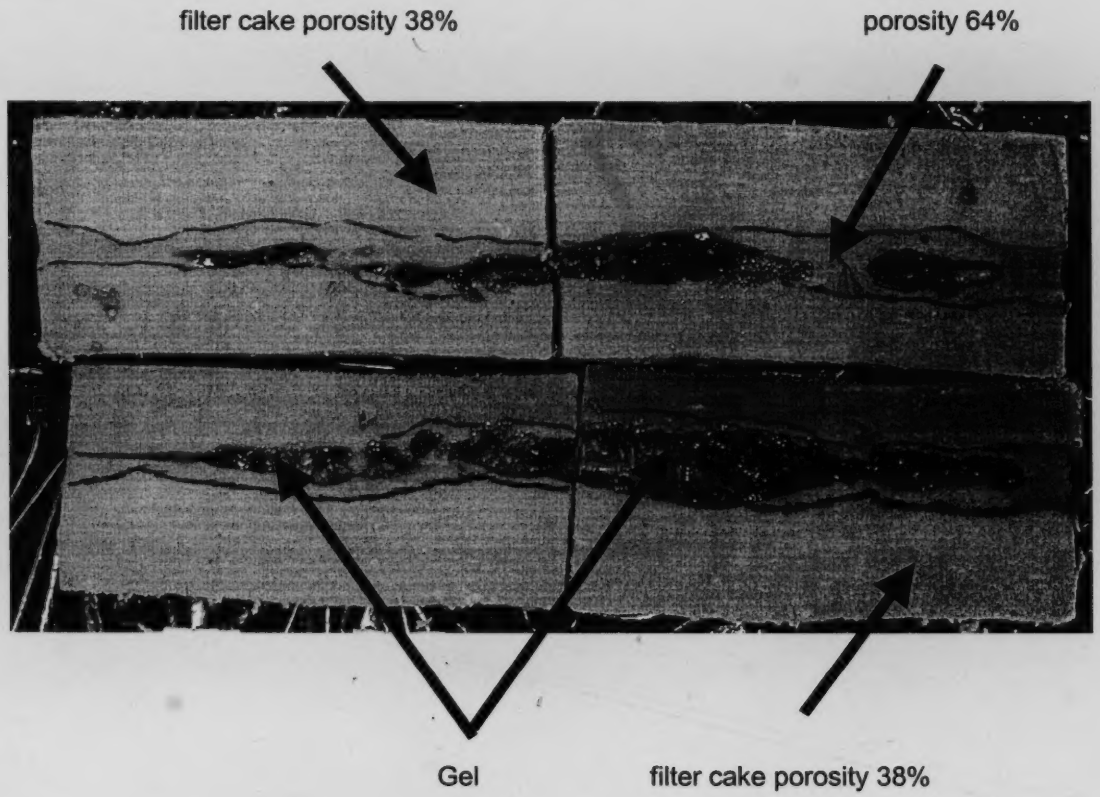

Figure 4.32 Sandy polymer gel plug sectioned longitudinally (second water shut-off experiment).

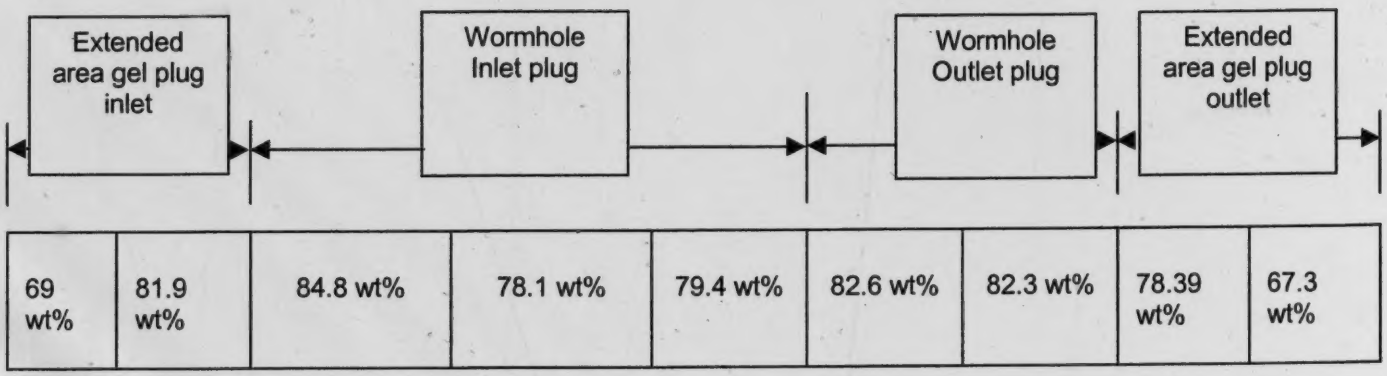

Figure 4.33 Wormhole gel plug excavation and sand concentration (wt%) (second water shut-off experiment).

CHAPTER 5

Discussion

The water shut-off experiments showed that a 10-cm diameter by 1.2 m screened pipe simulating a wormhole could be plugged to resist a field scale pressure gradient. The material strength measurements in addition to the viscosity, settling and gel degradation tests were used to simulate numerically the placement of the gel in the field and as a guide to planning field treatments. These calculations suggest that open channels (wormholes) could be blocked in the field.

5.1 Rheology, Settling and Degradation Tests

The viscosity measurements of the 60 wt% sandy polymer gel under different geometries, gelation time and shear history showed significant shear thinning. The viscosity of the 12,000 ppm polyacrylamide gel is high at low shear rates, reducing the settling rate of the sand. Shear thinning implies that the gel can be injected more easily. The gel did not show any significant thixotropy (viscosity reduction with time) effect (Figure 5.1) as observed when the gel was sheared through several sweeps.

The visual gel strength screening test showed that the 12,000 ppm gel was more elastic than the 10,000 ppm gel used in the first water shut-off experiment. This observation was made by flipping the test tubes. The elasticity of the 12,000 ppm gel within the sandy polymer gel would allow it to stretch before any irreversible deformation or cracks occurred. This may explain in part why water breakthrough occurred at a higher pressure drop in the second water shut-off experiment.

The settling test, could be employed to estimate the settling during the injection of the sandy polymer gel into the perforation and in the wormhole after the injection is stopped. The settling tests revealed the existence of a layer of pure gel at the top of the settled sand. This layer was of lower yield stress (approximately 1,200 Pa) compared to the settled sand layer (approximately 3,000 Pa). The high porosity measured in the settled sand layer (44 to 78% in Figures 4.5 and 4.6) compared to the porosity determined in the minimum density test (37 to 42%), may have resulted from the development of a yield stress of the gel which reduced the settling rate. The presence of air bubbles did not likely have a significant effect on the settling of the sand since the concentration of the bubbles within the slurry was low (less than 5% by volume) as seen in Figures 5.2 and 5.3. The final density of the settled sandy polymer gel was lowest for the 40 and 50 wt% sand concentrations for both settling tests (Tables 4.1 and 4.2).

In certain cases, the presence of iron particles in some high molecular weight polymer solutions can severely reduce the viscosity of the crosslinked polymer solution. The reduced viscosity can lead to the failure of polymer flooding treatments [74]. In addition, a critical shear stress level can be reached beyond which permanent shear degradation takes place [51]. In the degradation test, section (3.5.6), samples were circulated up to 120 times through the pump and the tubing for more than 2 hours at pump rates varying from 0.03 m^3/hour to the maximum capacity of 0.1 m^3/hour. In spite of its exposure to iron and high shear rates, the polymer gel was sufficiently viscous to carry the sand into the wormhole. The polymer gel was also able to regain its maximum strength within 7 to 9 days as displayed in Figure 4.8.

This finding is consistent with the earlier work of Yang and Treiber [75] in which the authors found that the addition of iron particles to polymer solution would not affect the gellation and strength of the gel. The polyacrylamide concentrations of

the gel tested by Wassmuth [74] was significantly lower (1,500 ppm) than for the water shut-off experiments (8,000 ppm, 10,000 ppm and 12,000 ppm). In field terms, this result would indicate that the exposure of the sandy polymer gel slurry to iron particles and high shear rates during its injection from the surface facilities, down the tubing to the proper location in the reservoir, would not prevent the sand from being transported at a 60 wt% sand concentration. In addition, the final strength of the sandy polymer gel would be sufficient to block the influx of water as observed in the water breakthrough experiment.

The relative viscosity for a wide range of sand concentrations was measured. For Newtonian (constant viscosity) fluids, the relative viscosity does not depend on the viscosity of the suspending fluid. Therefore, it can be used to estimate the viscosity of slurries prepared with different (Newtonian) fluids. For the sandy polymer gel, the relative viscosity was dependent on the shear rate since the gel itself was shear–thinning. By continuing the measurement of the relative viscosity for sand slurries prepared in polymer gels of different viscosities, it may be possible to obtain a common (universal) relative viscosity curve.

5.2 First Water Shut-off Experiment

In the first part of the first water shut-off experiment, the pressure drop across the simulated wormhole was very low during the entire injection process as shown in Figure 4.19 (Appendix L). The injection rate varied between 0.025 m^3/hour and 0.05 m^3/hour. The pressure gradient showed insensitivity to injection rate variation during the injection process. The pressure gradient was about 128 Pa/m at a flow rate of 0.05 m^3/hour. The lack of sensitivity of the injection rate on the pressure gradient is most likely due to the insufficient accuracy of the pressure transducers (± 7 kPa) to measure the change in pressure within the wormhole at the shear rates used in the experiment.

During the squeezing process, the pressure behavior inside the simulated wormhole exhibited gradual pressure build-up until it exceeded the pump shut-off pressure of 1.5 MPa as shown in Appendix L. The pressure build-up was most likely due to a dynamic compaction of the sandy polymer gel plug inside the wormhole (Appendix L). The squeezing process resulted in the leak-off of approximately 4.3 liters of polymer gel into the annulus.

The sandy polymer gel plug failed immediately after the start of the water breakthrough test at a pressure gradient of 16 kPa/m. The early failure of the plug may have been due to

- a lower strength of sandy polymer gel plug caused by a short shut-in period.
- water bypassing the sandy polymer gel plug due to the low strength of the gel in the annulus.
- fingering through the weakly gelled sandy polymer gel plug.

A stronger crosslinked polymer was prepared by increasing the polyacrylamide concentration to 12,000 ppm. The polymer was re-injected into the annulus. A three day shut-in period was allowed to improve the gelation inside the cell.

In the second part of the first experiment, the sandy polymer gel plug failed at a pressure gradient of 216 kPa/m. The initial effluent taken from the annulus during flooding with the enhanced crosslinked polymer solution reaffirmed that a weaker gel was formed in the first part of the first experiment within the annulus. Upon dismantling the cell, significant slumping of the sandy polymer gel plug (Table 4.9), as well as sand settling, were observed. This could be related to the inability of the weak gel to sustain the suspension of sand particles in the polymer gel. A relatively thick filter cake around the sandy polymer gel plug was observed. An average sand concentration of over 70 wt% was achieved along the sandy polymer gel plug. Figure 4.23 is a schematic diagram of sand concentration

(wt%) along the sections of the sandy polymer gel plug for the second part of the first water shut-off experiment. The yield stress of the sandy polymer gel plug at the wall of the screened pipe was calculated to be approximately 0.4 and 5 kPa for the first and second parts of the first water shut-off experiment respectively. Results of the first part of the first water shut-off experiment indicated that, in order to reduce the slumping and the settling of the sand particles, the gel had to be strengthened. This could be done through increasing either the polymer or crosslinker concentrations or both. Higher concentrations favored good gelation.

Most of the samples were pre-sheared for 10 seconds in a laboratory blender and compared to unsheared samples to evaluate the shear history dependence of the slurries.

5.3 Second Water Shut-off Experiment

The pressure behavior inside the simulated wormhole during the squeezing process maintained the same trend as observed in the first water shut-off test. The rising pressure inside the wormhole was an indication of a dynamic compaction of the sandy polymer gel plug inside the simulated wormhole (Appendix M). The squeezing process resulted in approximately 6 liters of polymer gel leaking-off into the annulus sand formation as compared to 4.3 liters leaked-off in the first water shut-off experiment. In the first experiment, the sandy polymer slurry was injected at 0.025 to 0.05 m^3/hour whereas in the second experiment it was injected at 0.05 to 0.1 m^3/hour. It was believed that the higher injection rate during the squeezing process of the second water shut-off experiment had contributed to the higher volume leaked-off. Polyacrylamide gel is not completely impermeable to water. An average permeability to water of approximately 2 milliDarcy was calculated for the plug before it yielded.

The plug yielded 30 hours after the start of the water breakthrough test at a pressure gradient varying between 225 kPa/m and 340 kPa/m as shown in Figure 4.29. This pressure gradient was calculated as the pressure drop across the sand pack divided by its length. A nearly uniform average sand concentration of more than 80% along the sandy polymer gel plug was achieved. Figure 4.33 is a schematic diagram of sand concentration (wt%) along the sections of the plug. A thicker filter cake was observed (Figure 4.32) surrounding the plug than in the first water shut-off experiment. The shear strength of the sand polymer gel plug at the wall of the screened pipe in the second water shut-off experiment was calculated to vary between 6 and 9 kPa, whereas it was approximately 5 kPa in the second part of the first water shut-off experiment. The greater leak-off in the second experiment may have been due to the ability of the more viscous gel to transport the sand without bridging at the inlet. The higher polymer concentration with the proper crosslinker concentration in the second experiment resulted in a gel with higher yield stress and consequently a stronger sandy polymer gel plug. Wiwchar et al. [76] observed that stronger gel was formed when leak-off was allowed in their experiment rather than without leak-off (Figure 5.4).

Under field conditions, leak-off of the polymer gel into the formation creates a strong bond between the sandy polymer gel plug and the formation leading to a stronger and more stable plug along the wormhole. In addition, the leaked-off polymer gel creates a barrier to water migration along the wormhole/formation interface.

In the second water shut-off experiment, the physical inspection of the sandy polymer gel plug showed that a small sand-free layer of pure gel was formed (Figure 4.32). The presence of this layer could be attributed to the sand settling along the wormhole axis as was observed in the settling tests. The pure gel layer might have also been formed due to the caking that occurred at the screened pipe (wormhole) inlet. This caking could have led to a deep squeezing of the

sandy gel at the wormhole inlet into the wormhole resulting into the creation of pure gel layer by further caking of the sand. This deep squeeze of the gel could also explain why the pure gel channel at the center of the plug was discontinuous.

The sandy polymer system developed in these experiments would not be sensitive to the water salinity of the formation since the gel was prepared in a brine solution. In spite of the lower injection rates in the water shut-off experiments (0.01 m^3/hour to 0.1 m^3/hour) compared to field rates (0.5 m^3/hour or more) the sand was uniformly caked onto the walls of the screened tube (2.54 cm I.D) without settling in the rubber hose connected the pump to the cell. In the water shut-off experiments, the sandy polymer gel could flow at the outlet of the screened tubing through narrow tubing without bridging and there was no evident injectivity loss.

Wiwchar et al. [76] showed that the addition of either produced sand (Husky sand contained 2 wt% residual oil and water) or cleaned sand (sand with no residual oil and water) would yield the same sandy polymer gel strength. Therefore, the sandy polymer gel system could make use of the produced sand as the mixing solid phase. This could result in cost reductions in the supply and transportation of the sand.

5.4 Application of Results: Field Treatment

The following section describes how the data and knowledge obtained in this thesis are being applied to design water shut-off treatments for cold production wells. The main concerns in designing a water shut-off treatment are:

1. the strength of the sandy polymer gel
2. the injectivity of the slurry

3. the placement of the gel
4. the cost of the treatment

These concerns were taken into account in selecting a sand concentration of 60 wt% and a polyacrylamide concentration of 12,000 ppm.

The placement of the sandy polymer gel was simulated using an approach described by Tremblay et al. [11] for three sand concentrations: 20 wt%, 40 wt% and 60 wt%. The power law coefficients and indices used to match the viscosity measurements (Appendix H and I) for the three sand concentrations, are listed in Table 5.1.

The gel treatment was modeled by assuming that the watered-out wormhole was a porous pipe 10 cm in diameter by 200 m long. The parameters used in the simulation are given in Table 5.1. For all three sand concentrations, the simulations were run until the wormhole caked completely at the inlet. The times required for the caking at the inlet (injection time) are listed in Table 5.2. In order to calculate the settling of the sand within the caked channel, the final settling height in percentage (Table 4.1) was used. When the sand in the sandy polymer gel within the caked channel settles, it leaves a top layer of pure gel (Figure 5.5). Although the filter cake was thicker (smallest radius of caked channel) for the lowest sand concentration, this lower concentration also led to the most settling as shown in Table 5.2.

Different yielding scenarios (1 to 3) were investigated. In the first scenario, the entire sandy polymer gel plug yields at the surface of the channel wall (location 1 in Figure 5.5).

In the second scenario, the pure gel plug yields at the surface locations 2. In the third scenario, the sandy polymer gel yields at the surface locations 3. The wormhole was assumed to be connected to an aquifer at a pressure of 4 MPa. The average shear stress on the surface locations 1, 2 and 3 was calculated using the following equation:

$$\tau = (\Delta P / L) \times (t / 2)$$

where: ΔP = 4 MPa

L = 200 m

t = open channel radius (scenario 1)

= height of pure gel (scenario 2)

= caked channel inner radius (scenario 3)

The shear stress for the different scenarios is given in Table 5.2. The yield stress of the pure gel was greater than 1,280 Pa as measured in the RT 20 shear rheometer. Higher shear stresses could not be reached with this rheometer. The yield stress of sandy polymer gel within the caked channel was measured by Wiwchar et al. [76] to be approximately 3,000 Pa (Figure 5.4). The yield stress of the caked sandy polymer plug at the surface of the original open channel was calculated in section 4.4 to be in the range of 6,000 to 9,000 Pa. In all three scenarios, the shear stress was lower than the yield stress measured in the second water shut-off experiment.

When the sand caked the inlet to the wormhole in the two water shut-off experiments, the progressive cavity pump (PCP) shut-off pressure was 1.5 MPa. The PCP in the field can go to higher pressures. More leak-off of the polymer gel around the well could be expected under field conditions if the sand cakes completely at the inlet of all the wormholes. In this case, leak-off of the polymer gel into the formation could have negative impact on the rock matrix permeability leading to a poor sweep efficiency and a lower productivity in water flooding and fractured reservoirs respectively.

Numerical calculations indicate that the watered-out wormhole will be the first wormhole to cake at the inlet first. If the injection is continued further the oil-filled wormhole will continue being filled until they also cake at the inlet. Before caking,

the pressure difference between the well and the formation is not large. If only the volume of slurry required to fill the watered-out wormhole is injected, then the pressure buildup should not occur within the well. The vertical wells may need to be reperforated to access the reservoir

The filter cake observations in both water shut-off experiments were in agreement with the numerical simulation by Tremblay et al. [11] of the build up of a sand filter cake within an open channel. The injection well was connected by an open channel to either a shut-in well or another injection well. Tremblay et al. found that a sand filter cake was formed in both cases. In the second case, the sandy filter cake was thicker. The volume of the gel that leaked-off in the second case was higher than in the first case (Figure 5.6).

Table 5.1 Parameters used in simulations

Permeability of the formation (Darcy)	15
Permeability of the filter cake (Darcy)	15
Injection flow rate (m^3/hour)	1
Initial open channel diameter (cm)	10
Outer radius of no-flow boundary (cm)	200
Length of the wormhole (m)	200
Gas saturation (%)	10
Oil viscosity (cP)	5,000
Power law coefficient (pure gel) (Pa)	0.672
Power law coefficient (20 wt% sand) (Pa)	0.8209
Power law coefficient (40 wt% sand) (Pa)	2.0102
Power law coefficient (60 wt% sand) (Pa)	8.835
Power law index (pure gel)	0.750
Power law index (20 wt% sand)	0.695
Power law index (40 wt% sand)	0.5659
Power law index (60 wt% sand)	0.4512

Table 5.2 Gel placement simulations

Sand (wt%)	Average diameter of caked channel d_{cake} (cm)	Sand-free layer height h_{gel} (cm)	Volume of gel injected (m^3)	Caking time (hours)	Shear stress at interface scenario 1 (Pa)	Shear stress at interface scenario 2 (Pa)	Shear stress at interface scenario 3 (Pa)	Average gel/oil interface radius (cm)
20	3.8	3.0	3.6	4	1,000	300	390	11.0
40	7.0	2.7	1.2	1.5	1,000	270	680	9.03
60	9.2	0.3	0.5	0.75	1,000	30	920	5.4

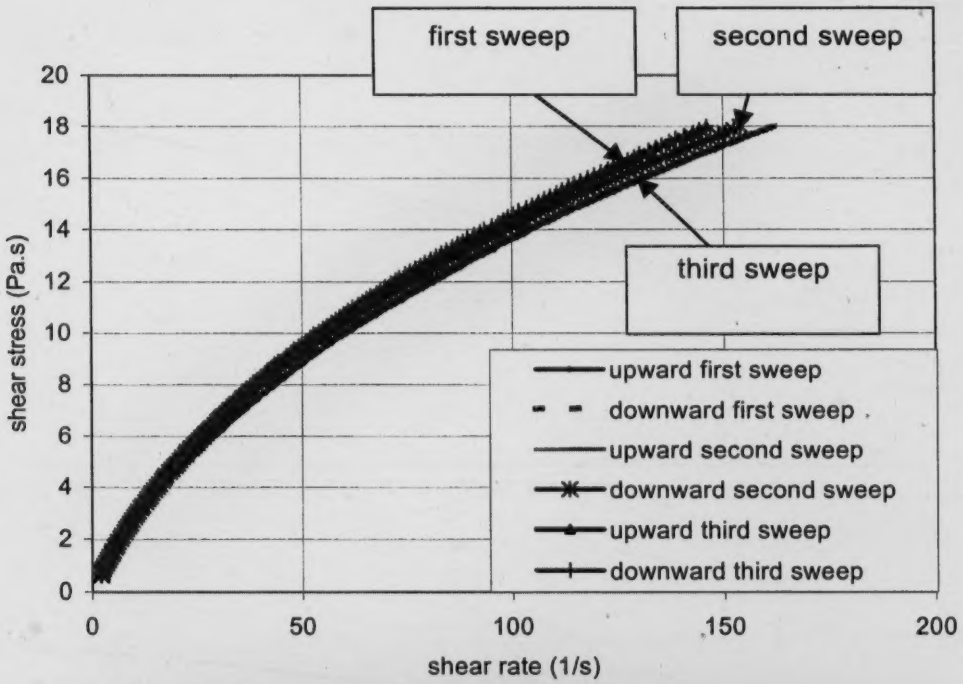

Figure 5.1 Thixotropy test (60 wt% sandy polymer gel).

Figure 5.2 Presence of air bubbles in high concentration sandy polymer gels. Numbers indicate sand concentrations (wt%).

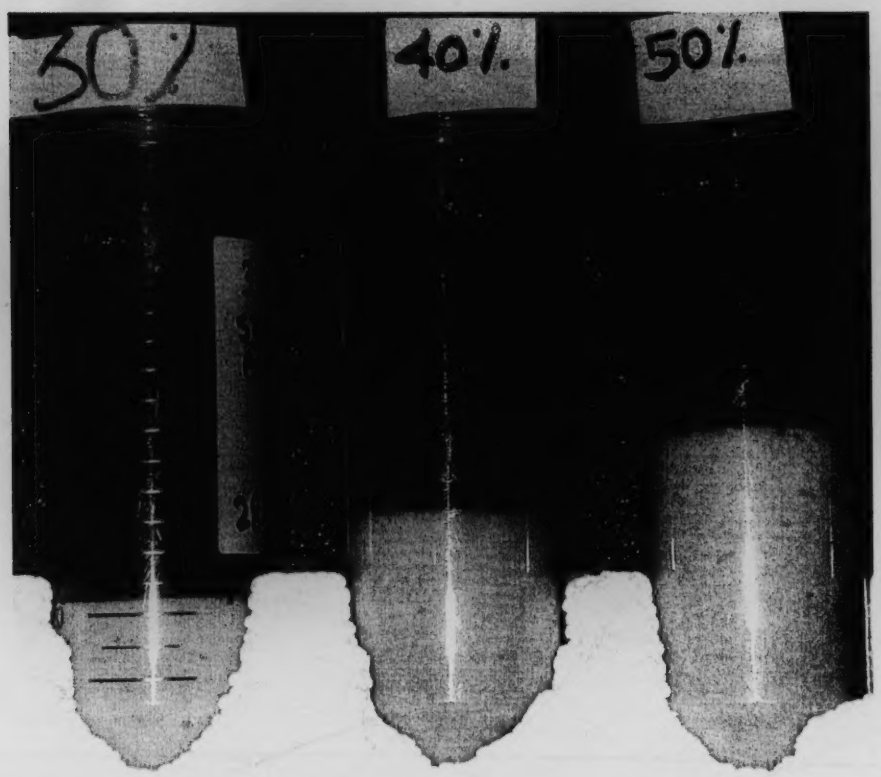

Figure 5.3 Presence of air bubbles in low concentration sandy polymer gels. Numbers indicate sand concentrations (wt%).

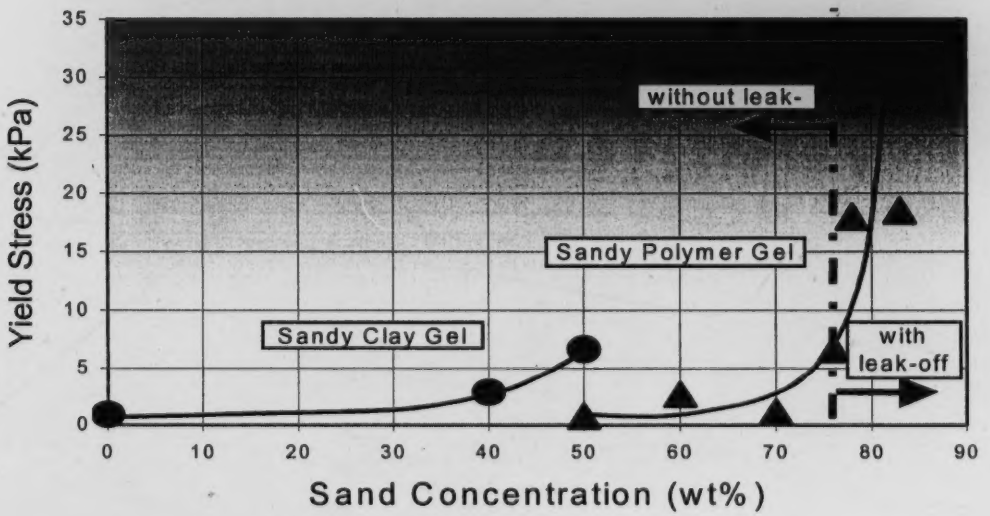

Figure 5.4 Effect of leak-off on yield stress.
Courtesy Wiwchar et al. [76].

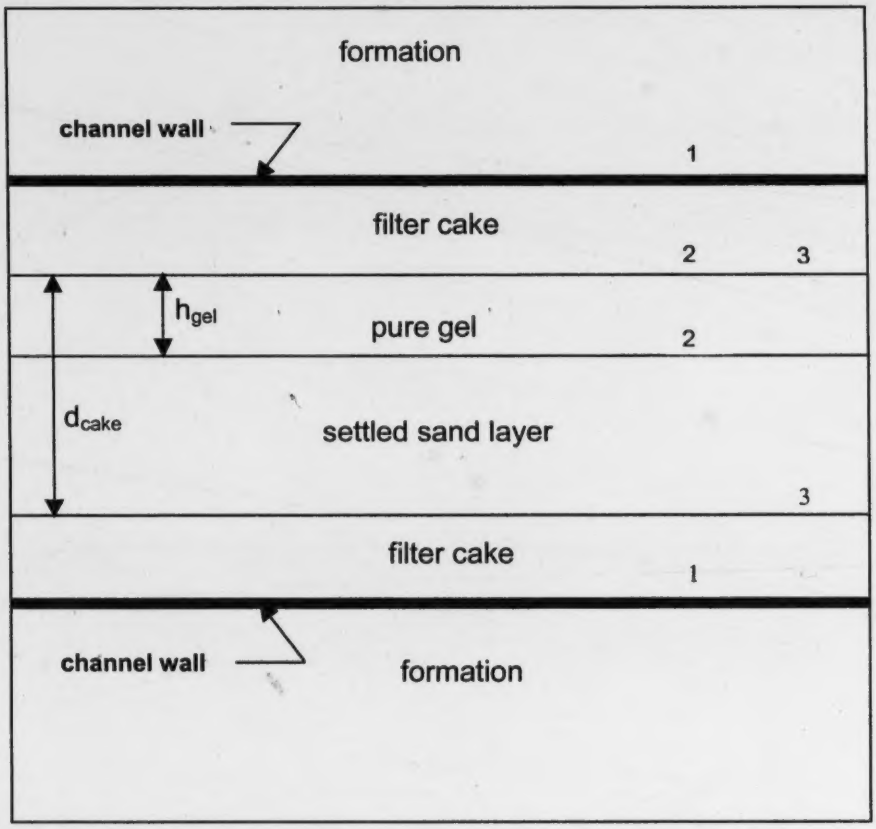

Figure 5.5 Sandy gel plug yielding, scenarios 1 to 3.

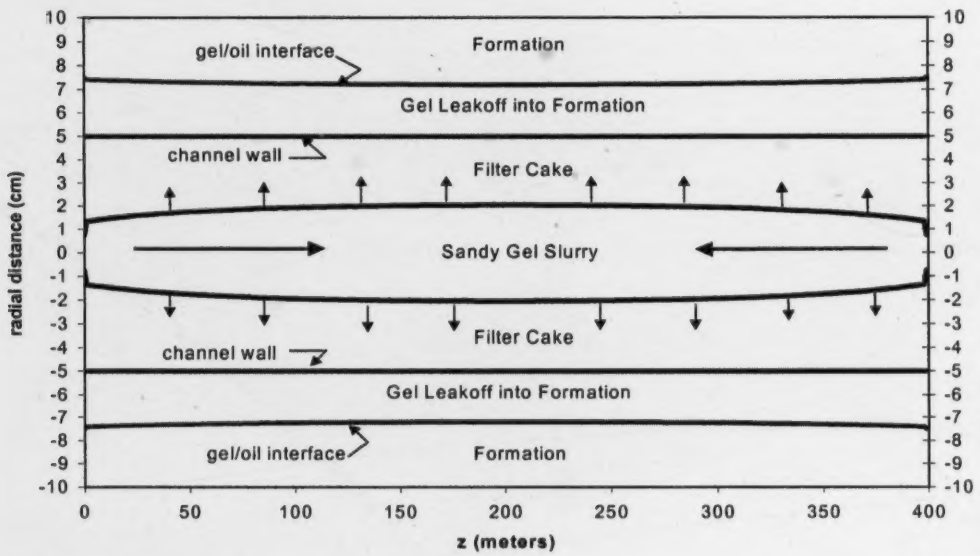

Figure 5.6 Filter cake formation within channel wall
Courtesy Tremblay et al. [11].

CHAPTER 6

Conclusions and Recommendations

6.1 Conclusion

As a result of the experimental work conducted, the following conclusions can be drawn:

1. The addition of sand to the crosslinked polymer solution increased the ultimate strength of the sandy polymer gel significantly with adequate gelation time.
2. The final strength of the sandy polymer gel used in these experiments was not affected by shear degradation and exposure to iron particles.
3. The viscosity measurements showed that the formulations were strongly shear thinning materials, with no significant wall slippage observed.
4. The relative viscosity calculations revealed that the relative viscosity for sandy polymer slurries at constant shear rate increased with increasing sand concentrations. Also, at the same sand concentration, the relative viscosity decreased with increasing shear rates.
5. It was observed that the higher the polymer concentration the stronger the gel plug.
6. The leak-off of polymer gel into the annulus formation likely contributed to strong bonding between the gel plug in the wormhole and the annulus formation, with high sand compaction inside the wormhole.
7. In water shut-off tests using sand-reinforced polyacrylamide (Hi Vis 350) gel systems, adequate gelation time (6 days or more) determined from the gel strength screen test would be required.
8. A thick filter cake was formed around the sandy polymer gel plug in both experiments.
9. A strong sandy polymer gel plug with sand content of more than 80%, capable of resisting a pressure gradient varying from approximately 225 to

340 kPa/m, was formed inside the wormhole. On a field perspective, the plug could block an aquifer pressure of 4MPa over a length of 20m.

6.2 Recommendation

Based on the experimental work and the results obtained, the following recommendations are suggested for future work in this area

1. Study the effect and influence of the sand grain diameter and size distribution on the injectivity, settling and compaction of the sand.
2. Perform water shut-off experiments at lower (40 wt%, 50 wt%) sand concentrations and using different types of polymer gel.
3. Use field sand in packing the formation annulus to investigate its influence on the leak-off, compaction and strength of the sandy polymer gel.
4. Study the effect of the screen on the bonding of the polymer gel across the wormhole into the annulus formation.
5. Perform a field trial of the sandy polymer gel system.
6. Develop a field model for wormhole growth. Such a model would provide significant technical assistance in designing a sandy polymer gel system.

REFERENCE

1. Tremblay, B., Sedgwick, G. and Vu, D, "A Review of Cold Production in Heavy Oil Reservoirs", Paper presented at the 10th European Symposium on Improved Oil Recovery, Brighton, UK, 18-20 August 1999.
2. Dusseault, M. B., Ormis, A. S. and El-sayed, S., "Heavy –Oil Production Enhancement by Encouraging Sand Production ", Paper SPE 59276, presented at Tulsa, Oklahoma, 3-5 April 2000.
3. Alberta Energy and Utility Board: Alberta Field/pool Production and Injection Monthly, EUB ST Series, 96-16A, 1996.
4. Sydansk, R. D., and Southwell, G.P., "More Than 12 Years, Experience With a Successful Conformance- Control Polymer- Gel Technology", Paper SPE 66558, presented at the 1998 SPE Annual Technical conference and exhibition held in New Orleans, 27-30 September 1998.
5. Fullevlove, R. J., Morgan, J.C., Stevens, D. G. and Thrasher, D. R., "Water Shut-Off in Oil Production Wells-Lesson from 12 Treatments", Paper SPE 36211, presented at the 7th Abu Dhabi international petroleum and conference, held in Abu Dhabi, UAE 13-16 October 1996.
6. Boreng, R. and Svenendsen, O. B., "A Successful Water Shut-Off. Case Study from the Stratford Field", Paper SPE 37466, presented at the 1997 SPE Production operation symposium held in Oklahoma U.S.A, 9-11 March 1997.
7. Zhou et al. "Process for Reducing Permeability in a Subterranean Formation", Pat. No. 6,143,699 issued November 7, 2000.
8. AEUB "Alberta field/pool production and injection monthly", Alberta Energy and Utility Board, Statistical Series, 97-16A, 1997.
9. Zhou, Z. J., " Clay Gel for Water Shut-off in Heavy Oil Production", presented at the 1998 CIM Heavy Oil Technical Symposium, Lloydminister, Alberta, Canada. September 16 – 17, 1998.

10. Squires, A., "Inter Well Tracer Results and Gel Blocking Program", Paper presented at the 10th annual Heavy Oil and Oil Sands Technical Symposium, Calgary, Alberta, March 9, 1993.
11. Tremblay, B., Wiwchar, B., Huang, H., Bani, E., Cameron, S. and Polikar, M., "Development and Testing of a Sandy Polyacrylamide Gel for Water Shut-off of Large Channels". Alberta Research Council Inc., AACI Report 0102-2, January 2002.
12. Tremblay, B., Sedgwick, G. and Vu, D., "C T Imaging of Sand Production in a Horizontal Sand Pack Using Live Oil", Paper presented at the 49th Annual Technical Meeting of The Petroleum Society in Calgary, Alberta, Canada at June 8- 10 –1998.
13. Wang, Y. and Chen, C. C., "Improved Production and Sand (Cold) Production in Conventional and Heavy Oil Reservoir-A Field Case and Simulation", Paper SPE 57290, presented at the 1999 SPE Asia Pacific Improved Oil Recovery Conference held in Kuala Lumpur, Malaysia, October 25-26, 1999.
14. Tremblay, B., Sedgwick, G. and Vu, D., "CT Imaging of Wormholes Growth under Solution-Gas Drive", SPE Reservoir Eval. & Eng., Vol. 2, No. 1, February 1999.
15. Denbina, E. S., Baker, R. O., Gegunde, G. G., Klesken, A. J. and Sodero, S. F., "Modeling Cold Production for Heavy Oil Reservoirs", Paper presented at the 49thAnnual Technical Meeting of the petroleum Society in Calgary, Alberta, Canada, June 8 –10 1998.
16. Wang, Y. and Yuan, J. Y., "Cold Production and Wormholes Propagation in Poorly Consolidated Reservoirs", 7th UNITAR International Conference on Heavy Crude and Tar Sands, Beijing, China, October 1998.
17. Ehlig-Economides, C. A., Fernandez, B. G. and Gonora, C. A., "Global Experiences and Practice for Cold Production of Moderate and Heavy Oil", Paper SPE 58773, presented at the 2000 SPE International Symposium on Formation Damage Control held in Lafayette, Louisiana, 23- 24 February 2000.

18. Chalaturnyk, R.J. and Wagg, B. T., "The Mechanisms of Solids Production in Unconsolidated Heavy-Oil Reservoirs", Paper SPE 23780, presented at the SPE Inti. Symposium on Formation Damage Control held in Lafayette, Louisiana, February 26-27 1992.
19. Geilikman, M. B. and Dusseault, M. B., "Fluid Rate Enhancement from Massive Sand Production in Heavy Oil Reservoirs", Journal of Petroleum Science and Engineering Vol. 17, 5-18, 1997.
20. Hu, C., Liu, X., Wang, J., Song, Z., Fan, Z. and Yang, F., "Cold Production of Thin –bedded Heavy Oil Reservoir in Henan Oilfield", Paper SPE 50885, presented at the 1998 SPE International Conference and Exhibition in China held in Beijing, 2-6 November 1998.
21. Wang, Y., " Sand Production and Foamy Oil Flow in Heavy-Oil Reservoirs", Paper presented at the 1997 SPE International Thermal Operations & Heavy Oil Symposium held in Bakersfield, CA., and 10-12 February 1997.
22. Vaziri, H. H., Palmer, I. D., McLennan, J. and Islam, R., " How Can Sand Production Yield a Several Increase in Productivity: Experimental and Field Data", Paper SPE 63235, presented at the 2000 SPE Annual Technical Conference and Exhibition held in Dallas, Texas, 1-4 October 2000.
23. Vaziri, H. H., Phillips, R and Hurley, S., " Physical Modelling of Sand Production", Paper presented at the 36Th Rock Mechanics Symposium (NYROCK '97), New York. June 29- July 2 1997.
24. Dusseault, M. B., Geilikman, M. B. and Spanos, T., "Mechanism of Massive Sand Production in Heavy Oils", Paper presented at the 7th UNITAR conference, Beijing, China, 1998.
25. Dusseault, M. B. and Geilikman, M. B., "Heavy Oil Production from Unconsolidated Sandstones using Sand Production and SAGD", Paper SPE 48890, presented at the 1998 SPE International Conference and Exhibition in China held Beijing, China, 2-6 November 1998.

26. Tremblay, B., Sedgwick, G. and Forshner, K., "Simulation of Cold Production in Heavy Oil Reservoirs: Wormhole Dynamics", Paper SPE 35387, presented at 1996 SPE/DOE Tenth Symposium on Improved Oil Recovery, Tulsa, OK., 21-24 April 1996.
27. Tremblay, B., Sedgwick, G. and Forshner, K., " Modeling of Sand Production from Wells on Primary recovery", JCPT, Vol. 37, No 3, page 41-50, 1998.
28. McCaffrey, W.J. and Bowman, R.D., "Recent Successes in Primary Bitumen Production", Paper presented at the 1991 heavy Oil and Oil Sands Technical Symposium, March 14, 1991.
29. Elkins, L.F., Morton, D. and Blackwell, W. A., "Experimental Firefloods in a very Viscous Oil Unconsolidated Sand Reservoir", Paper presented at the 47th Annual Meeting of the SPE in San Antonio, Texas, Oct. 8 – 11 1992.
30. Yeung, K. C., "Cold Flow Production of Crude Bitumen at the Burnt Lake Project, Northeast Alberta, Canada", Paper presented at the 1995UNITAR Intl. Conference on Heavy Crude and Tar Sands, Houston, 12-17 February 1995.
31. Loughead, D. J. and Saltuklaroglu, M., "Lloydminister heavy oil production why so unusual?", Paper presented at the ninth annual heavy oil and sands technology symposium, Calgary, Alberta, Canada, March 11 1992.
32. Dusseault, M. B. and Geilikman, M. B., "Practical Requirement for sand Production Implementation in Heavy Oil Applications", Paper SPE 30250, presented at the International Heavy Oil Symposium held in Calgary, Alberta, Canada, 19-21 June 1995.
33. Geilikman, M. B., Dusseault, M. B. and Dullien, F. A., "Sand Production as a Viscoplastic Granular Flow", Paper SPE 27343, presented at the International Symposium on Formation Damage Control, Lafayette, Louisiana, 9-10 February 1994.
34. Smith, G. E., "Fluid Flow and Sand Production in Heavy Oil Reservoirs under Solution Gas Drive", SPE Production Engineering, Vol 3, No 2, 169-189, May 1988.

35. Solanki, S. and Metwally, M., "Heavy Oil Reservoir Mechanisms, Lindbergh and Frog Lake Fields, Alberta, Part : Geomechanical Evaluation", Paper SPE 30249, presented at the International Heavy Oil Symposium held in Calgary, Alberta, Canada, 19-21 June 1995.
36. Metwally, M and Solanki, S., "Heavy Oil Reservoir Mechanisms, Lindberg and Frog Lake Fields, Alberta, Part : Field Observations and Reservoir Simulation", Paper 95-63 presented at the 46th Annual Technical Meeting of the Petroleum Society of CIM in Banff, Alberta, Canada, 14-17 May 1995.
37. McCaffrey, W. J. and Bowman, R. D " Recent Successes in Primary Bitumen Production", Paper presented at the Challenges and Innovation 1991 Heavy Oil and Sand Oil Sands Technical Symposium at March 14,1991.
38. Yuan, J., Tremblay, B. and Babchin, A., "A Wormhole Network Model of Cold Production in heavy Oil", Paper SPE 54097, presented at 1999 SPE International Thermal Operations & Heavy Oil Symposium held in Bakersfield, CA., 17-19 March 1999.
39. Tremblay, B., Sedgwick, G. and Forshner, K. "Imaging of Sand Production in Horizontal Pack by X-Ray Computed Tomography", Paper presented at the International Heavy Oil Symposium, Calgary, Alberta, Canada, 19 –21 June 1995.
40. Dusseault, M. B., " Cold Production and Enhanced Oil Recovery", Journal of Canadian Petroleum Technology. Vol. 32, No. 9, November 1993.
41. Huerta, M., Otero, C., Rico, A., Jimenez, I., de Miracle, M. and Rojas, G., "Understanding Foamy Oil Mechanisms for Heavy Oil Reservoirs during Primary Production", Paper SPE 36749, presented at the 1996 SPE Annual Technical Conference and Exhibition held in Denver, Colorado, U.S.A., 6-9 October1996.
42. Maini, B., "Foamy Oil Flow in Heavy Oil Production", JCPT, Vol. 35, No.6, 21 – 24 June 1996.

43. Islam, M.R. and Chakma, A., "Mechanics of Bubble Flow in Heavy Oil Reservoir", Paper SPE 20070, presented at the 60th California Regional Meeting, Ventura, CA, April 1990.
44. Claridge, E.L. and Prats, M., "A proposed Model and Mechanism for Anomalous Foamy Heavy Oil Behaviour", Paper SPE 29243, presented at the International Heavy Oil Symposium, Calgary, Alberta, June 19 – 21, 1995.
45. Maini, B. B., "Foamy-Oil Flow", Page 54-64, JPT SPE 68885, October 2001.
46. Poon, D. and Kisman, K., "Non – Newtonian effects on the Primary production of Heavy Oil", Paper presented at the Petroleum Society of CIM/AOSTRA annual Technical Meeting, Banff, Alberta, 1991.
47. Pooladi-Darvish, M. and Firoozabadi, A., "Solution- Gas Drive in Heavy Oil Reservoirs", JCPT, Vol. 38, No 4, 54 – 61, April 1999.
48. Maini, B.B., Sarma, H.K. and George, A.E., "Significance of Foamy Oil Behaviour in Primary Production of Heavy Oils", JCPT, Vol. 32, No 9, 50 – 54, November 1993.
49. Bora, R., Maini, B. and Chakma, A., "Flow Visualization studies of Solution Gas Drive Process in Heavy Oil Reservoirs Using a Glass Micromodel", Paper SPE 37519, presented at the SPE International Thermal Operations and Heavy Oil Symposium held in Bakersfield, California, USA, 10 – 12 February 1997.
50. Chierici, G. L., "Principles of Petroleum Reservoir Engineering 2", Springer – Verlag, Berlin 1994.
51. Sorbie, K. S., " Polymer Improved Oil Recovery", 1991 Blackie and Son Ltd. Boca Raton, Florida, first edition, 1991
52. Forrest F. Craig Jr. "The Reservoir Aspect of Waterflooding", Monograph Vol. 3. SPE AIME New York 1971.
53. Wiwchar, B., Cameron, S., Tremblay, B., McCarthy, C. and Zhou, Z., " Produced Sand and Reinforced Polymer Gel: Application for Water Shut

off in Cold Production", Alberta Research Council Inc., Report 0001-5, June 2000.

54. Hill, H. J., Brew, J. R., Claridge, E. L., Hite, J. R. and Pope, G. A., "The behavior of polymer in porous media", Proceedings of the SPE Improved Oil Recovery Symposium, Tulsa, Oklahoma, SPE 4748, 1974.
55. Martin, F. D., "Laboratory investigation in the use polymers in low permeability reservoirs", Proceedings of the SPE 49th Annual Fall Conference, SPE 5100, 6 – 9 October 1974.
56. Agarwal, S. H. and Porter, R. S. J. Appl. Polymer Sci. 25, 173 – 185, 1980.
57. Martin, F. D., "Improved water-soluble polymers for enhanced recovery of oil", Proceeding of the SPE International Symposium on Oilfields and Geothermal Chemistry, Denver, CO, 1 – 3 June 1983.
58. Akstinant, M. H., "Polymers for enhanced oil recovery in reservoirs of extremely high salinities and high temperature", Proceedings of the SPE 5th International Symposium on Oilfield and Geothermal Chemistry". Stanford, CA, SPE 8979, 28 – 30 May 1980.
59. Bird, R. B., Armstrong, R.C and Hassager, O., "Dynamics of Polymer Liquids", Vol: 1. Fluid Mechanics, second edition, John Willy and Sons, Toronto, 1987.
60. O'Brien, W. J., Stratton Jr., J. J. and Lane, R. H., " Mechanistic Reservoir Modeling Improves Fissure Treatment Gel Design in Horizontal Injectors, Iidd El Shargi North Dome Field, Qatar", Paper SPE 56743, presented at the 1999 SPE Annual technical Conference and Exhibition held in Houston, Texas, 3 – 6 October 1999.
61. Seright, R. S., "Gel propagation Through Fractures", Paper SPE 59316, presented at the 2000 SPE/DOE Improved Oil Recovery Symposium held in Tulsa, Oklahoma, 3 – 5 April 2000.
62. Seright, R. S., "Polymer gel Dehydration during Extraction through Fractures", SPE Prod. & Facilities 14 (2), SPE 56126, May 1999.

63. Seright, R. S., "Gel Placement in Fractured Systems", SPE Production and Facilities, 241 – 248. SPE 27740, November 1995.
64. Seright, R. S., "Mechanism for Gel Propagation through Fractures", Paper SPE 55628, presented at the 1999 SPE Rocky Mountain Meeting held in Gillette, Wyoming, 15 – 18 May 1999.
65. Liu, J and Seright, R. S., "Rheology of Gel Used for Conformance Control in Fractures", Paper SPE 59318, presented at the 2000 SPE/DOE Improved Oil Recovery Symposium held in Tulsa, Oklahoma, 3 – 5 April 2000.
66. Seright, R. S., "Use of preformed Gel for Conformance Control in Fractured Systems", SPE Production and Facilities 59 – 65, Feb. 1997.
67. Broseta, D., Marquer, O., Zaitoun, A., Baylocq, P. and Fery, J., "Shear Effects on Polyacrylamide/Chromium (III) Acetate Gelation", SPE Reservoir Eval. & Eng. 3 (3), SPE 64500, June 2000.
68. Lai, Q. J. and Newhouse, D. P., "Well treatment with artificial matrix and gel composition", U. S. Pat. No. 5404951, issued April 11, 1995.
69. Dovan, H. T., (SPE), Hutchins, R. D., (SPE, UNOCAL), Sandiford, B.B. (SPE, Polymer Applications), (1997): "Delaying Gelation of Aqueous Polymer at Elevated Temperatures Using Novel Organic Crosslinkers", Paper SPE 37246, presented at the SPE International Symposium on Oilfield Chemistry, Houston, Texas, USA, 18-21 February, 1997.
70. American Society for Testing and Materials, "Standard Test Method for Particle-Size Analysis of Soils", Designation: D442-63 (Reapproved 1998).
71. American Society for Testing and Materials, "Standard Test Method for Rubber Chemicals-Density", Designation: D 1817-96.
72. American Society for Testing and Materials, "Standard Test Method for Maximum Index Density and Unit Weight of Soils Using a Vibratory Table", Designation: D 4253-93.
73. American Society for Testing and Materials, "Standard Test Method for Minimum Index Density and Unit Weight of Soils and Calculation of Relative Density", Designation: D 4254-91.

74. Wassmuth, A., private communication, 2002.

75. Yang, S. H., and Treiber, L. E., "Chemical Stability of Polyacrylamide Under Simulated Field Conditions", Paper SPE 14232, presented at the 60th Annual Conference and Exhibition of the SPE held in Las Vegas, NV. 22-25 September 1985.

76. Wiwchar, B., Cameron, S., Tremblay, B., McCarthy, C. and Zhou, Z., " Produced Sand and Reinforced Polymer Gel: Application for Water Shut off in Cold Production", Alberta Research Council Inc., Report 0001-5, June 2000.

77. Seright, R. S., "Improved Methods for Water Shut-off", Final Technical Progress Report (U.S. DOE Report DOE/PC/91008-14) U.S DOE Contract DE-AC22-94 PC 91008, BDM – Oklahoma. Subcontract G 4560330, 21 – 54, Oct. 1998.

Appendix A:
A.1 Grain size distribution and density

Table A.1 Sieve opening sizes

Sieve # U.S. mesh	Size (mm)	Size (in)
45	0.355	0.0139
60	0.250	0.0117
80	0.180	0.0070
100	0.150	0.0059
120	0.125	0.0049
140	0.106	0.0041
170	0.090	0.0035
200	0.075	0.0029
230	0.063	0.0025
325	0.045	0.0017
400	0.038	0.0015
BP	<0.038	<0.0015

Table A.2 Wormhole and annulus sand analysis from the grain size distribution.

Parameter	Annulus sand (mm)	Wormhole sand (mm)
Graphical mean (M)	0.149	0.098
Graphical Standard Deviation (D)	0.796	0.731
Graphical Skewness (S)	0.870	1.000
Graphical Kurtosis (K)	0.468	0.461

A.2 Permeability calculation for wormhole and annulus sands

The permeability was measured by flowing water at a known flow rate through a sand pack of known length and cross-sectional area. The pressure drop across the sand back was measured. These values were used in Darcy's law to calculate the permeability.

$$K(darcy) = \frac{L}{A} \times \frac{Q}{\Delta p} \times (1.01325 \times 10^{12}) \qquad (A.1)$$

Three tests at different flow rates were conducted and then averaged for both the wormhole and the annulus sand pack. Data for these tests are given below:

Table A.3 Permeability calculation for annulus (70/140) sand

Packing volume (ml)	148
Sand mass (g)	258.8
Porosity (%)	33.8

	Test #1	Test #2	Test #3
Flow-rate (cc/h)	500	1,000	1,500
Pressure drop (kPa)	9.90	19.90	29.65
Length (m)	0.279	0.279	0.279
Diameter (m)	0.022	0.022	0.022
μ (Pa.s)	1.00E-03	1.00E-03	1.00-03
K (darcy)	10.5	10.4	10.5

Table A.4 Permeability calculation for wormhole (F 110) sand

Packing volume (ml)	155
Sand mass (g)	260
Porosity (%)	36.6

	Test # 1	Test # 2	Test # 3
Flow-rate (cc/h)	500	1000	1500
Pressure drop (kPa)	25.197	17.191	17.211
Length (m)	0.279	0.279	0.279
Diameter (m)	0.22	0.22	0.22
μ (Pa-s)	1.00E-03	1.00E-03	1.00E-03
K (darcy)	4.1	6.01	6.01

Appendix B:
Pump calibration

The progressive cavity pump (PCP) was calibrated by measuring the weight of effluent at the outlet of the pump versus time.

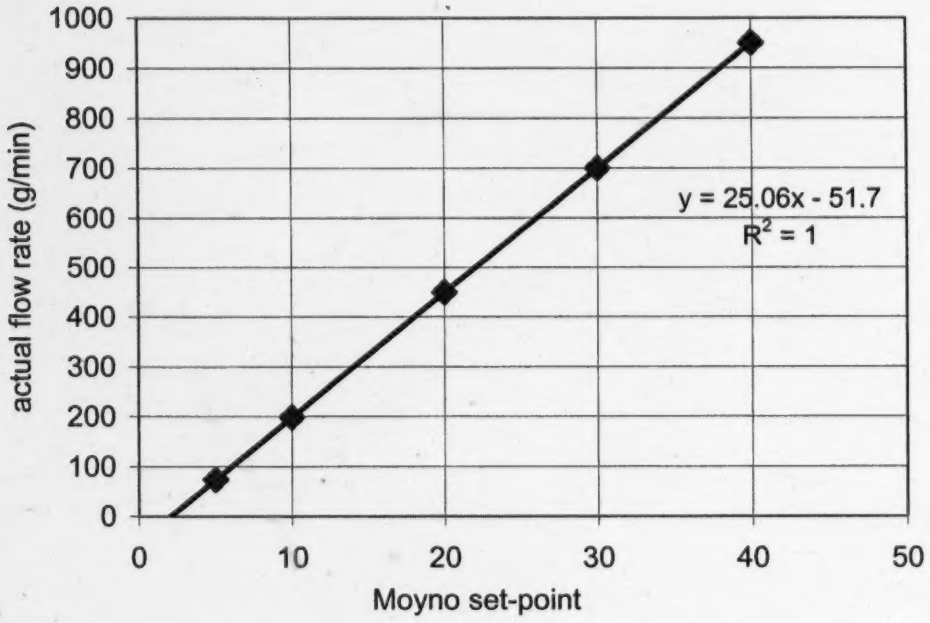

Figure B.1 Calibration for the Moyno pump

Appendix C: Gel strength

Table C.1 Gel strength rating and description

UNOCAL Code	Detailed Gel Description
1+	No detectable gel formed; gel has same viscosity as original polymer solution.
2	Highly flowing gel; gel is slightly more viscous than original polymer solution.
3-	Flowing gel; most of the gel flows to the vial/tube top upon inversion.
3+	Moderately flowing gel; only a small portion (5% – 15%) of the gel does not readily flow to vial/tube top upon inversion.
4+	Barely flowing gel; gel barely flows to the vial/top top; a significant portion (>15%0 of the gel does not flow upon inversion.
5-	Highly deformed non-flowing; gel does not quite reach the vial/tube top upon inversion.
5	Moderately deformable non-flowing gel; gel deforms about half the distance to the vial/tube top upon inversion.
5+	Slightly deformable non-flowing gel; gel surface slightly deform upon inversion.
5++	Rigid gel; no gel surface deformation upon inversion.
6	Ringing rigid gel; a tuning fork-like mechanical vibration upon tapping
/N%	Syneresis; volume percent of free water separated from the gel based upon the total volume of sample.

Table C.2 Gel strength rating and equivalence scale

Scale (UNOCAL Code)	Equivalence
1+	1
2	2
3-	3
3+	4
4+	5
5-	6
5	7
5+	8
5++	9
6	10

Table C.3 Gel strength screening test

Time (days)	Crosslinked polymer 0 wt% sand	20 wt% sand Concentration	30 wt% sand Concentration	40 wt% sand Concentration	50 wt% sand Concentration	60 wt% sand Concentration	65 wt% sand Concentration	70 wt% sand Concentration	75 wt% sand Concentration
	Gel strength	Gel strength	Gel strength	Gel strength	Gel strength	Gel strength	Gel strength	Gel strength	Gel strength
0.00	1	2	2	2	3	4	4	5	5
0.13	1	2	2	2	3	4	4	5	5
0.25	1	2	2	3	3	4	4	5	5
0.38	1	2	2	3	3	5	5	5	5
0.50	2	2	3	3	3	5	5	5	5
1.00	2	2	3	3	4	5	5	5	7
1.13	2	2	3	3	4	5	5	7	7
1.25	2	3	3	3	4	5	5	7	7
1.38	2	3	3	3	4	5	7	7	9
1.50	2	3	3	4	4	7	7	7	9
2.00	3	3	3	4	5	7	7	7	9
2.13	3	3	3	4	5	7	7	8	9
2.25	3	3	4	4	5	7	8	8	9
2.38	3	3	4	4	5	7	8	8	10
2.50	3	4	4	5	6	8	8	9	10
3.00	3	4	4	5	6	8	9	9	10
3.13	3	4	5	5	7	8	9	9	10
3.25	3	4	5	5	7	9	9	9	10
3.38	3	4	5	7	7	9	9	9	10
3.50	3	5	5	7	7	9	9	10	10
4.00	3	5	5	7	8	9	9	10	10
4.13	3	5	7	7	8	9	9	10	10
4.25	4	5	7	7	8	9	9	10	10
4.38	4	5	7	8	8	9	9	10	10
4.50	5	5	7	8	8	9	9	10	10
5.00	5	5	8	8	8	9	9	10	10
6.00	5	7	8	8	8	9	9	10	10
7.00	5	7	8	8	8	9	9	10	10
8.00	5	7	8	8	8	9	9	10	10
9.00	5	7	8	8	8	9	9	10	10
10.00	6	7	8	8	8	9	9	10	10
11.00	6	7	8	8	8	9	9	10	10
12.00	6	7	8	8	8	9	9	10	10
13.00	6	7	8	8	8	9	9	10	10
14.00	6	7	8	8	8	9	9	10	10
15.00	6	7	8	8	8	9	9	10	10
16.00	6	7	8	8	8	9	9	10	10
17.00	6	7	8	8	8	9	9	10	10

Appendix D:
Injectivity

D.1 Calibration of the capillary tube radius with deionized water

Since the precise diameter of the capillary tube was not known, a calibration test was performed to calculate an average tube radius. Water was injected at a constant rate and the pressure drop across the tube was measured.

Table D.1 Input data

Water viscosity @ 20 °C	0.001006 Pa.s
Water density @ 20 °C	1 (g/cc)
Deionized water injection rate	1.10 cc/s
Capillary tube length	457 cm
Pressure drop	700 Pa

From Poiseuille's law

$$r = \left(\frac{8\mu L}{\pi \Delta P}\right)^{1/4} \qquad \text{(D.1)}$$

The corrected radius for the capillary tube was: 0.207 cm

D.2 Viscosity measurement of 60 wt% sandy polymer

The shear rate at the walls of the capillary tube was corrected by the power law model (Bird et al. 1960) [59] as described below. The shear stress at the wall of the tube was calculated from:

$$\tau = (R/2)(\Delta P/L) \qquad \text{(D.2)}$$

The apparent shear rate at the wall was calculated from:

$$\gamma_{app} = 8U_m / D \qquad \text{(D.3)}$$

where:

$$U_m = Q/(\pi R^2) \qquad \text{(D.4)}$$

The logarithm of τ was plotted versus the logarithm of γ_{app} and the data was fitted to a straight line. The slope of this line is the power law index, n. The y intercept is equal to log k^1.

The corrected shear rate is calculated from:

$$\gamma_{corr} = (3n+1)/(4n)\gamma_{app} \qquad \text{(D.5)}$$

The viscosity was calculated from:

$$\eta = \tau / \gamma_{corr} \qquad \text{(D.6)}$$

The power law constant k was calculated from:

$$k = k^1 / ((3n+1)/(4n))^n \qquad \text{(D.7)}$$

The shear stress (Table D.3) of the sandy polymer gel plug at the wall of the screened pipe was calculated from equation D.2. The density of the sandy polymer gel (Table D.2) was measured at the exit of the capillary to make sure that the slurry concentration was correct.

Table D.2 Slurry densities

Sand to polymer weight ratio	Slurry density (g/cm^3)
60:40	1.614
75:25	1.802

Table D.3 Final (stable) pressure drop (DP) versus flow rate.

Rate (g/min)	Rate (cc/min)	DP (kPa)
110	68	155
292	181	270
480	297	345
665	412	422

The diameter of the capillary tube was 0.414 cm. The length of the capillary tube was 457 cm.

Table D.4 Power Law Index Determination

Shear stress (Pa)	Shear rate app. (1/s)	Avg. velocity (cm/sec)	Shear rate corr. (1/s)	Viscosity (Pa.s)	Log shear stress	Log shear rate app.	n	k'	k
35.10	162.77	8.42	195.93	0.18	1.55	2.21	0.55	0.33	0.30
61.15	433.26	22.42	521.52	0.12	1.79	2.64	0.55	0.33	0.30
78.13	710.93	36.79	855.76	0.09	1.89	2.85	0.55	0.33	0.30
95.57	986.20	51.04	1187.11	0.08	1.98	2.99	0.55	0.33	0.30

Viscosity measurements (Fann 35) were performed at no delay and 2 hour delay time.

Table D.5 Fan35 viscometer viscosity measurements

Measurement	RPM	Dial Reading θ_N	Apparent Viscosity μ_{app} (Pa.s)	Shear rate (1/s)	Shear stress (kPa)	Polyacrylamide concentration (ppm) and polymer crosslinker ratio	
1	6	7	0.4	10.214	0.053	12,000 ppm, 10:1 ratio	no delay
1	3	6	0.6	5.107	0.046		
2	6	4	0.2	10.214	3.040	8,000 ppm, 40:1 ratio	no delay
2	3	3	0.3	5.107	2.280		
3	6	16	0.8	10.214	12.160	12,000 ppm, 10:1 ratio	2 hour delay
3	3	14	1.4	5.107	10.640		
4	6	8	0.4	10.214	6.080	8,000 ppm, 40:1 ratio	2 hour delay
4	3	6	0.6	5.107	4.560		
5	6	50	2.5	10.214	38.000	12,000 ppm 40:1 ratio	no delay
5	3	45	4.5	5.107	34.200		
6	6	16	0.8	10.214	12.160	12,000 ppm 10:1 ratio	no delay
6	3	14	1.4	5.107	10.640		
7	6	17	0.9	10.214	12.920	12,000 ppm 10:1 ratio	no delay
7	3	15	1.5	5.107	11.400		
8	6	78	3.9	10.214	59.281	12,000 ppm 40:1 ratio	2 hour delay
8	3	60	6.0	5.107	45.601		

Table D.6 Shear rate regime for the experiments

Flow rate (L/hr)	Flow rate (m^3/s)	Avg. velocity (m/s)	Pressure drop (kPa)	Power index (n)
15.0	4.17E-06	0.0082	1,552.68	0.551
17.0	4.72E-06	0.0093	1,759.70	0.551
20.0	5.56E-06	0.0110	2,070.23	0.551
25.0	6.94E-06	0.0137	2,587.79	0.551
30.0	8.33E-06	0.0165	3,105.35	0.551

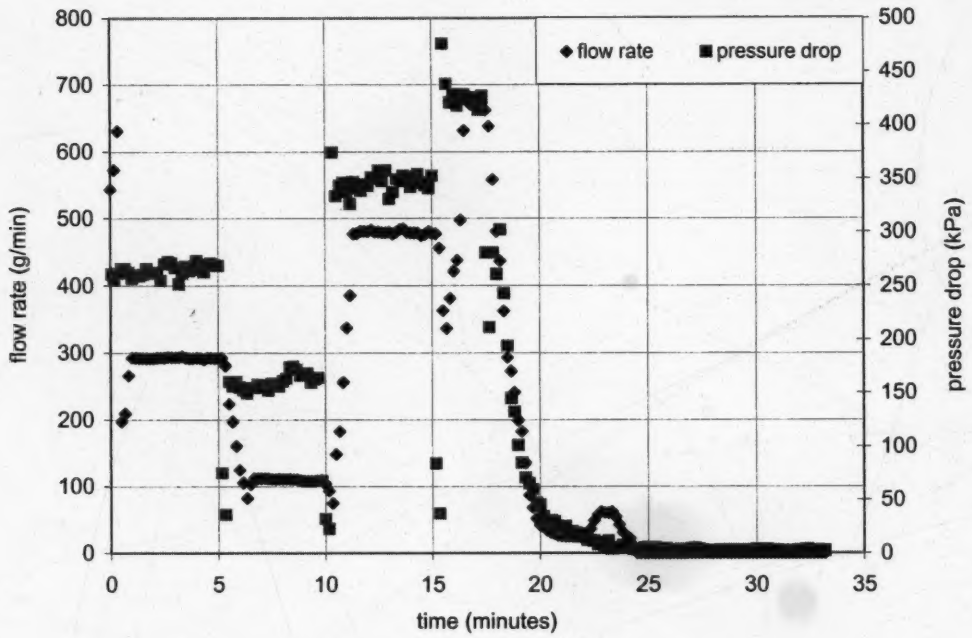

Figure D.1 Pressure drop and flow rate using the capillary viscometer

Appendix E:
Degradation test

These tests were conducted to investigate the effects of shear and iron contact on gelation. The gel was re-circulated through the pump at different flow rates for various times. The residence time is the time the gel spends in the pump for one circulation. The number of circulations through the pump was calculated from the pump flow rate and the pump capacity. The shear rate was calculated at the tubing wall from equation D.5 for a 2.5 cm inner diameter hose.

Table E.1 Degradation test data (gel strength)

Sample #	Flow rate pump (%) of maximum rate	Flow rate pump (L/min)	Time (min) cumulative	No. of circulations through pump	Gel strength Number of days							
					1	2	3	6	7	8	9	14
4	25	0.5748	5	1.08	3-	5+	5++	5++	6	6	6	6
3	25	0.5748	10	2.17	3-	5+	5+	5++	6	6	6	6
2	25	0.5748	15	3.25	3-	5+	5+	5++	6	6	6	6
1	25	0.5748	20	4.34	2	5+	5+	5++	6	6	6	6
10	50	1.2013	25	11.33	3+	5+	5++	5++	6	6	6	6
9	50	1.2013	30	13.59	3+	5+	5+	5++	6	6	6	6
8	50	1.2013	35	15.86	3-	5+	5+	5++	6	6	6	6
7	50	1.2013	40	18.12	3-	5	5+	5++	6	6	6	6
15	100	2.4543	45	41.65	3+	5+	5++	5++	6	6	6	6
14	100	2.4543	50	46.28	3+	5+	5++	5++	6	6	6	6
13	100	2.4543	55	50.91	3+	5+	5+	5+	6	6	6	6
12	100	2.4543	60	55.54	3-	5+	5+	5+	5++	5++	6	6
11	100	2.4543	130	120.33	3-	5	5	5	5	5+	5+	5+

Table E.2 Flow rate and residence time.

Flow rate (% of maximum rate)	Flow rate (g/min)	Flow rate (L/min)	Residence time (min)
25.0	574.8	0.5748	4.61
50.0	1201.3	1.2013	2.21
100.0	2454.3	2.4543	1.08

Table E.3 Degradation test shear rate (at the wall of the 2.5 cm (1.D) hose).

Sample #	Time (min) cumulative	Flow rate (L/min)	Residence time (min)	No. of circulations through pump	Avg. Velocity (cm/s)	Shear rate (apparent) 1/s	Shear rate (corrected) (1/s)
1	5	0.5748	4.61	1.08	1.8916	5.9578	7.1715
2	10	0.5748	4.61	2.17	1.8916	5.9578	7.1715
3	15	0.5748	4.61	3.25	1.8916	5.9578	7.1715
4	20	0.5748	4.61	4.34	1.8916	5.9578	7.1715
5	25	1.2013	2.21	11.33	3.9533	12.4514	14.9880
6	30	1.2013	2.21	13.59	3.9533	12.4514	14.9880
7	35	1.2013	2.21	15.86	3.9533	12.4514	14.9880
8	40	1.2013	2.21	18.12	3.9533	12.4514	14.9880
9	45	2.4543	1.08	41.65	8.0768	25.4387	30.6211
10	50	2.4543	1.08	46.28	8.0768	25.4387	30.6211
11	55	2.4543	1.08	50.91	8.0768	25.4387	30.6211
12	60	2.4543	1.08	55.54	8.0768	25.4387	30.6211
13	130	2.4543	1.08	120.33	8.0768	25.4387	30.6211

Appendix F:
Settling tests

Table F.1 First settling test data.

(first settling test) 75:25 sand : polymer weight ratio formulation: (SPG = sandy polymer gel)

	Specific gravity	Volume (cc)	Volume (%)	Mass (gm)
Sand	2.65	28.52	53.58	140.92
Polymer gel	1.012	24.70	46.42	43.82
Salt				3.15

Time (hours)	Init. vol. (cc)	Init. len. (cm)	Measured vol. (cc)	Measured Length (cm)	Settling % (vol)	Settling % (length)	Settling rate (cm/hr)	Sand vol. (cc)	Poly. gel vol. (cc)	Initial porosity (%)	Final porosity (%)	Initial density of SPG (kg/m^3)	Final density of SPG (kg/m^3)	Vol. poly gel in settled layer (cc)	Mass poly gel in settled layer (g)	Porosity change (%)	Density change (%)
0.00	100	18.7	100	18.70	0.00	0.00	0.000	53.58	46.42	46	46	1847.43	1847.43			0.00	0.00
1.00	100	18.7	98	18.31	2.00	2.11	0.390	53.58	46.42	46	45	1847.43	1896.66	44.42	44.95	-2.36	2.04
2.00	100	18.7	98	18.31	2.00	2.11	0.195	53.58	46.42	46	45	1847.43	1896.66	44.42	44.95	-2.36	2.04
3.00	100	18.7	97	18.10	3.00	3.21	0.200	53.58	46.42	46	45	1847.43	1905.78	43.42	43.94	-3.57	3.09
4.00	100	18.7	96.5	18.04	3.50	3.53	0.165	53.58	46.42	46	44	1847.43	1910.41	42.92	43.43	-4.19	3.63
6.00	100	18.7	96.5	18.04	3.50	3.53	0.165	53.58	46.42	46	44	1847.43	1910.41	42.92	43.43	-4.19	3.63
30.00	100	18.7	96.5	18.04	3.50	3.53	0.165	53.58	46.42	46	44	1847.43	1910.41	42.92	43.43	-4.19	3.63
54.00	100	18.7	96.5	18.04	3.50	3.53	0.165	53.58	46.42	46	44	1847.43	1910.41	42.92	43.43	-4.19	3.63
120.00	100	18.7	96.5	18.04	3.50	3.53	0.165	53.58	46.42	46	44	1847.43	1910.41	42.92	43.43	-4.19	3.63

(first settling test) 70:30 sand : polymer weight ratio formulation: (SPG = sandy polymer gel)

	Specific gravity	Volume (cc)	Volume (%)	Mass (gm)
Sand	2.65	26.62	47.31	124.42
Polymer gel	1.012	29.64	52.69	49.74
Salt				3.58

Time (hours)	Init. vol. (cc)	Init. len. (cm)	Measured vol. (cc)	Measured length (cm)	Settling % (vol)	Settling % (length)	Settling rate (cm/hr)	Sand vol. (cc)	Poly. gel vol. (cc)	Initial porosity (%)	Final porosity (%)	Initial density of SPG (kg/m^3)	Final density of SPG (kg/m^3)	Vol.poly gel in settled layer (cc)	Mass poly gel in settled layer (g)	Porosity change (%)	Density change (%)
0.00	100	18.8	100	18.80	0.00	0.00	0.000	47.31	52.69	53	53	1741.65	1741.65			0.00	0.00
1.00	100	18.8	98	18.40	2.00	2.13	0.400	47.31	52.69	53	52	1741.65	1793.08	50.69	51.30	-1.83	2.04
2.00	100	18.8	96	18.00	4.00	4.26	0.350	47.31	52.69	53	51	1741.65	1809.35	48.69	49.28	-3.74	4.17
3.00	100	18.8	96	18.00	4.00	4.26	0.400	47.31	52.69	53	51	1741.65	1809.35	48.69	49.28	-3.74	4.17
4.00	100	18.8	96	18.00	4.00	4.26	0.400	47.31	52.69	53	51	1741.65	1809.35	48.69	49.28	-3.74	4.17
5.00	100	18.8	96	18.00	4.00	4.26	0.400	47.31	52.69	53	51	1741.65	1809.35	48.69	49.28	-3.74	4.17
6.00	100	18.8	96	18.00	4.00	4.26	0.400	47.31	52.69	53	51	1741.65	1809.35	48.69	49.28	-3.74	4.17
30.00	100	18.8	96	18.00	4.00	4.26	0.400	47.31	52.69	53	51	1741.65	1809.35	48.69	49.28	-3.74	4.17
54.00	100	18.8	96	18.00	4.00	4.26	0.400	47.31	52.69	53	51	1741.65	1809.35	48.69	49.28	-3.74	4.17
120.00	100	18.8	96	18.00	4.00	4.26	0.400	47.31	52.69	53	51	1741.65	1809.35	48.69	49.28	-3.74	4.17

(first settling test) 65:35 sand : polymer weight ratio formulation: (SPG = sandy polymer gel)

	Specific gravity	Volume (cc)	Volume (%)	Mass (gm)
Sand	2.65	24.71	41.68	109.61
Polymer gel	1.012	34.58	58.32	55.06
Salt				3.96

Time (hours)	Init. vol. (cc)	Init. len. (cm)	Measured vol. (cc)	Measured length (cm)	Settling % (vol)	Settling % (length)	Settling rate (cm/hr)	Sand vol. (cc)	Poly. gel Vol. (cc)	Initial porosity (%)	Final porosity (%)	Initial density of SPG (kg/m^3)	Final density of SPG (kg/m^3)	Vol.poly gel in settled layer (cc)	Mass poly gel in settled layer (g)	Porosity change (%)	Density change (%)
0.00	100	19	100	19.00	0.00	0.00	0.000	41.68	58.32	58	58	1646.72	1646.72			0.00	0.00
1.00	100	19	95	18.00	5.00	5.26	1.000	41.68	58.32	58	56	1646.72	1721.84	53.32	53.96	20.92	0.05
2.00	100	19	93.5	17.80	6.50	6.32	0.600	41.68	58.32	58	55	1646.72	1733.23	51.82	52.44	19.41	0.07
3.00	100	19	93	17.60	7.00	7.37	0.467	41.68	58.32	58	55	1646.72	1737.10	51.32	51.94	18.89	0.08
4.00	100	19	93	17.60	7.00	7.37	0.467	41.68	58.32	58	55	1646.72	1737.10	51.32	51.94	18.89	0.08
5.00	100	19	93	17.60	7.00	7.37	0.467	41.68	58.32	58	55	1646.72	1737.10	51.32	51.94	18.89	0.08
6.00	100	19	93	17.60	7.00	7.37	0.467	41.68	58.32	58	55	1646.72	1737.10	51.32	51.94	18.89	0.08
30.00	100	19	93	17.60	7.00	7.37	0.467	41.68	58.32	58	55	1646.72	1737.10	51.32	51.94	18.89	0.08
54.00	100	19	93	17.60	7.00	7.37	0.467	41.68	58.32	58	55	1646.72	1737.10	51.32	51.94	18.89	0.08
120.00	100	19	93	17.60	7.00	7.37	0.467	41.68	58.32	58	55	1646.72	1737.10	51.32	51.94	18.89	0.08

(first settling test) 60:40 sand : polymer weight ratio formulation: (SPG = sandy polymer gel)

	Specific gravity	Volume (cc)	Volume (%)	Mass (gm)
Sand	2.65	22.81	36.60	96.25
Polymer gel	1.012	39.53	63.40	59.86
Salt				4.31

Time (hours)	Init. vol. (cc)	Init. len. (cm)	Measured vol. (cc)	Measured length (cm)	Settling % (vol)	Settling % (length)	Settling rate (cm/hr)	Sand vol. (cc)	Poly. gel vol. (cc)	Initial porosity (%)	Final porosity (%)	Initial density of SPG (kg/m^3)	Final density of SPG (kg/m^3)	Vol.poly gel in settled layer (cc)	Mass poly gel in settled layer (g)	Porosity change (%)	Density change (%)
0.00	100	18.6	100	18.60	0.00	0.00	0.000	36.60	63.40	63	63	1561.04	1561.04			0.00	0.00
1.00	100	18.6	94.5	17.58	5.50	5.48	1.020	36.60	63.40	63	61	1561.04	1638.58	57.90	58.60	32.01	0.06
2.00	100	18.6	93	17.30	7.00	6.99	0.650	36.60	63.40	63	61	1561.04	1648.69	56.40	57.08	30.66	0.08
3.00	100	18.6	92	17.10	8.00	8.06	0.500	36.60	63.40	63	60	1561.04	1655.61	55.40	56.07	29.74	0.09
4.00	100	18.6	92	17.10	8.00	8.06	0.500	36.60	63.40	63	60	1561.04	1655.61	55.40	56.07	29.74	0.09
5.00	100	18.6	92	17.10	8.00	8.06	0.500	36.60	63.40	63	60	1561.04	1655.61	55.40	56.07	29.74	0.09
6.00	100	18.6	92	17.10	8.00	8.06	0.500	36.60	63.40	63	60	1561.04	1655.61	55.40	56.07	29.74	0.09
30.00	100	18.6	92	17.10	8.00	8.06	0.500	36.60	63.40	63	60	1561.04	1655.61	55.40	56.07	29.74	0.09
54.00	100	18.6	92	17.10	8.00	8.06	0.500	36.60	63.40	63	60	1561.04	1655.61	55.40	56.07	29.74	0.09
120.00	100	18.6	92	17.10	8.00	8.06	0.500	36.60	63.40	63	60	1561.04	1655.61	55.40	56.07	29.74	0.09

(first settling test) 50:50 sand : polymer weight ratio formulation: (SPG = sandy polymer gel)

	Specific gravity	Volume (cc)	Volume (%)	Mass (gm)
Sand	2.65	19.01	27.79	73.08
Polymer gel	1.012	49.41	72.21	68.17
Salt				4.91

Time (hours)	Init. vol. (cc)	Init. len. (cm)	Measured vol. (cc)	Measured length (cm)	Settling % (vol)	Settling % (length)	Settling rate (cm/hr)	Sand vol. (cc)	Poly. gel vol. (cc)	Initial porosity (%)	Final porosity (%)	Initial density of SPG (kg/m^3)	Final density of SPG (kg/m^3)	Vol.poly gel in settled layer (cc)	Mass poly gel in settled layer (g)	Porosity change (%)	Density change (%)
0.00	100	18.7	100	18.70	0.00	0.00	0.000	27.79	72.21	0.72	72	1412.52	1412.52			0.00	0.00
1.00	100	18.7	92	17.20	8.00	8.02	1.500	27.79	72.21	0.72	70	1412.52	1500.69	64.21	64.98	50.37	0.09
2.00	100	18.7	87	16.25	13.00	13.10	1.225	27.79	72.21	0.72	68	1412.52	1528.77	59.21	59.92	46.63	0.15
3.00	100	18.7	84	15.70	16.00	16.04	1.000	27.79	72.21	0.72	67	1412.52	1547.23	56.21	56.89	44.17	0.19
4.00	100	18.7	84	15.70	16.00	16.04	1.000	27.79	72.21	0.72	67	1412.52	1547.23	56.21	56.89	44.17	0.19
5.00	100	18.7	84	15.70	16.00	16.04	1.000	27.79	72.21	0.72	67	1412.52	1547.23	56.21	56.89	44.17	0.19
6.00	100	18.7	84	15.70	16.00	16.04	1.000	27.79	72.21	0.72	67	1412.52	1547.23	56.21	56.89	44.17	0.19
30.00	100	18.7	84	15.70	16.00	16.04	1.000	27.79	72.21	0.72	67	1412.52	1547.23	56.21	56.89	44.17	0.19
54.00	100	18.7	84	15.70	16.00	16.04	1.000	27.79	72.21	0.72	67	1412.52	1547.23	56.21	56.89	44.17	0.19
120.00	100	18.7	84	15.70	16.00	16.04	1.000	27.79	72.21	0.72	67	1412.52	1547.23	56.21	56.89	44.17	0.19

(first settling test) 40:60 sand : polymer weight ratio formulation: (SPG = sandy polymer gel)

	Specific gravity	Volume (cc)	Volume (%)	Mass (gm)
Sand	2.65	15.21	20.42	53.69
Polymer gel	1.012	59.29	79.58	75.13
Salt				5.41

Time (hours)	Init. vol. (cc)	Init. len. (cm)	Measured vol. (cc)	Measured length (cm)	Settling % (vol)	Settling % (length)	Settling rate (cm/hr)	Sand vol. (cc)	Poly. gel vol. (cc)	Initial porosity (%)	Final porosity (%)	Initial density of SPG (kg/m^3)	Final density of SPG (kg/m^3)	Vol.poly gel in settled layer (cc)	Mass poly gel in settled layer (g)	Porosity change (%)	Density change (%)
0.00	100	18.5	100	18.50	0.00	0.00	0.000	20.42	79.58	80	80	1288.25	1288.25			0.00	0.00
1.00	100	18.5	87	16.10	13.00	12.97	2.400	20.42	79.58	80	77	1288.25	1391.68	66.58	67.38	64.88	0.15
2.00	100	18.5	75	13.85	25.00	25.14	2.325	20.42	79.58	80	73	1288.25	1452.43	54.58	55.24	56.79	0.33
3.00	100	18.5	65	12.00	35.00	35.14	2.167	20.42	79.58	80	69	1288.25	1520.19	44.58	45.12	47.77	0.54
4.00	100	18.5	63	11.60	37.00	37.30	1.725	20.42	79.58	80	68	1288.25	1536.32	42.58	43.10	45.62	0.59
5.00	100	18.5	60	11.10	40.00	40.00	1.480	20.42	79.58	80	66	1288.25	1562.54	39.58	40.06	42.13	0.67
6.00	100	18.5	60	11.10	40.00	40.00	1.480	20.42	79.58	80	66	1288.25	1562.54	39.58	40.06	42.13	0.67
30.00	100	18.5	55	10.10	45.00	45.41	0.280	20.42	79.58	80	63	1288.25	1612.59	34.58	35.00	35.47	0.82
54.00	100	18.5	55	10.10	45.00	45.41	0.280	20.42	79.58	80	63	1288.25	1612.59	34.58	35.00	35.47	0.82
120.00	100	18.5	55	10.10	45.00	45.41	0.280	20.42	79.58	80	63	1288.25	1612.59	34.58	35.00	35.47	0.82

(first settling test)30:70 sand : polymer weight ratio formulation: (SPG = sandy polymer gel)

	Specific gravity	Volume (cc)	Volume (%)	Mass (gm)
Sand	2.65	14.16	14.16	37.23
Polymer gel	1.012	85.84	85.84	81.04
Salt				5.83

Time (hours)	Init. Vol. (cc)	Init. len. (cm)	Measured vol. (cc)	Measured length (cm)	Settling % (vol)	Settling % (length)	Settling rate (cm/hr)	Sand vol. (cc)	Poly. gel vol. (cc)	Initial porosity (%)	Final porosity (%)	Initial density of SPG (kg/m^3)	Final density of SPG (kg/m^3)	Vol.poly gel in settled layer (cc)	Mass poly gel in settled layer (g)	Porosity change (%)	Density change (%)
0.00	100	18	100	18.00	0.00	0.00	0.000	14.16	85.84	86	86	1182.72	1182.72			0.00	0.00
1.00	100	18	66	11.84	34.00	34.22	6.160	14.16	85.84	86	79	1182.72	1359.05	51.84	52.47	69.23	0.52
2.00	100	18	50	9.00	50.00	50.00	4.500	14.16	85.84	86	72	1182.72	1470.10	35.84	36.27	54.44	1.00
3.00	100	18	39	7.00	61.00	61.11	3.667	14.16	85.84	86	64	1182.72	1599.31	24.84	25.14	37.24	1.56
4.00	100	18	35	6.30	65.00	65.00	2.925	14.16	85.84	86	60	1182.72	1666.43	20.84	21.09	28.30	1.86
5.00	100	18	35	6.30	65.00	65.00	2.340	14.16	85.84	86	60	1182.72	1666.43	20.84	21.09	28.30	1.86
6.00	100	18	35	6.30	65.00	65.00	2.340	14.16	85.84	86	60	1182.72	1666.43	20.84	21.09	28.30	1.86
30.00	100	18	30	5.40	70.00	70.00	0.420	14.16	85.84	86	53	1182.72	1775.51	15.84	16.03	13.78	2.33
54.00	100	18	30	5.40	70.00	70.00	0.420	14.16	85.84	86	53	1182.72	1775.51	15.84	16.03	13.78	2.33
120.00	100	18	30	5.40	70.00	70.00	0.420	14.16	85.84	86	53	1182.72	1775.51	15.84	16.03	13.78	2.33

(first settling test) 20:80 sand : polymer weight ratio formulation: (SPG = sandy polymer gel)

	Specific gravity	Volume (cc)	Volume (%)	Mass (gm)
Sand	2.65	7.60	8.78	23.08
Polymer gel	1.012	79.05	91.22	86.12
Salt				6.20

Time (hours)	Init. vol. (cc)	Init. len. (cm)	Measured vol. (cc)	Measured length (cm)	Settling % (vol)	Settling % (length)	Settling rate (cm/hr)	Sand vol. (cc)	Poly. gel vol. (cc)	Initial porosity (%)	Final porosity (%)	Initial density of SPG (kg/m^3)	Final density of SPG (kg/m^3)	Vol.poly gel in settled layer (cc)	Mass poly gel in settled layer (g)	Porosity change (%)	Density change (%)
0.00	100	18.7	100	18.70	0.00	0.00	0.000	8.78	91.22	91	91	1092.00	1092.00			0.00	0.00
1.00	100	18.7	60	11.20	40.00	40.11	7.500	8.78	91.22	91	85	1092.00	1248.65	51.22	51.84	83.93	0.67
2.00	100	18.7	40	7.45	60.00	60.16	5.630	8.78	91.22	91	78	1092.00	1366.97	31.22	31.60	68.17	1.50
3.00	100	18.7	29	5.40	71.00	71.12	4.430	8.78	91.22	91	70	1092.00	1501.62	20.22	20.47	50.24	2.45
4.00	100	18.7	25	4.60	75.00	75.40	3.530	8.78	91.22	91	65	1092.00	1579.96	16.22	16.42	39.81	3.00
5.00	100	18.7	25	4.60	75.00	75.40	3.530	8.78	91.22	91	65	1092.00	1579.96	16.22	16.42	39.81	3.00
6.00	100	18.7	25	4.60	75.00	75.40	3.530	8.78	91.22	91	65	1092.00	1579.96	16.22	16.42	39.81	3.00
30.00	100	18.7	18	3.30	82.00	82.35	0.510	8.78	91.22	91	51	1092.00	1800.83	9.22	9.34	10.40	4.56
54.00	100	18.7	18	3.30	82.00	82.35	0.510	8.78	91.22	91	51	1092.00	1800.83	9.22	9.34	10.40	4.56
120.00	100	18.7	18	3.30	82.00	82.35	0.51	8.78	91.22	91	51	1092.00	1800.83	9.22	9.34	10.40	4.56

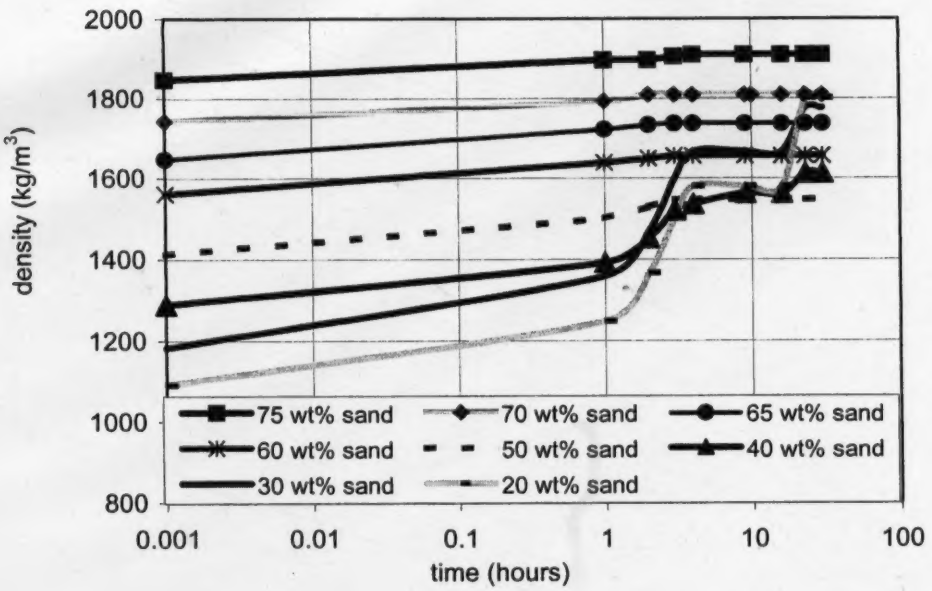

Figure F.1 Sandy polymer gel densities versus time for different concentrations (first settling test).

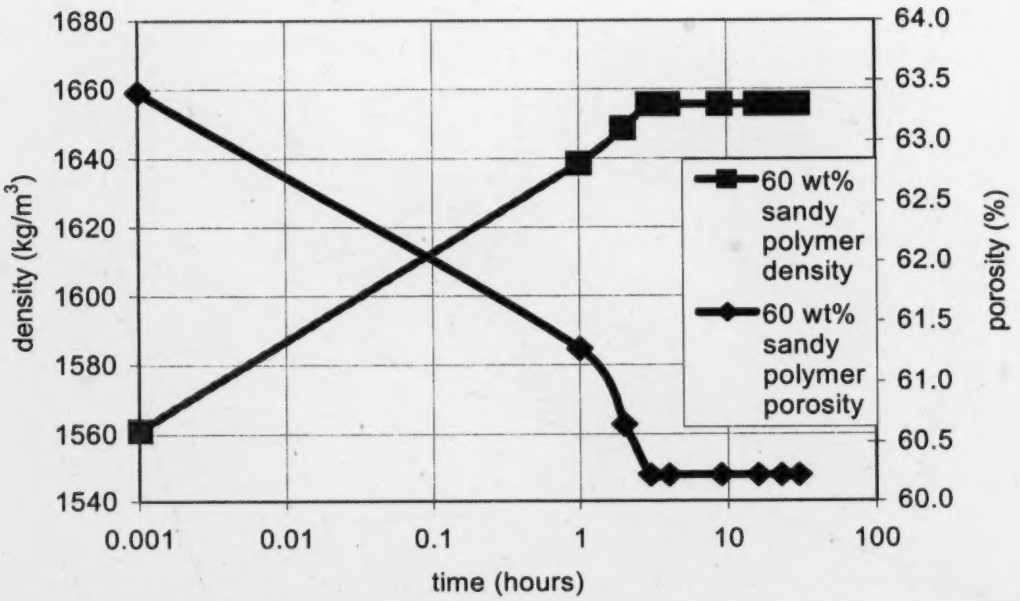

Figure F.2 60 wt% sandy polymer density and porosity versus time (first settling test).

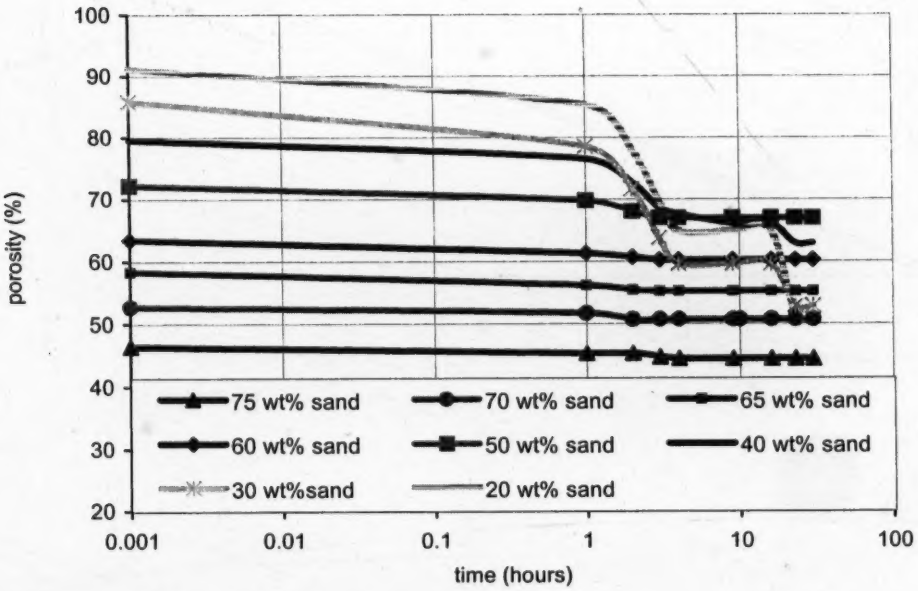

Figure F.3 Sandy polymer gel porosity versus time for different sand concentrations (first settling test).

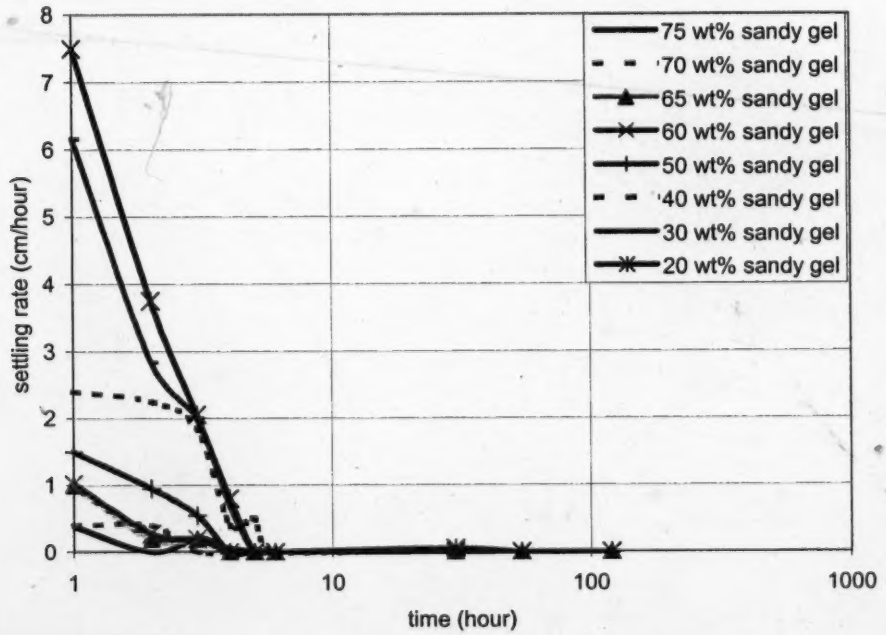

Figure F.4 Settling rate versus time for different sand concentrations (first settling test).

Table F.2 Second settling test data.

(second settling test) 75:25 sand : polymer weight ratio formulation: (SPG = sandy polymer gel)

	Specific gravity	Volume (cc)	Volume (%)	Mass (gm)
Sand	2.65	28.52	53.58	140.92
Polymer gel	1.012	24.70	46.42	43.82
Salt				3.15

Time (hours)	Init. vol. (cc)	Init. len. (cm)	Measured vol. (cc)	Measured length. (cm)	Settling % (vol)	Settling % (length)	Settling rate (cm/hr)	Sand vol (cc)	Poly gel. vol. (cc)	Initial porosity (%)	Final porosity (%)	Initial density of SPG (kg/m^3)	Final density of SPG (kg/m^3)	Vol. poly gel in settled layer (cc)	Mass poly gel in settled layer (g)	Porosity change %	Density change %
0.00	100	18.9	100	18.9	0.00	0.00	0.000	53.58	46.42	46	46	1847.43	1847.43			0.00	0.00
0.58	100	18.9	99	18.7	1.00	1.06	0.345	53.58	46.42	46	46	1847.43	1887.73	45.42	45.96	-0.01	1.01
1.50	100	18.9	98	18.5	2.00	2.12	0.267	53.58	46.42	46	45	1847.43	1896.66	44.42	44.95	-0.02	2.04
2.25	100	18.9	97	18.3	3.00	3.17	0.267	53.58	46.42	46	45	1847.43	1905.78	43.42	43.94	-0.04	3.09
3.33	100	18.9	96	18.1	4.00	4.23	0.240	53.58	46.42	46	44	1847.43	1915.09	42.42	42.93	-0.05	4.17
120.00	100	18.9	96	18.1	4.00	4.23	0.240	53.58	46.42	46	44	1847.43	1915.09	42.42	42.93	-0.05	4.17

(second settling test) 70:30 sand : polymer weight ratio formulation: (SPG = sandy polymer gel)

	Specific gravity	Volume (cc)	Volume (%)	Mass (gm)
Sand	2.65	26.62	47.31	124.42
Polymer gel	1.012	29.64	52.69	49.74
Salt				3.58

Time (hours)	Init. vol. (cc)	Init. len. (cm)	Measured vol. (cc)	Measured length. (cm)	Settling % (vol)	Settling % (length)	Settling rate (cm/hr)	Sand vol (cc)	Poly gel. vol. (cc)	Initial porosity (%)	Final porosity (%)	Initial density of SPG (kg/m^3)	Final density of SPG (kg/m^3)	Vol. poly gel in settled layer (cc)	Mass poly gel in settled layer (g)	Porosity change %	Density change %
0.00	100	18.7	100	19.0	0.00	0.00	0.000	47.31	52.69	53	53	1741.65	1741.65			0.00	0.00
0.08	100	18.7	100	19.0	0.00	0.00	0.000	47.31	52.69	53	53	1741.65	1777.45	52.69	53.32	0.00	0.00
0.25	100	18.7	99	18.5	1.00	1.07	0.800	47.31	52.69	53	52	1741.65	1785.19	51.69	52.31	-0.01	0.01
0.50	100	18.7	98	18.3	2.00	2.14	0.800	47.31	52.69	53	52	1741.65	1793.08	50.69	51.30	-0.02	0.02
0.58	100	18.7	97	18.1	3.00	3.21	1.034	47.31	52.69	53	51	1741.65	1801.13	49.69	50.29	-0.03	0.03
1.25	100	18.7	96	18	4.00	3.74	0.560	47.31	52.69	53	51	1741.65	1809.35	48.69	49.28	-0.04	0.04
2.75	100	18.7	95	17.8	5.00	4.81	0.327	47.31	52.69	53	50	1741.65	1817.74	47.69	48.26	8.15	0.05
120.00	100	18.7	95	17.8	5.00	4.81	0.327	47.31	52.69	53	50	1741.65	1817.74	47.69	48.26	8.15	0.05

(second settling test) 65:35 sand : polymer weight ratio formulation: (SPG = sandy polymer gel)

	Specific gravity	Volume (cc)	Volume (%)	Mass (gm)
Sand	2.65	24.71	41.68	109.61
Polymer gel	1.012	34.58	58.32	55.06
Salt				3.96

Time (hours)	Init. vol. (cc)	Init. len. (cm)	Measured vol. (cc)	Measured length. (cm)	Settling % (vol)	Settling % (length)	Settling rate (cm/hr)	Sand vol (cc)	Poly gel. vol. (cc)	Initial porosity (%)	Final porosity (%)	Initial density of SPG (kg/m^3)	Final density of SPG (kg/m^3)	Vol. poly gel in settled layer (cc)	Mass poly gel in settled layer (g)	Porosity change %	Density change %
0.00	100	18.6	100	18.6	0.00	0.00	0.000	41.68	58.32	58	58	1096.12	1646.72			0.00	0.00
0.08	100	18.6	99	18.5	1.00	1.08	1.250	41.68	58.32	58	58	1096.12	1693.16	57.32	58.01	-0.01	1.01
0.33	100	18.6	98	18.3	2.00	1.61	0.909	41.68	58.32	58	57	1096.12	1700.11	56.32	57.00	-0.01	2.04
0.75	100	18.6	97	18.1	3.00	2.69	0.667	41.68	58.32	58	57	1096.12	1707.20	55.32	55.99	-0.02	3.09
1.08	100	18.6	96	17.9	4.00	3.76	0.648	41.68	58.32	58	57	1096.12	1714.44	54.32	54.97	-0.03	4.17
1.75	100	18.6	95	17.7	5.00	4.84	0.514	41.68	58.32	58	56	1096.12	1721.84	53.32	53.96	-0.04	5.26
2.58	100	18.6	94	17.5	6.00	5.91	0.426	41.68	58.32	58	56	1096.12	1729.39	52.32	52.95	-0.05	6.38
120.00	100	18.6	94	17.5	6.00	5.91	0.426	41.68	58.32	58	56	1096.12	1729.39	52.32	52.95	-0.05	6.38

(second settling test) 60:40 sand : polymer weight ratio formulation: (SPG = sandy polymer gel)

	Specific gravity	Volume (cc)	Volume (%)	Mass (gm)
Sand	2.65	22.81	36.60	96.25
Polymer gel	1.012	39.53	63.40	59.86
Salt				4.31

Time (hours)	Init. vol. (cc)	Init. len. (cm)	Measured vol. (cc)	Measured length. (cm)	Settling % (vol)	Settling % (length)	Settling rate (cm/hr)	Sand vol (cc)	Poly gel. Vol. (cc)	Initial porosity (%)	Final porosity (%)	Initial density of SPG (kg/m^3)	Final density of SPG (kg/m^3)	Vol. poly gel in settled layer (cc)	Mass poly gel in settled layer (g)	Porosity change %	Density change %
0.00	100	19	100	19	0.00	0.00	0.000	36.60	63.40	63	63	1561.04	1561.04			0.00	0.00
0.08	100	19	99	18.9	1.00	1.05	1.250	36.60	63.40	63	63	1561.04	1610.10	62.40	63.15	-0.01	0.01
0.42	100	19	98	18.6	2.00	2.11	0.952	36.60	63.40	63	63	1561.04	1616.21	61.40	62.14	-0.01	0.02
0.75	100	19	97	18.4	3.00	3.16	0.800	36.60	63.40	63	62	1561.04	1622.44	60.40	61.13	-0.02	0.03
1.08	100	19	96	18.2	4.00	4.21	0.741	36.60	63.40	63	62	1561.04	1628.79	59.40	60.12	-0.02	0.04
1.50	100	19	95	18	5.00	5.26	0.667	36.60	63.40	63	61	1561.04	1635.29	58.40	59.10	-0.03	0.05
2.00	100	19	94	17.8	6.00	6.32	0.600	36.60	63.40	63	61	1561.04	1641.92	57.40	58.09	-0.04	0.06
2.58	100	19	93	17.6	7.00	7.37	0.543	36.60	63.40	63	61	1561.04	1648.69	56.40	57.08	-0.04	0.08
120.00	100	19	93	17.6	7.00	7.37	0.543	36.60	63.40	63	61	1561.04	1648.69	56.40	57.08	-0.04	0.08

(second settling test) 50:50 sand : polymer weight ratio formulation: (SPG = sandy polymer gel)

	Specific gravity	Volume (cc)	Volume (%)	Mass (gm)
Sand	2.65	19.01	27.79	73.08
Polymer gel	1.012	49.41	72.21	68.17
Salt				4.91

Time (hours)	Init. vol. (cc)	Init. len. (cm)	Measured vol. (cc)	Measured length (cm)	Settling % (vol)	Settling % (length)	Settling rate (cm/hr)	Sand vol (cc)	Poly gel. Vol. (cc)	Initial porosity (%)	Final porosity (%)	Initial density of SPG (kg/m^3)	Final density of SPG (kg/m^3)	Vol. poly gel in settled layer (cc)	Mass poly gel in settled layer (g)	Porosity change %	Density change %
0.00	100	17.9	100	17.9	0.00	0.00	0.000	27.79	72.21	72	72	1412.52	1412.52			0.00	0.00
0.08	100	17.9	99	17.7	1.00	0.56	2.500	27.79	72.21	72	72	1412.52	1466.13	71.21	72.07	0.00	1.01
0.17	100	17.9	98	17.5	2.00	1.68	2.353	27.79	72.21	72	72	1412.52	1470.77	70.21	71.06	-0.01	2.04
0.25	100	17.9	97	17.3	3.00	3.35	2.400	27.79	72.21	72	71	1412.52	1475.50	69.21	70.04	-0.01	3.09
0.33	100	17.9	96	17.1	4.00	4.47	2.424	27.79	72.21	72	71	1412.52	1480.33	68.21	69.03	-0.02	4.17
0.50	100	17.9	95	17	5.00	5.03	1.800	27.79	72.21	72	71	1412.52	1485.26	67.21	68.02	-0.02	5.26
0.58	100	17.9	94	16.9	6.00	5.59	1.724	27.79	72.21	72	70	1412.52	1490.29	66.21	67.01	-0.02	6.38
0.67	100	17.9	93	16.7	7.00	6.70	1.791	27.79	72.21	72	70	1412.52	1495.43	65.21	66.00	-0.03	7.53
0.83	100	17.9	93	16.6	7.50	7.26	1.566	27.79	72.21	72	70	1412.52	1498.05	64.71	65.49	-0.03	8.11
0.92	100	17.9	91	16.3	9.00	8.94	1.739	27.79	72.21	72	69	1412.52	1506.06	63.21	63.97	-0.04	9.89
1.17	100	17.9	90	16.1	10.00	10.06	1.538	27.79	72.21	72	69	1412.52	1511.55	62.21	62.96	-0.04	11.11
1.42	100	17.9	89	15.9	11.00	11.17	1.408	27.79	72.21	72	69	1412.52	1517.16	61.21	61.95	-0.05	12.36
1.50	100	17.9	88	15.7	12.00	12.29	1.467	27.79	72.21	72	68	1412.52	1522.90	60.21	60.94	-0.05	13.64
1.58	100	17.9	87	15.5	13.00	13.41	1.519	27.79	72.21	72	68	1412.52	1528.77	59.21	59.92	-0.06	14.94
1.75	100	17.9	86	15.3	14.00	14.53	1.486	27.79	72.21	72	68	1412.52	1534.78	58.21	58.91	-0.06	16.28
1.83	100	17.9	85	15.1	15.00	15.64	1.530	27.79	72.21	72	67	1412.52	1540.93	57.21	57.90	-0.07	17.65
1.92	100	17.9	84	14.9	16.00	16.76	1.563	27.79	72.21	72	67	1412.52	1547.23	56.21	56.89	-0.07	19.05
2.00	100	17.9	83	14.7	17.00	17.88	1.600	27.79	72.21	72	67	1412.52	1553.68	55.21	55.88	-0.08	20.48
2.08	100	17.9	82	14.5	18.00	18.99	1.635	27.79	72.21	72	66	1412.52	1560.28	54.21	54.86	-0.08	21.95
2.25	100	17.9	81	14.3	19.00	20.11	1.600	27.79	72.21	72	66	1412.52	1567.05	53.21	53.85	-0.09	23.46
2.92	100	17.9	80	14.1	20.00	21.23	1.301	27.79	72.21	72	65	1412.52	1573.99	52.21	52.84	-0.10	25.00
120.00	100	17.9	80	14	20.00	21.79	0.033	27.79	72.21	72	65	1412.52	1573.99	52.21	52.84	-0.10	25.00
130.00	100	17.9	80	14	20.00	21.79	0.033	27.79	72.21	72	65	1412.52	1573.99	52.21	52.84	-0.10	25.00

(second settling test) 40:60 sand : polymer weight ratio formulation: (SPG = sandy polymer gel)

	Specific gravity	Volume (cc)	Volume (%)	Mass (gm)
Sand	2.65	15.21	20.42	53.69
Polymer gel	1.012	59.29	79.58	75.13
Salt				5.41

Time (hours)	Init. vol. (cc)	Init. len. (cm)	Measured vol. (cc)	Measured length. (cm)	Settling % (vol)	Settling % (length)	Settling rate (cm/hr)	Sand vol (cc)	Poly gel. Vol. (cc)	Initial porosity (%)	Final porosity (%)	Initial density of SPG (kg/m^3)	Final density of SPG (kg/m^3)	Vol. poly gel in settled layer (cc)	Mass poly gel in settled layer (g)	Porosity change %	Density change %
0.00	100	19	100	19.0	0.00	0.00	0.000	20.42	79.58	80	80	536.93	1288.25			0.00	0.00
0.08	100	19	99	18.7	1.00	1.58	3.750	20.42	79.58	80	79	536.93	1345.66	78.58	79.53	0.00	0.01
0.17	100	19	98	18.5	2.00	2.63	2.941	20.42	79.58	80	79	536.93	1349.07	77.58	78.52	-0.01	0.02
0.25	100	19	97	18.3	3.00	3.68	2.800	20.42	79.58	80	79	536.93	1352.54	76.58	77.50	-0.01	0.03
0.33	100	19	96	18.1	4.00	4.74	2.727	20.42	79.58	80	79	536.93	1356.09	75.58	76.49	-0.01	0.04
0.42	100	19	95	17.9	5.00	5.79	2.619	20.42	79.58	80	79	536.93	1359.71	74.58	75.48	-0.01	0.05
0.58	100	19	94	17.8	6.00	6.32	2.069	20.42	79.58	80	78	536.93	1363.41	73.58	74.47	-0.02	0.06
0.67	100	19	93	17.6	7.00	7.37	2.090	20.42	79.58	80	78	536.93	1367.19	72.58	73.46	-0.02	0.08
0.75	100	19	92	17.4	8.00	8.42	2.133	20.42	79.58	80	78	536.93	1371.05	71.58	72.44	-0.02	0.09
0.83	100	19	91	17.1	9.00	10.00	2.289	20.42	79.58	80	78	536.93	1374.99	70.58	71.43	-0.03	0.10
0.92	100	19	89	16.8	11.00	11.58	2.391	20.42	79.58	80	77	536.93	1383.15	68.58	69.41	-0.03	0.12
1.00	100	19	88	16.6	12.00	12.63	2.400	20.42	79.58	80	77	536.93	1387.37	67.58	68.40	-0.03	0.14
1.08	100	19	87	16.4	13.00	13.68	2.407	20.42	79.58	80	77	536.93	1391.68	66.58	67.38	-0.04	0.15
1.17	100	19	86	16.2	14.00	14.74	2.393	20.42	79.58	80	76	536.93	1396.10	65.58	66.37	-0.04	0.16
1.33	100	19	85	16.0	15.00	15.79	2.256	20.42	79.58	80	76	536.93	1400.62	64.58	65.36	-0.05	0.18
1.58	100	19	84	15.8	16.00	16.84	2.025	20.42	79.58	80	76	536.93	1405.24	63.58	64.35	-0.05	0.19
1.92	100	19	84	15.7	16.00	17.37	1.719	20.42	79.58	80	76	536.93	1405.24	63.58	64.35	-0.05	0.19
2.17	100	19	83	15.6	17.00	17.89	1.567	20.42	79.58	80	75	536.93	1,409.98	62.58	63.34	-0.05	0.20
2.42	100	19	82	15.4	18.00	18.95	1.488	20.42	79.58	80	75	536.93	1,14.83	61.58	62.32	-0.06	0.22
3.92	100	19	79	14.8	21.00	22.11	1.071	20.42	79.58	80	74	536.93	1,430.13	58.58	59.29	-0.07	0.27
4.75	100	19	69	13.0	31.00	31.58	1.263	20.42	79.58	80	70	536.93	1,490.73	48.58	49.17	-2.49	0.45
5.75	100	19	62	11.4	38.00	40.00	1.322	20.42	79.58	80	67	536.93	1,544.78	41.58	42.08	-7.12	0.61
120.00	100	19	62	11.4	38.00	40.00	1.322	20.42	79.58	80	67	536.93	1,544.78	41.58	42.08	-7.12	0.61

(second settling test) 30:70 sand : polymer weight ratio formulation: (SPG = sandy polymer gel)

	Specific gravity	Volume (cc)	Volume (%)	Mass (gm)
Sand	2.65	14.16	14.16	37.23
Polymer gel	1.012	85.84	85.84	81.04
Salt				5.83

Time (hours)	Init. vol. (cc)	Init. len. (cm)	Measured vol. (cc)	Measured length. (cm)	Settling % (vol)	Settling % (length)	Settling rate (cm/hr)	Sand vol (cc)	Poly gel. Vol. (cc)	Initial porosity (%)	Final porosity (%)	Initial density of SPG (kg/m^3)	Final density of SPG (kg/m^3)	Vol. poly gel in settled layer (cc)	Mass poly gel in settled layer (g)	Porosity change %	Density change %
0.0	100	19	100	18.5	0.00	0.00	0.000	14.16	85.84	86	86	1182.72	1182.72			0.00	0.00
0.08	100	19	98	18.3	2.00	1.08	8.750	14.16	85.84	86	86	1182.72	1245.73	83.84	84.85	0.00	2.04
0.17	100	19	97	18	3.00	2.70	5.882	14.16	85.84	86	85	1182.72	1248.14	82.84	83.84	-0.01	3.09
0.25	100	19	96	17.7	4.00	4.32	5.200	14.16	85.84	86	85	1182.72	1250.60	81.84	82.83	-0.01	4.17
0.33	100	19	95	17.5	5.00	5.41	4.545	14.16	85.84	86	85	1182.72	1253.11	80.84	81.81	-0.01	5.26
0.50	100	19	94	17.3	6.00	6.49	3.400	14.16	85.84	86	85	1182.72	1253.11	79.84	80.80	-0.01	6.38
0.67	100	19	92	17	8.00	8.11	2.985	14.16	85.84	86	85	1182.72	1255.67	77.84	78.78	-0.01	8.70
0.75	100	19	90	16.4	10.00	11.35	3.467	14.16	85.84	86	84	1182.72	1255.67	75.84	76.75	-0.02	11.11
0.83	100	19	85	15.6	15.00	15.68	4.096	14.16	85.84	86	83	1182.72	1260.97	70.84	71.69	-0.03	17.65
0.92	100	19	80	14.7	20.00	20.54	4.674	14.16	85.84	86	82	1182.72	1266.50	65.84	66.63	-0.04	25.00
1.00	100	19	76	14.1	24.00	23.78	4.900	14.16	85.84	86	81	1182.72	1281.47	61.84	62.59	-0.05	31.58
1.08	100	19	70	12.8	30.00	30.81	5.741	14.16	85.84	86	80	1182.72	1298.31	55.84	56.51	-0.07	42.86
1.17	100	19	65	11.9	35.00	35.68	6.068	14.16	85.84	86	78	1182.72	1313.38	50.84	51.45	-0.09	53.85
1.25	100	19	60	11	40.00	40.54	6.400	14.16	85.84	86	76	1182.72	1339.22	45.84	46.39	-0.11	66.67
1.33	100	19	55	10	45.00	45.95	6.767	14.16	85.84	86	74	1182.72	1364.39	40.84	41.33	-0.13	81.82
1.42	100	19	40	7.1	60.00	61.62	8.380	14.16	85.84	86	65	1182.72	1393.75	25.84	26.15	-0.25	150.00
1.50	100	19	37	6.5	63.00	64.86	8.333	14.16	85.84	86	62	1182.72	1428.46	22.84	23.12	-0.28	170.27
2.17	100	19	34	6	66.00	67.57	5.991	14.16	85.84	86	58	1182.72	1685.68	19.84	20.08	-0.32	194.12
2.83	100	19	32	5.1	68.00	72.43	4.912	14.16	85.84	86	56	1182.72	1727.79	17.84	18.06	-0.35	212.50
6.33	100	19	29	4.2	71.00	77.30	2.338	14.16	85.84	86	51	1182.72	1801.83	14.84	15.02	-0.40	244.83
120.00	100	19	29	4.2	71.00	77.30	2.338	14.16	85.84	86	51	1182.72	1801.83	14.84	15.02	-0.40	244.83

(second settling test) 20:80 sand : polymer weight ratio formulation: (SPG = sandy polymer gel)

	Specific gravity	Volume (cc)	Volume (%)	Mass (gm)
Sand	2.65	7.60	8.78	23.08
Polymer gel	1.012	79.05	91.22	86.12
Salt				6.20

Time (hours)	Init. vol. (cc)	Init. len. (cm)	Measured vol. (cc)	Measured length. (cm)	Settling % (vol)	Settling % (length)	Settling rate (cm/hr)	Sand vol (cc)	Poly gel. Vol. (cc)	Initial porosity (%)	Final porosity (%)	Initial density of SPG (kg/m^3)	Final density of SPG (kg/m^3)	Vol. poly gel in settled layer (cc)	Mass poly gel in settled layer (g)	Porosity change %	Density change %
0.00	100	19	100	18.9	0.00	0.00	0.000	8.78	91.22	91	91	1092.00	1092.00			0.00	0.00
0.08	100	19	99	18.7	1.00	1.06	3.750	8.78	91.22	91	91	1092.00	1155.42	90.22	91.31	0.00	0.01
0.17	100	19	98	18.4	2.00	2.65	3.529	8.78	91.22	91	91	1092.00	1156.89	89.22	90.30	0.00	0.02
0.25	100	19	97	18.2	3.00	3.70	3.200	8.78	91.22	91	91	1092.00	1158.38	88.22	89.28	0.00	0.03
0.33	100	19	96	17.9	4.00	5.29	3.333	8.78	91.22	91	91	1092.00	1159.91	87.22	88.27	0.00	0.04
0.42	100	19	95	17.7	5.00	6.35	3.095	8.78	91.22	91	91	1092.00	1161.46	86.22	87.26	-0.01	0.05
0.50	100	19	94	17.5	6.00	7.41	3.000	8.78	91.22	91	91	1092.00	1163.05	85.22	86.25	-0.01	0.06
0.58	100	19	92	17.2	8.00	8.99	3.103	8.78	91.22	91	90	1092.00	1166.34	83.22	84.22	-0.01	0.09
0.67	100	19	90	16.7	10.00	11.64	3.433	8.78	91.22	91	90	1092.00	1169.77	81.22	82.20	-0.01	0.11
0.75	100	19	85	15.8	15.00	16.40	4.267	8.78	91.22	91	90	1092.00	1179.05	76.22	77.14	-0.02	0.18
0.83	100	19	80	14.8	20.00	21.69	5.060	8.78	91.22	91	89	1092.00	1189.49	71.22	72.08	-0.02	0.25
0.92	100	19	70	13.1	30.00	30.69	6.413	8.78	91.22	91	87	1092.00	1214.84	61.22	61.96	-0.04	0.43
1.00	100	19	60	11	40.00	41.80	8.000	8.78	91.22	91	85	1092.00	1248.65	51.22	51.84	-0.06	0.67
1.08	100	19	50	9.1	50.00	51.85	9.167	8.78	91.22	91	82	1092.00	1295.98	41.22	41.72	-0.10	1.00
1.17	100	19	40	7.1	60.00	62.43	10.171	8.78	91.22	91	78	1092.00	1366.97	31.22	31.60	-0.14	1.50
1.25	100	19	25	4.3	75.00	77.25	11.760	8.78	91.22	91	65	1092.00	1579.96	16.22	16.42	-0.29	3.00
2.67	100	19	25	4.3	75.00	77.25	5.506	8.78	91.22	91	65	1092.00	1579.96	16.22	16.42	-0.29	3.00
2.75	100	19	20	3.4	80.00	82.01	5.673	8.78	91.22	91	56	1092.00	1721.94	11.22	11.36	-0.38	4.00
3.67	100	19	18	3	82.00	84.13	4.360	8.78	91.22	91	51	1092.00	1800.83	9.22	9.34	-40.30	4.56
120.00	100	19	18	3	82.00	84.13	4.360	8.78	91.22	91	51	1092.00	1800.83	9.22	9.34	-40.30	4.56

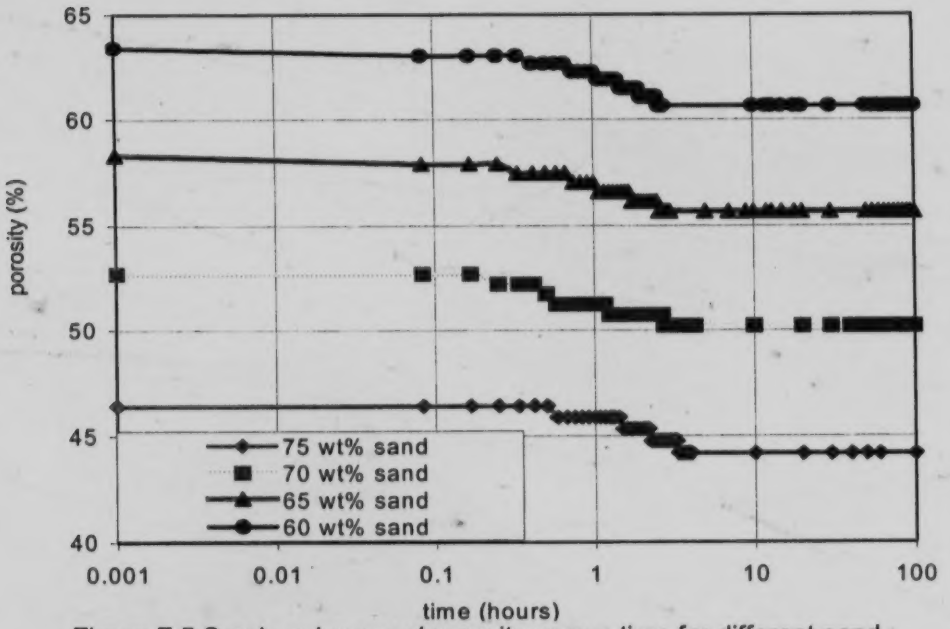

Figure F.5 Sandy polymer gel porosity versus time for different sand concentrations (second settling test).

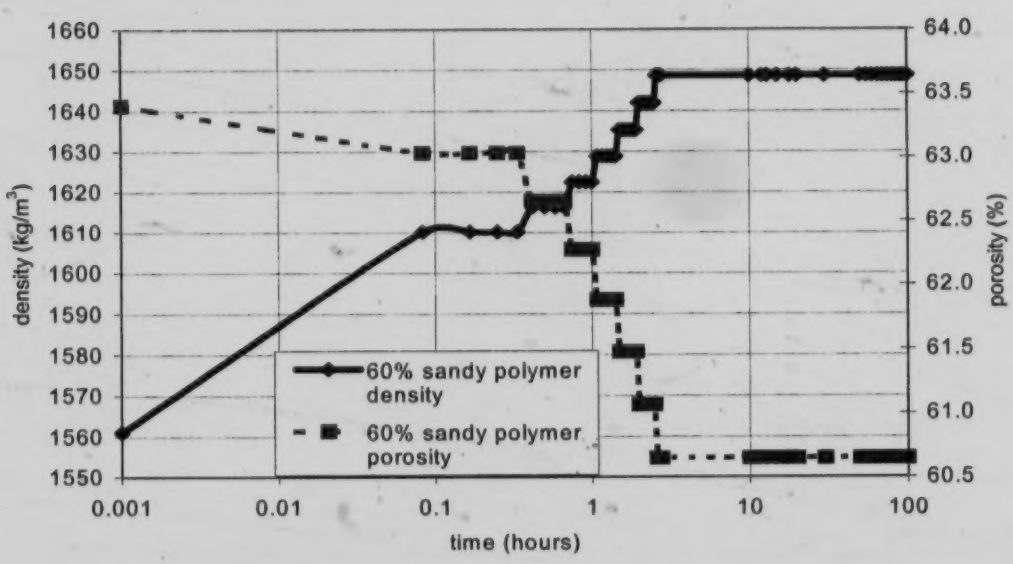

Figure F.6 60 wt% sandy polymer gel density and porosity versus time (second settling test).

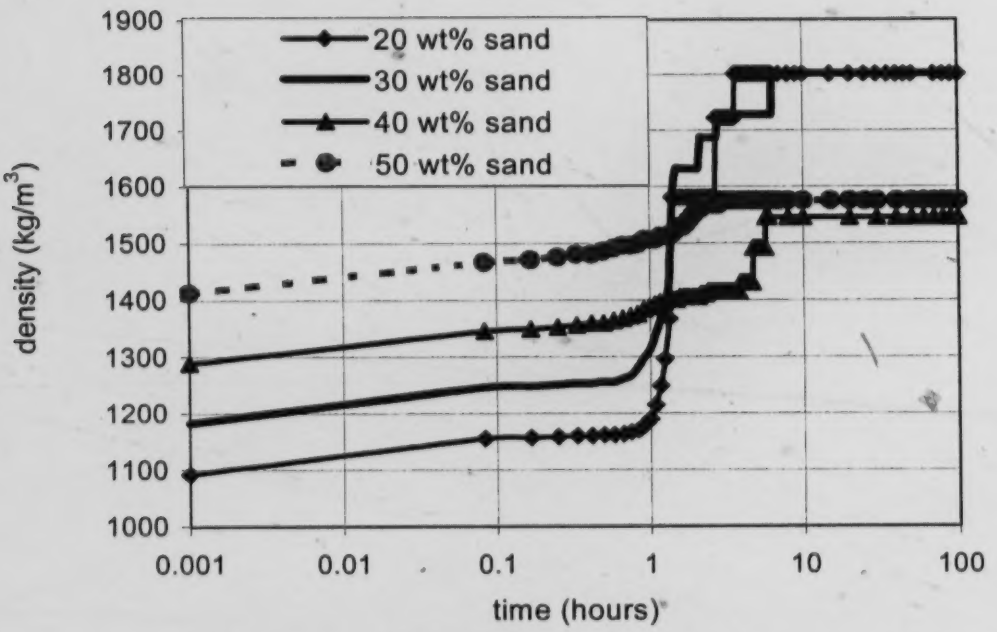

Figure F.7 Sandy polymer gel densities of settled sand layer for low sand concentrations (second settling test).

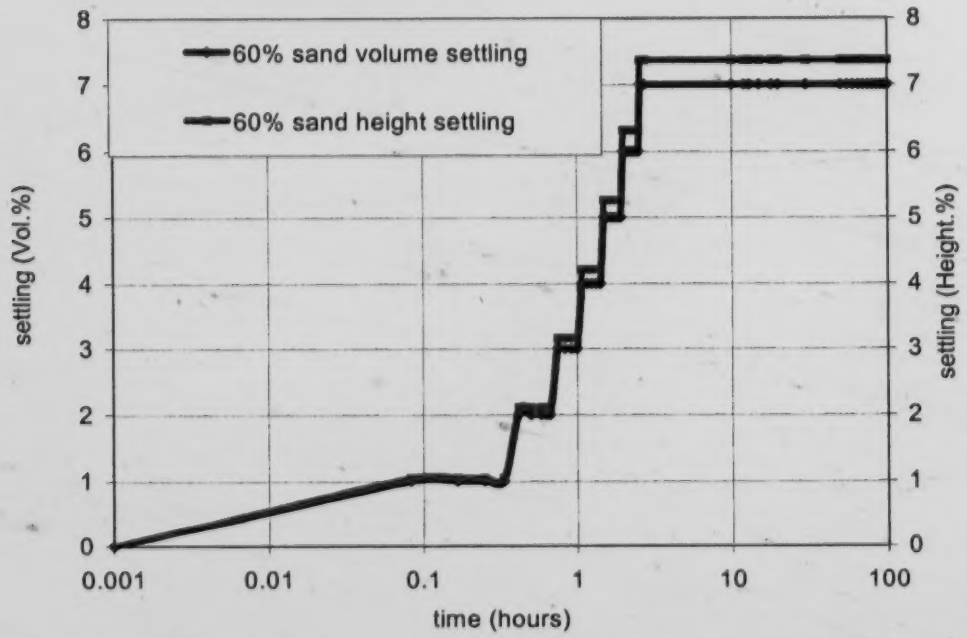

Figure F.8 Settling of sand in 60 wt% sand polymer gel in terms of height and volume percentage (second settling test).

Appendix G:
Effect of geometry on slippage

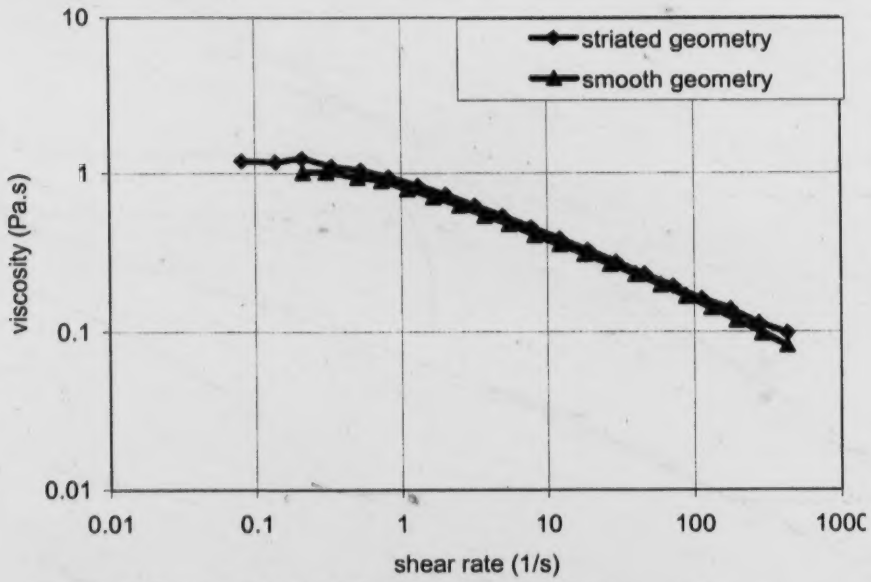

Figure G.1 Slip effect (1.5 hour delay), pure gel (no sand).

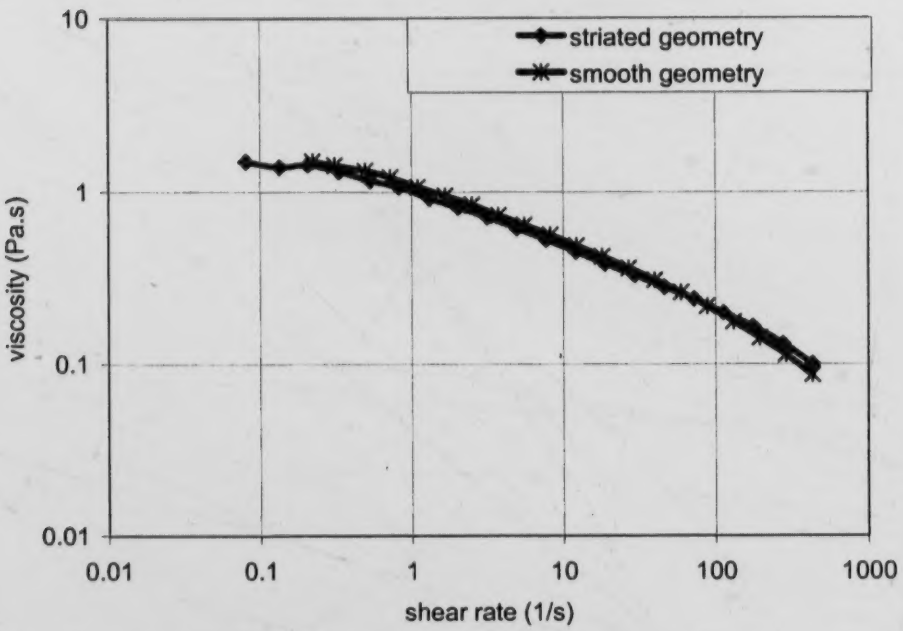

Figure G.2 Slip effect (2.5 hour delay), pure gel (no sand).

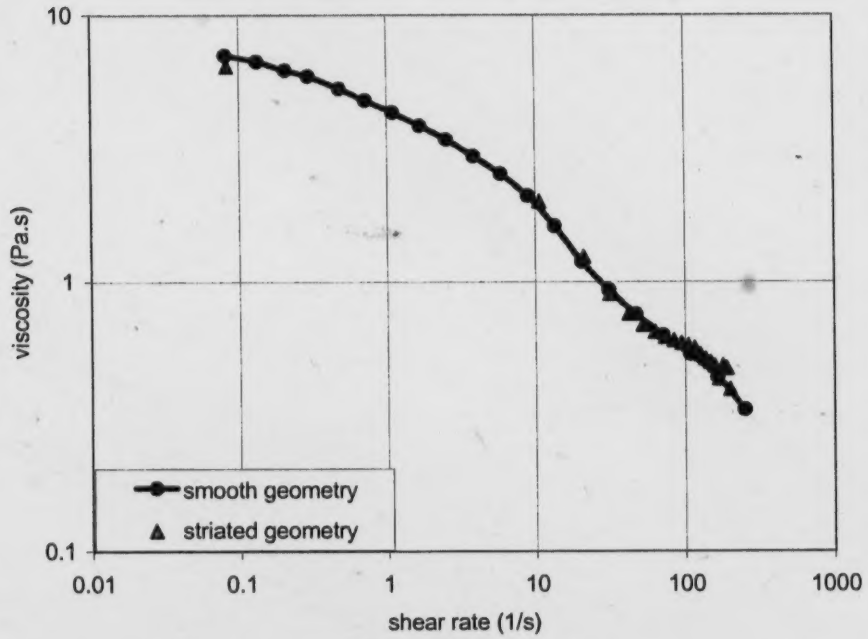

Figure G.3 Slip effect for 60 wt% sandy polymer gel (no delay).

Appendix H: Rheological models fitted

H.1 Rheological models

Casson model

The shear stress is given by:

$$\tau = \sqrt[n]{\tau_0^n + (\overset{0}{\gamma}\eta_0)^n} \qquad \text{(H.1)}$$

The viscosity is given by:

$$\eta = \sqrt[n]{(\tau_0/\gamma)^n + (\eta_0)^n} \qquad \text{(H.2)}$$

Cross model

The shear stress is given by:

$$\tau = \gamma(\eta_\infty + (\eta_0 - \eta_\infty))/(1 + (\gamma/\gamma_b)^n) \qquad \text{(H.3)}$$

The viscosity is given by:

$$\eta = \eta_\infty + (\eta_0 - \eta_\infty)/(1 + (\gamma/\gamma_b)^n) \qquad \text{(H.4)}$$

Bingham model

The shear stress is given by:

$$\tau = \tau_0 + \eta_0\gamma \qquad \text{(H.5)}$$

The viscosity is given by ($\tau > \tau_o$)

$$\eta = \tau_0/\gamma \qquad \text{(H.6)}$$

Rheological models fitted

Table H.1 Carreau and Herschel-Bulkley (H-B) rheological models fitted to the sheared sandy polymer slurries.
(R = 1 perfect fit)

Model	Parameters								Sand concentration
	η_o	η_∞	λ	n	a	k	τ_o	R (regression coefficient)	
Carreau model	1.39	0.000	1.323	0.6655	2			0.9952	40% no delay
Carreau model	9.41	0.000	5.296	0.4718	2			0.9929	40% 1.5 hour delay
Carreau model	7.029	0.000	3.985	0.5191	2			0.9814	40% 2.5 hour delay
Carreau model	2.43	0.000	0.5581	0.5406	2			0.9917	50% no delay
Carreau model	8.228	0.000	4.487	0.5271	2			0.9821	50% 1.5 hour delay
Carreau model	22.6	0.000	11.67	0.4748	2			0.986	50% 2.5 hour delay
Carreau model	27.2	0.000	7.495	0.4272	2			0.9661	60% no delay
Carreau model	15.08	0.000	1.306	0.3564	2			0.958	60% no delay
Carreau model	350.6	0.000	141.5	0.337	2			0.9831	60% 1.5 hour delay
H-B model				0.4559		13.47	1.627	0.9751	60% 2.5 hour delay
Carreau model	11.33	0.000	0.5005	0.2852	2			0.972	65% no delay
H-B model				0.533		8.629	2.277	0.9908	65% 1.5 hour delay
HI-B model				0.4738		14.71	2.395	0.9987	65% 2.5 hour delay
H-B model				0.5276		85.01	42.56	0.9952	75% 1.5 hour delay

Table H.2 Rheological models fitted to the sheared sandy polymer slurries.
(R = 1 perfect fit)

Model	Parameters						Sand concentration
	η_o	η_∞	n	γ_b^o	k	R (regression coefficient)	
Power law			0.801		0.4874	0.9988	20% no delay
Power law			0.7524		0.6887	0.9943	20% 1.5 hour delay
Power law			0.9861		0.1986	0.9938	20% 2.5 hour delay
Power law			0.8264		0.4502	0.9959	30% no delay
Power law			0.6404		1.2336	0.9886	30% 1.5 hour delay
Power law			0.9437		0.2703	0.9946	30% 2.5 hour delay
Cross model	39.71	0.3167	1.104	1.072		0.9805	60% no delay
Cross model	48.92	0.2428	0.8487	0.3973		0.9698	60% 1.5 hour delay
Cross model	192.5	0.3313	0.907	0.1453		0.9399	65% 1.5 hour delay

Cross model	109.3	1.264	1.901	2.321		0.9553	70 % on delay
Cross model	103.6	1.042	2.07	2.462		0.9729	70% 1.5 hour delay
Cross model	262.2	1.038	1.515	1.181		0.95	70% 2.5 hour delay
Power law			0.3794		75.66	0.9945	75 % no delay
Power law			0.3498		88.05	0.996	75% 1.5 hour delay
Power law			0.2867		167	0.9872	75% 2.5 hour delay

Table H.3 Carreau and Herschel-Bulkley (H-B) rheological models fitted to unsheared sandy polymer slurries.
(R = 1 perfect fit)

Model	Parameters								Sand concentration
	η_o	η_∞	λ	n	a	k	τ_o	R (regression coefficient)	
Carreau model	1.543	0.000	1.093	0.6643	2			0.9917	30% unsheared no delay
H-B model				0.6563		1.299	1.742	0.9778	30% unsheared 1.5 hour delay
H-B model				0.5751		2.026	1.429	0.972	30% unsheared 2.5 hour delay
Carreau model	1.336	0.000	0.066	0.4044	2			0.9892	40% unsheared 2.5 hour delay
Carreau model	9.63	0.000	2.149	0.4504	2			0.995	50% unsheared no delay
Carreau model	7.886	0.000	1.508	0.4468	2			0.9965	50% unsheared 1.5 hour delay
Carreau model	13.73	0.000	2.032	0.4321	2			0.9997	50% unsheared 2.5 hour delay
Carreau model	37.93	0.000	7.532	0.4242	2			0.9871	60% unsheared no delay
Carreau model	23.3	0.000	2.967	0.4082	2			0.9716	60% unsheared 1.5 hour delay
Carreau model	33.42	0.000	5.799	0.4110	2			0.9963	60% unsheared 2.5 hour delay
Carreau model	154	0.000	214.7	0.5234	2			0.9925	65% unsheared 1.5 hour delay
H-B model				0.4742		31.37	9.131	0.9921	65% unsheared 2.5 hour delay
Carreau model	197.9	0.000	55.47	0.4137	2			0.9931	70% unsheared no delay
Carreau model	2669	0.000	1950	0.3798	2			0.9984	70% unsheared 1.5 hour delay
H-B model				0.5296		35.16	182.9	0.9983	70% unsheared 1.5 hour delay
H-B model				0.5296		35.16	182.9	0.9983	70% unsheared 2.5 hour delay
H-B model				0.5071		13.46	10.43	0.9961	75% unsheared no delay
Carreau model	992	0.000	13.14	0.1468	2			0.9924	75% unsheared 1.5 hour delay

Table H.4 Unsheared rheological models fitted to the sandy polymer slurries.
(R = 1 perfect fit)

Model	Parameters						Sand concentration
	η_o	η_∞	n	$\dot{\gamma}_o$	k	R (regression coefficient)	
Cross model	49.14	0.07	0.6736	0.2894		0.9766	65% unsheared no delay
Power law			0.7018		1.3942	0.9959	40% unsheared no delay
Power law			0.6859		1.4177	0.9864	40% unsheared 1.5 hour delay
Power law			0.1948		225.17	0.931	75% unsheared 2.5 hour delay

Table H.5 Rheological models fitted to the crosslinked polymer (pure gel).
(R = 1 perfect fit)

Model	Parameters						Sand concentration
	η_o	η_∞	λ	n	a	R (regression coefficient)	
Carreau model	1.193	0.00	2.606	0.6539	2	0.9909	no delay
Carreau model	1.196	0.00	2.4	0.662	2	0.9950	1.5 hour delay
Carreau model	1.299	0.00	3.128	0.683	2	0.9855	2.5 hour delay
Carreau model	0.8808	0.00	1.355	0.6402	2	0.9962	no delay
Carreau model	0.9634	0.00	1.536	0.6562	2	0.9949	1.5 hour delay
Carreau model	1.424	0.00	2.419	0.6500	2	0.9912	2.5 hour delay

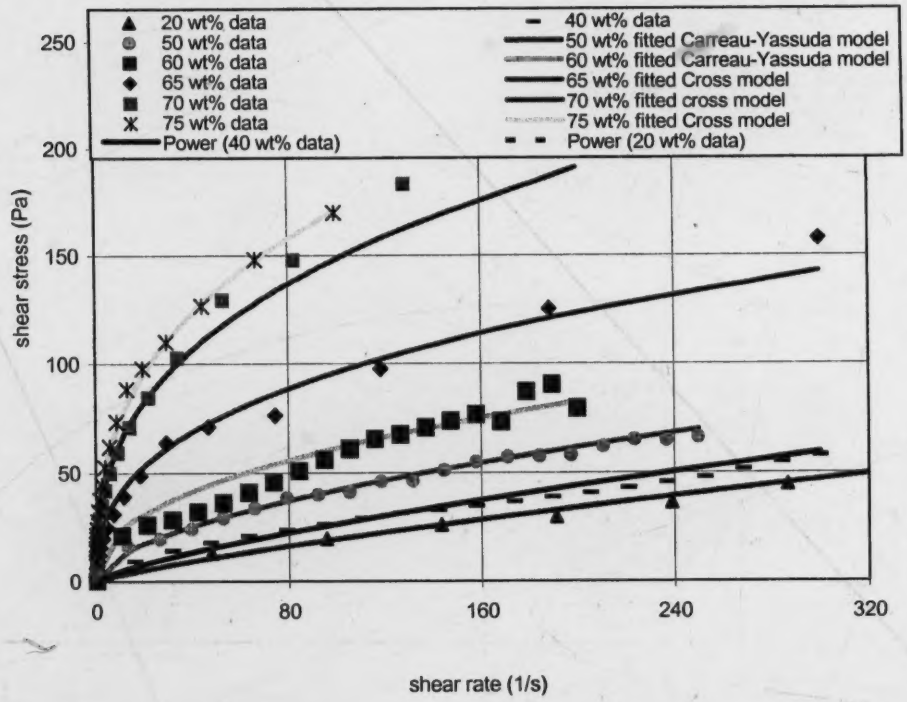

Figure H.1 Shear stress versus shear rate for different sand concentrations (data fitted with different models).

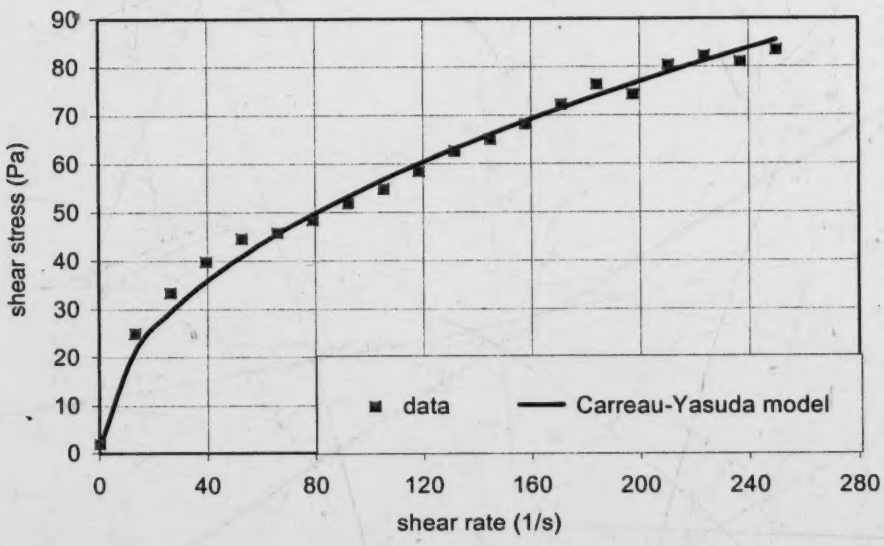

Figure H.2 Shear stress versus shear rate for 60 wt% sandy polymer slurry (data fitted to Carreau-Yasuda rheological model, no delay).

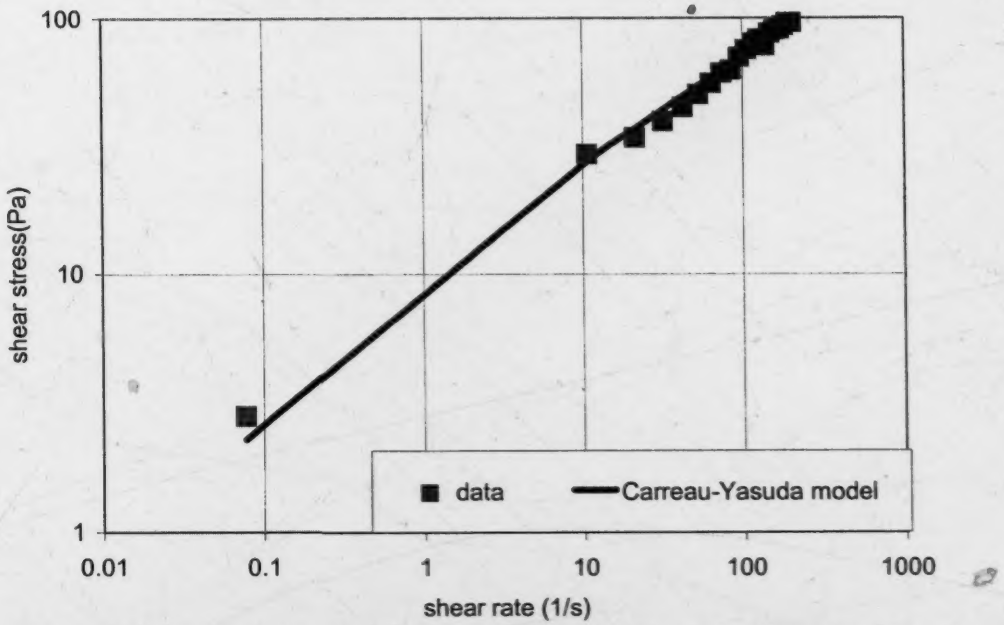

Figure H.3 Shear stress versus shear rate for 60 wt% sand polyacrylamide gel slurry (data fitted to Carreau-Yasuda rheological model, 1.5 hour delay).

Appendix I:
Viscosity of sandy polymer gels

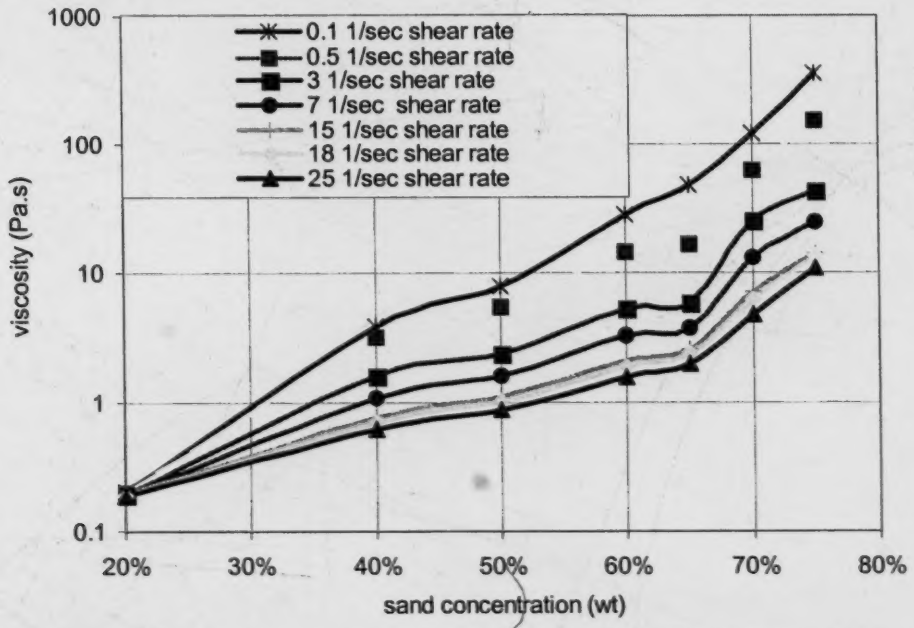

Figure I.1 Viscosity versus sand concentrations (1.5 hour delay, striated geometry).

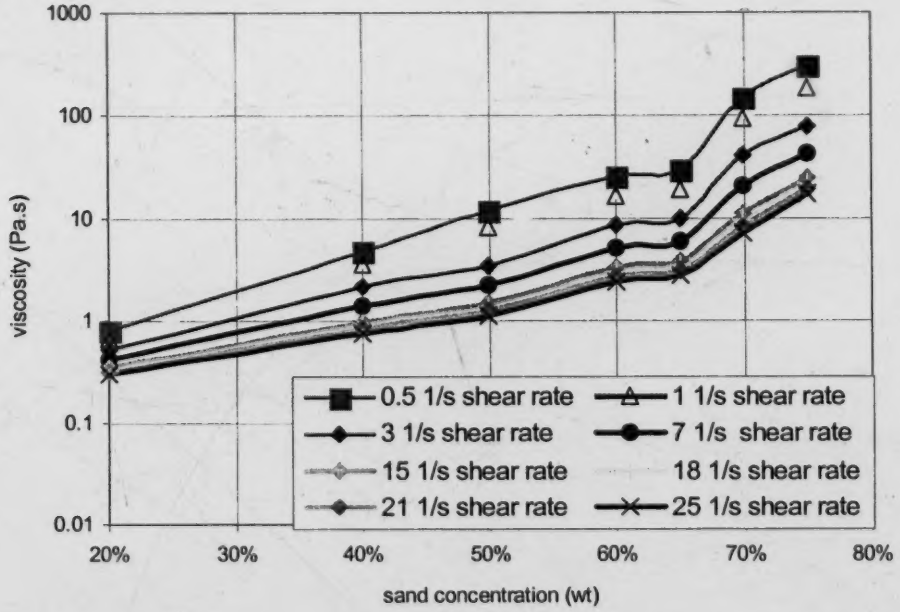

Figure I.2 Viscosity versus sand concentrations (2.5 hour delay, striated geometry).

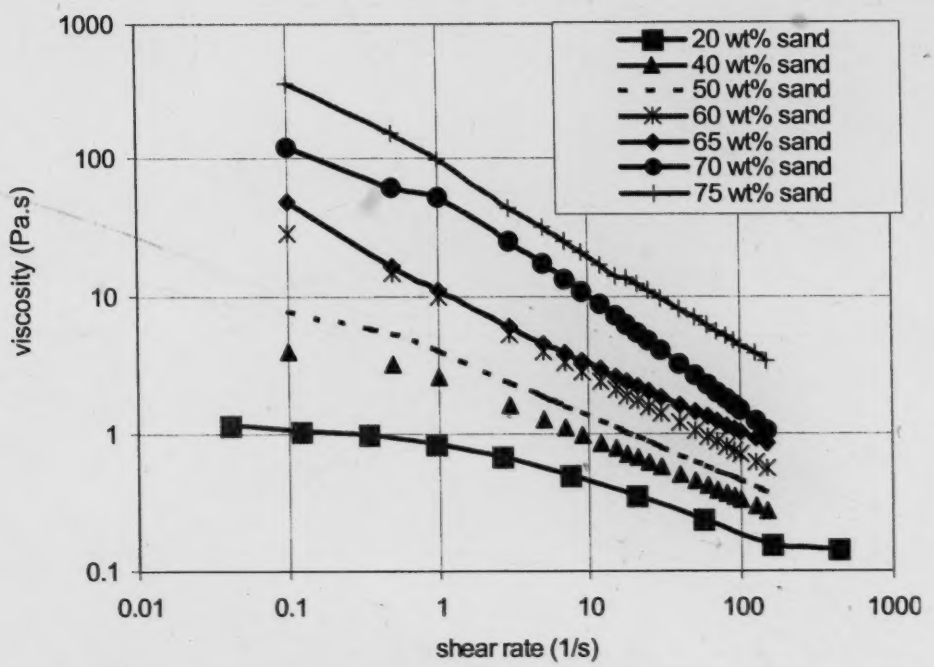

Figure I.3 Viscosity versus shear rate striated geometry (1.5 hour delay). Sandy polymer slurries.

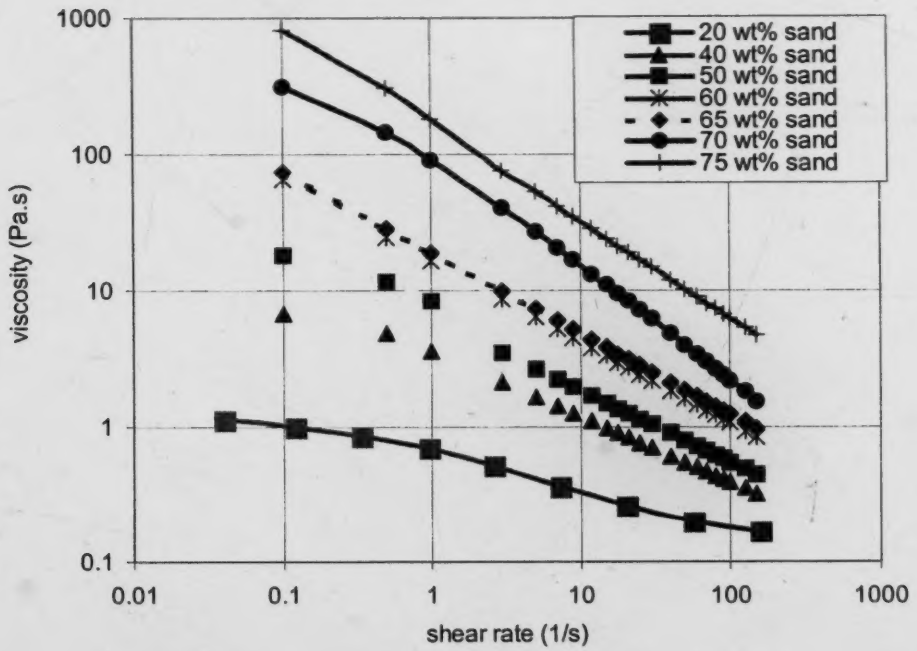

Figure I.4 Viscosity versus shear rate striated geometry (2.5 hour delay). Sandy polymer slurries.

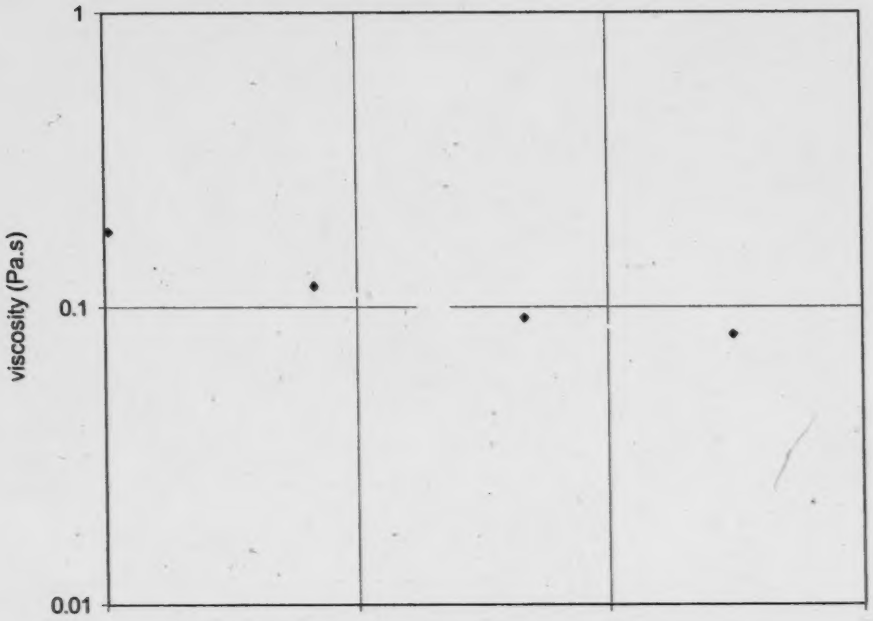

Figure I.5 Viscosity versus shear rate for the 60 wt% sandy polymer gel (capillary tube viscometer).

Appendix J:
Relative viscosity of sandy polymer gels

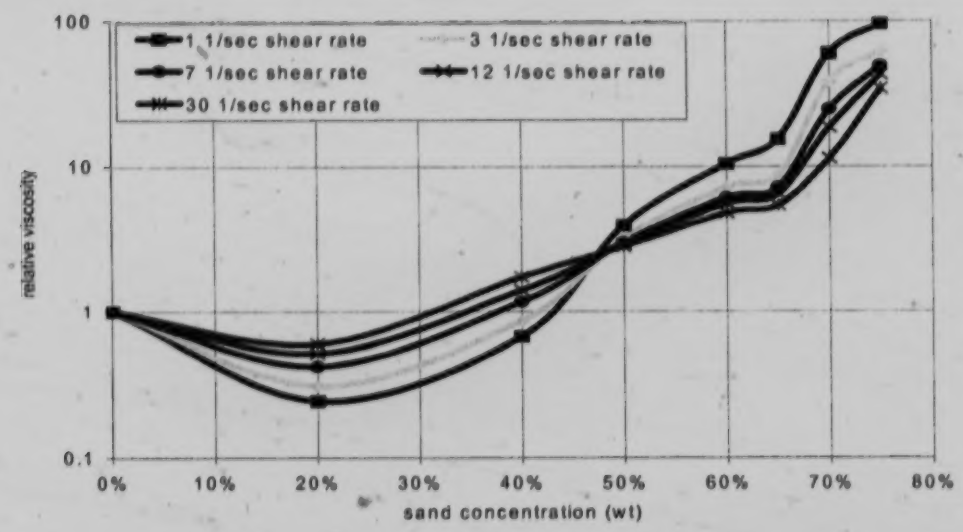

Figure J.1 Relative viscosity versus sand concentration (striated geometry, no delay, sheared samples).

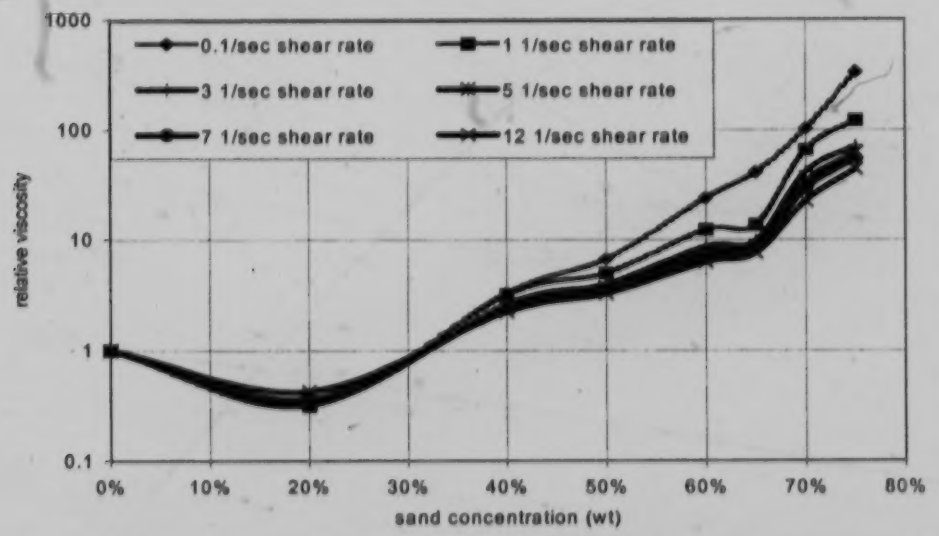

Figure J.2 Relative viscosity versus sand concentration (striated geometry, 1.5 hour delay, sheared samples).

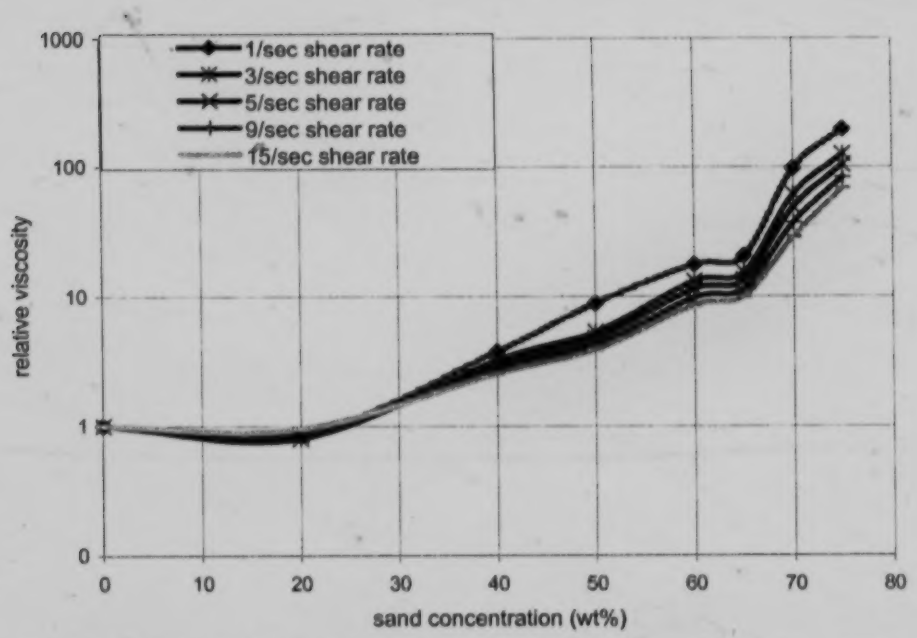

Figure J.3 Relative viscosity versus sand concentration. (striated geometry, 2.5 hour delay, presheared samples).

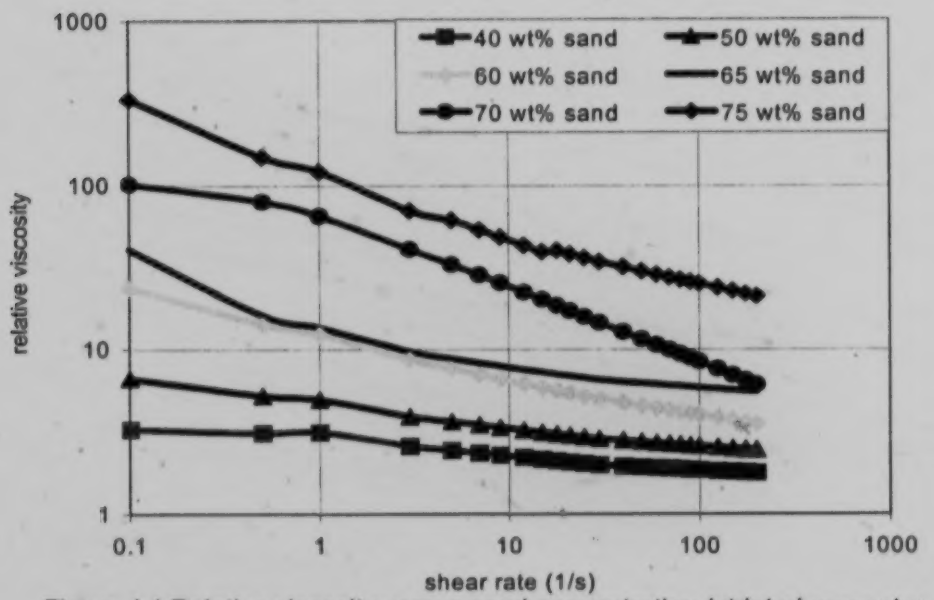

Figure J.4 Relative viscosity versus sand concentration (striated geometry, 1.5 hour delay, sheared samples).

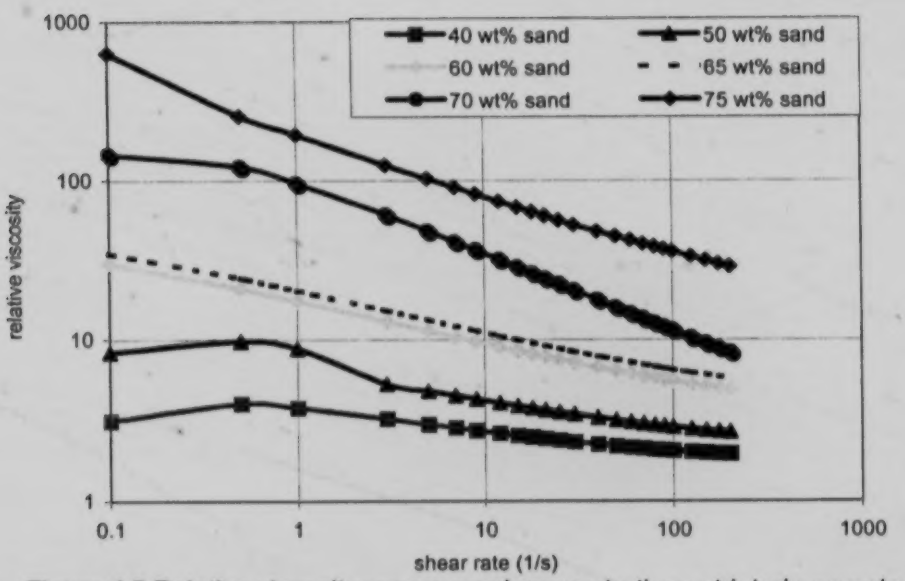

Figure J.5 Relative viscosity versus sand concentrations striated geometry, 2.5 hour delay, sheared samples).

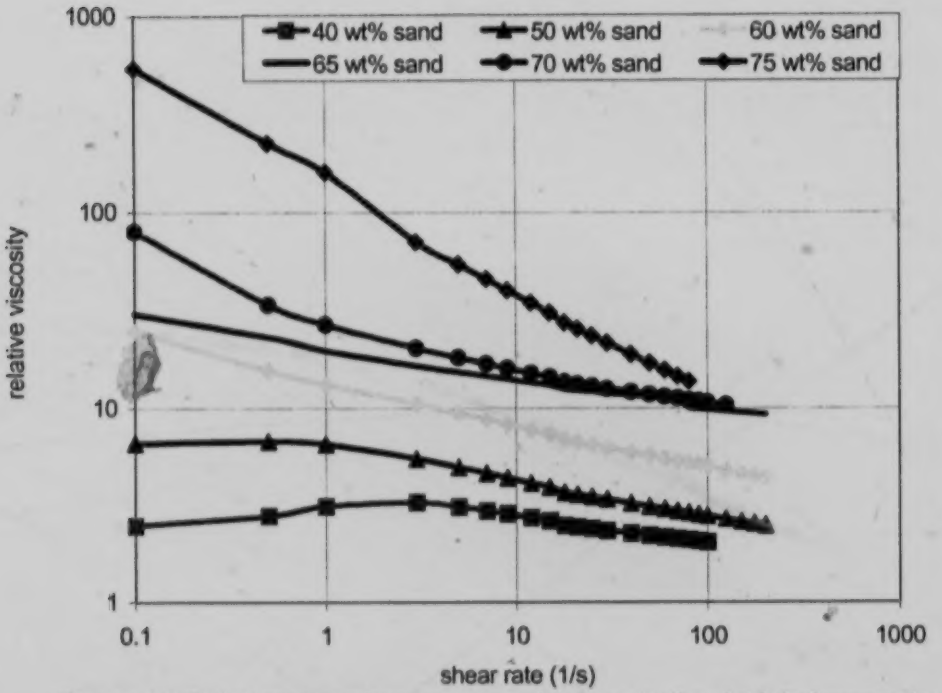

Figure J.6 Relative viscosity versus sand concentration (striated geometry, 1.5 hour delay, unsheared samples).

Appendix K:
60 wt% sandy polyacrylamide slurries

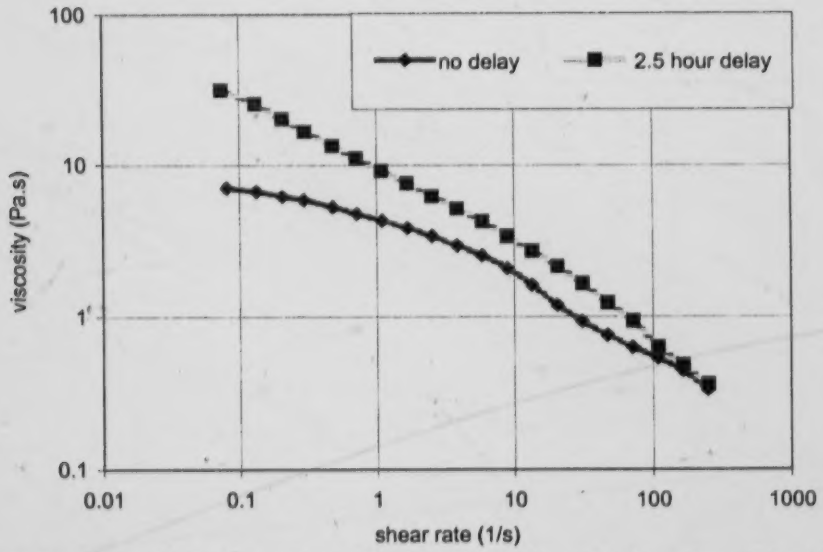

Figure K.1 60 wt% sandy polyacrylamide slurry viscosity (presheared, striated geometry).

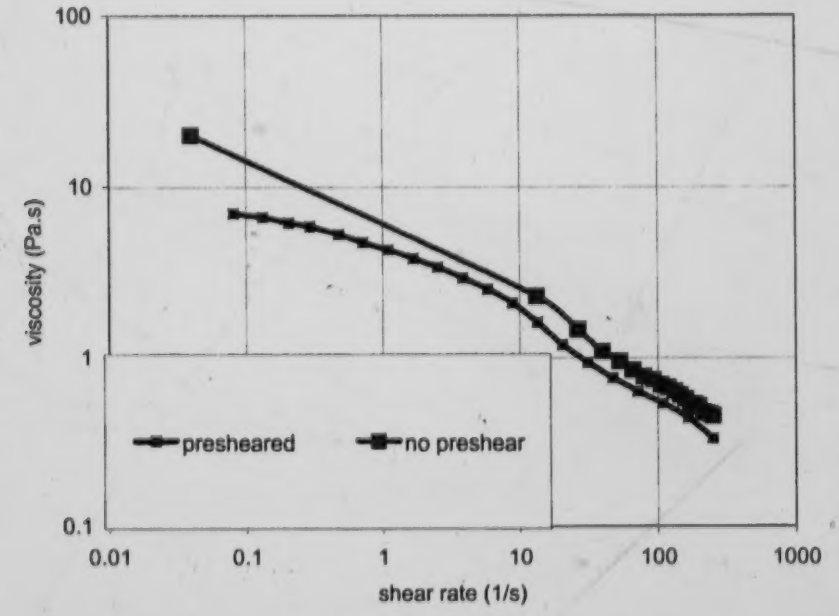

Figure K.2 Preshear effect on 60 wt% sandy polyacrylamide slurry viscosity (no delay, smooth geometry).

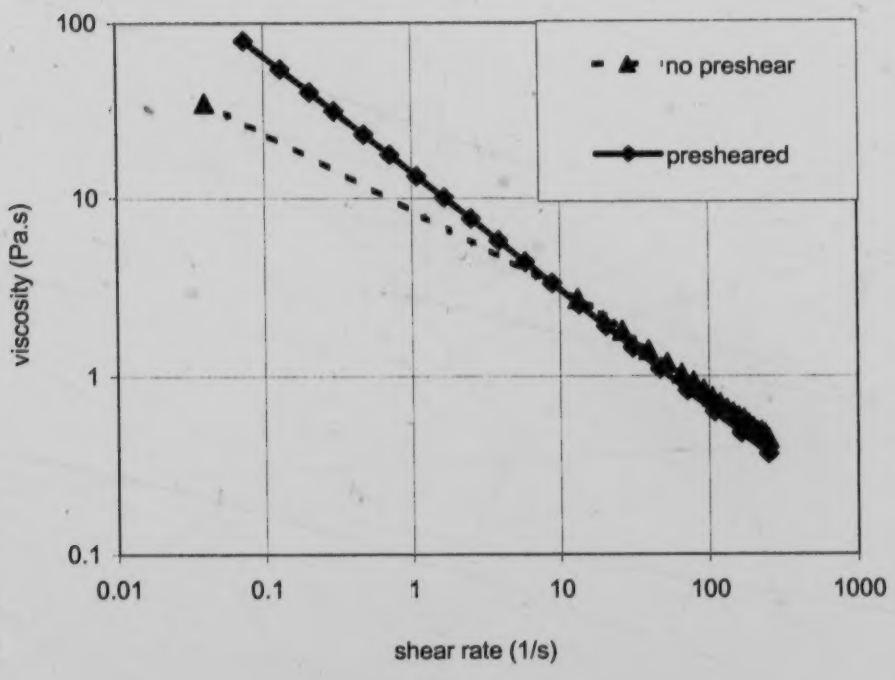

Figure K.3 Preshear effect on 60 wt% sandy polyacrylamide slurry (0.5 hour delay, smooth geometry).

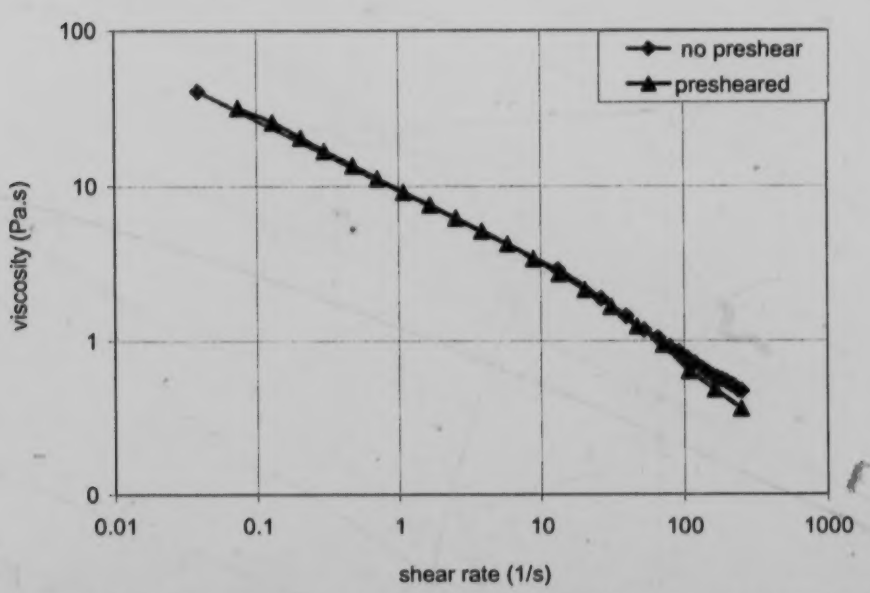

Figure K.4 Preshear effect on 60 wt% sandy polyacrylamide viscosity (2.5 hour delay, smooth geometry).

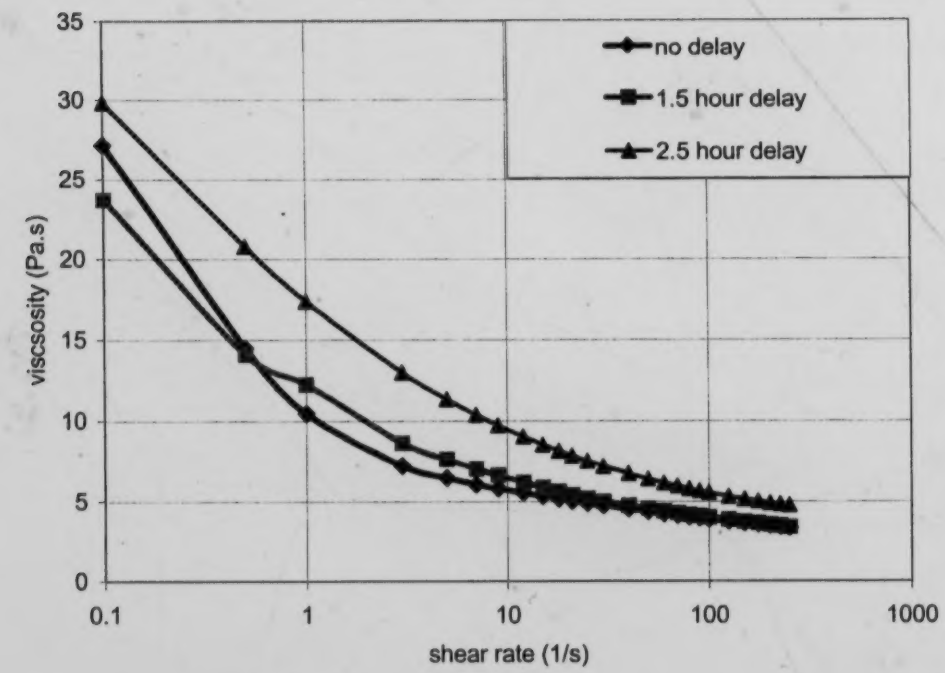

Figure K.5 Effect of delay time on 60 wt% sandy polyacrylamide slurry (striated geometry).

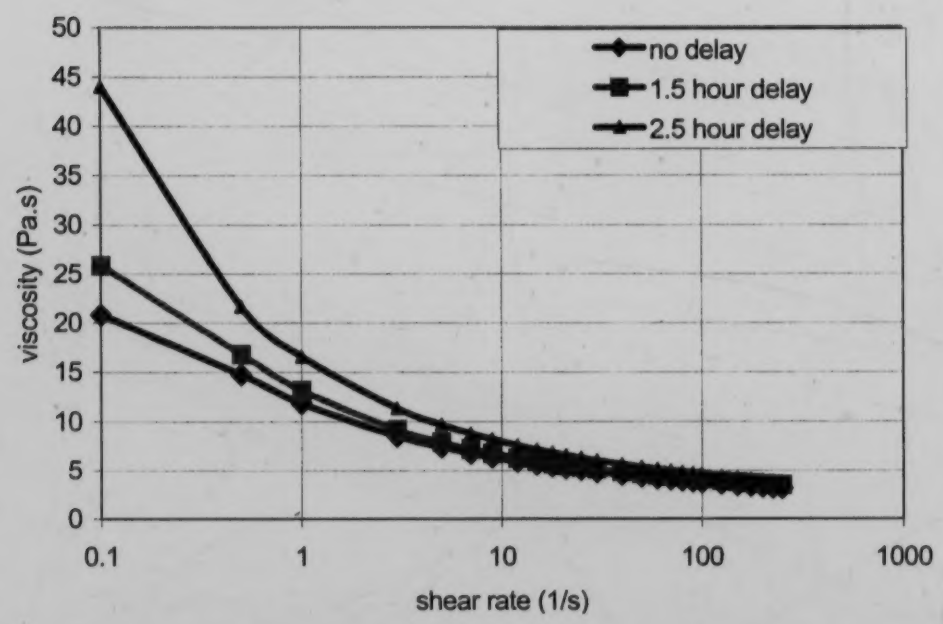

Figure K.6 Effect of delay time on 60 wt% sandy polyacrylamide slurry (smooth geometry).

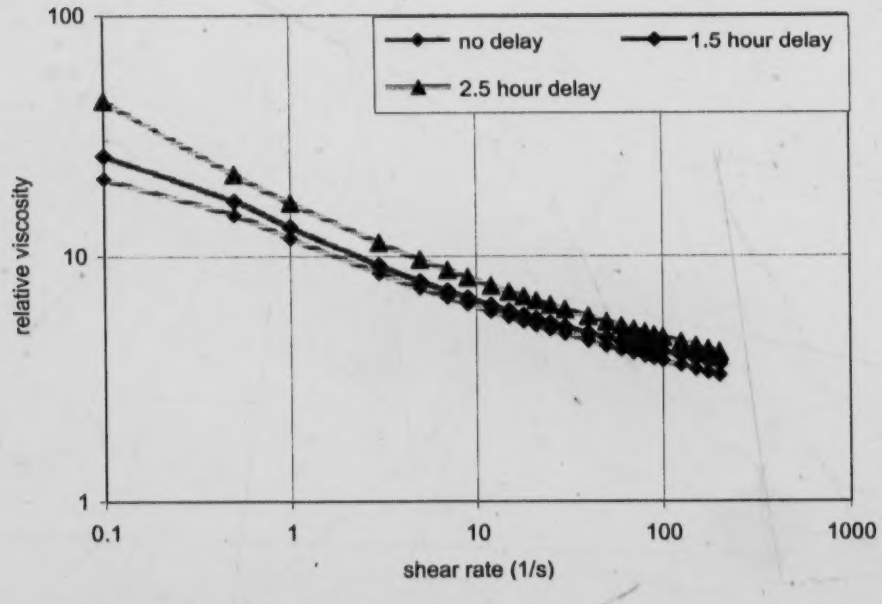

Figure K.7 Effect of delay time on 60 wt% sandy polyacrylamide slurry relative viscosity (smooth geometry).

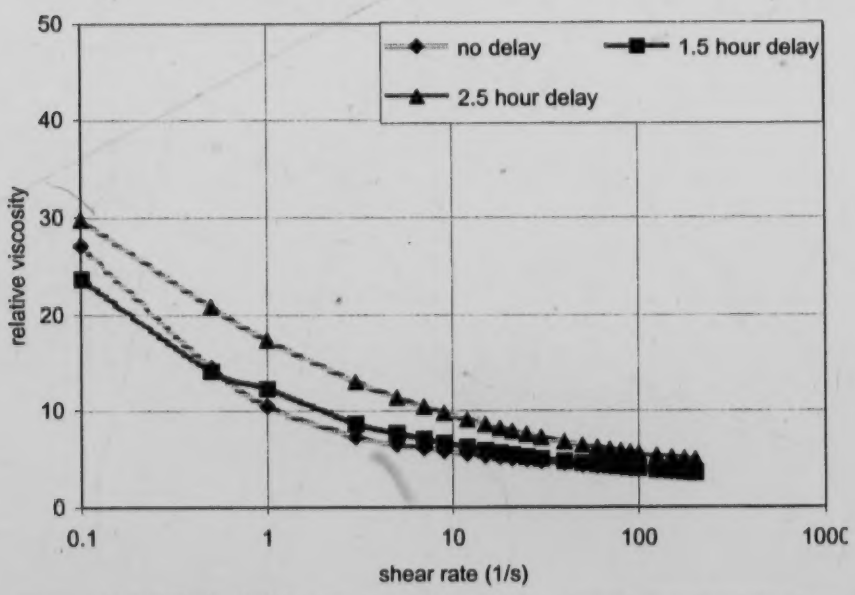

Figure K.8 Effect of delay time on 60 wt% sandy polyacrylamide slurry relative viscosity (striated geometry).

Appendix L:
First water shut-off experiment

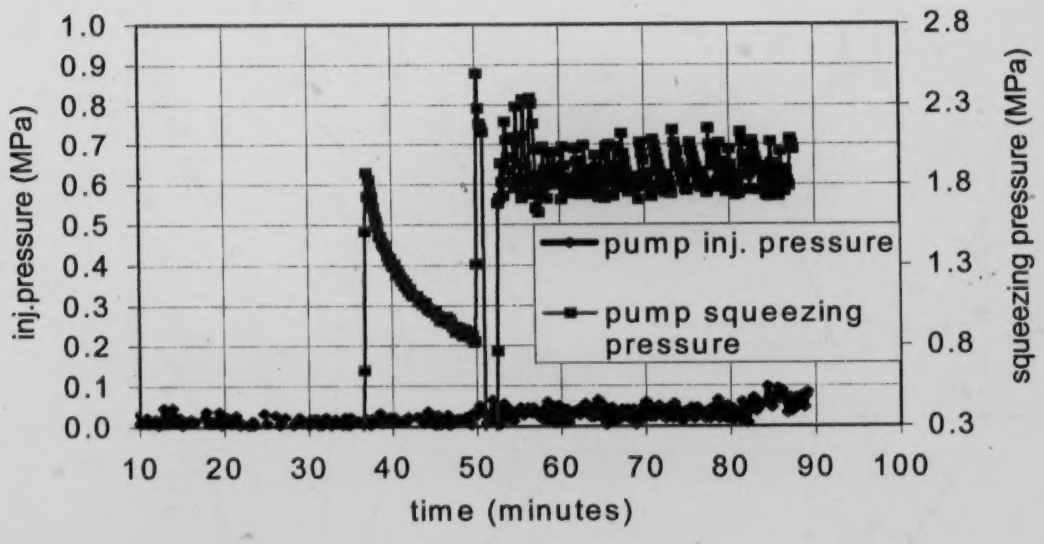

Figure L.1 Injection and squeezing pressures (first water shut-off experiment (first part)).

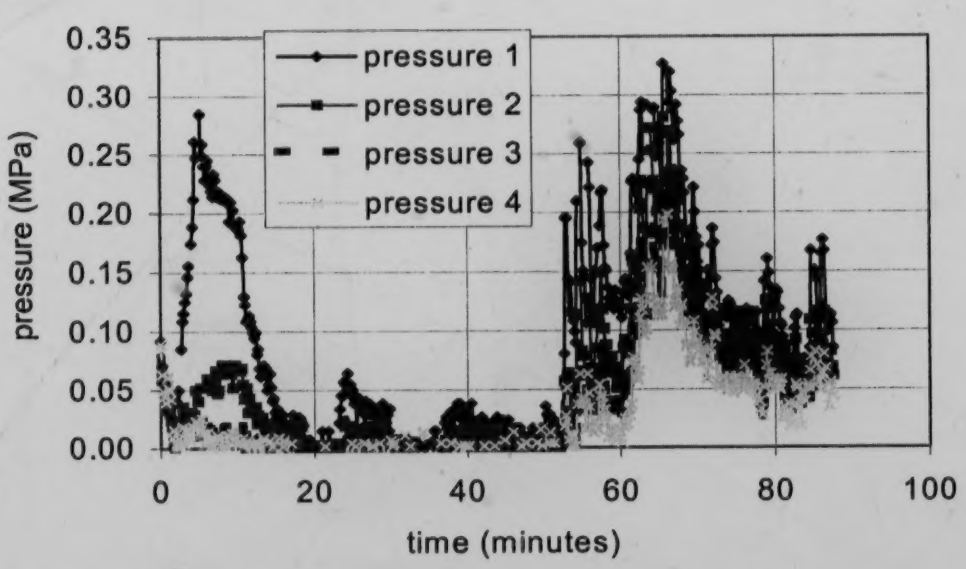

Figure L.2 Pressure versus time during crosslinked polymer squeezing into annulus (first water shut-off experiment (first part)). See Figure 3.3 for pressure port locations.

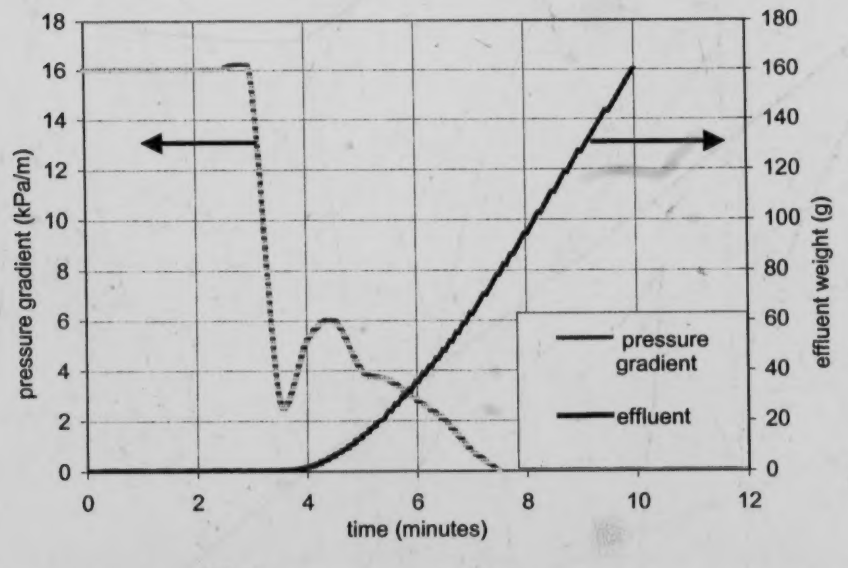

Figure L.3 Water breakthrough test (first water shut-off experiment (first part)).

Appendix M:
Second water shut-off experiment

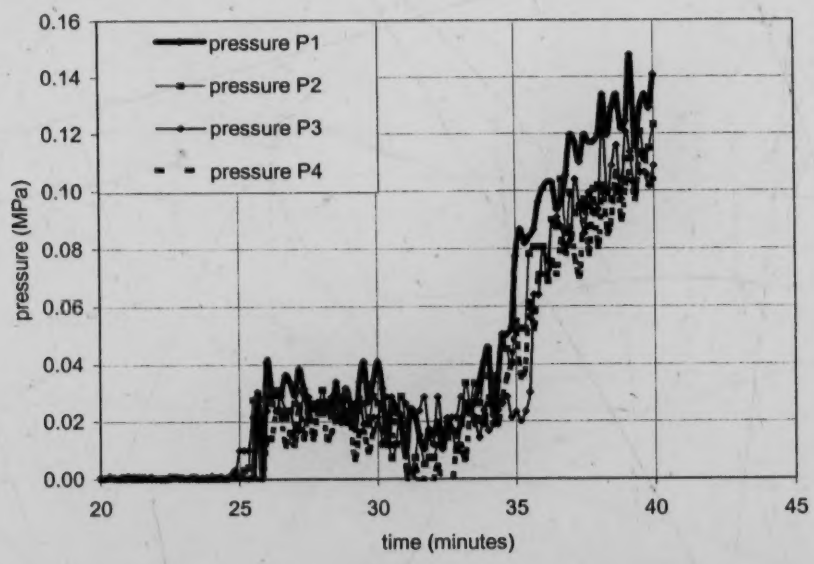

Figure M.1 Pressure inside wormhole during slurry injection (second water shut-off experiment). See Figure 3.3 for pressure port locations.

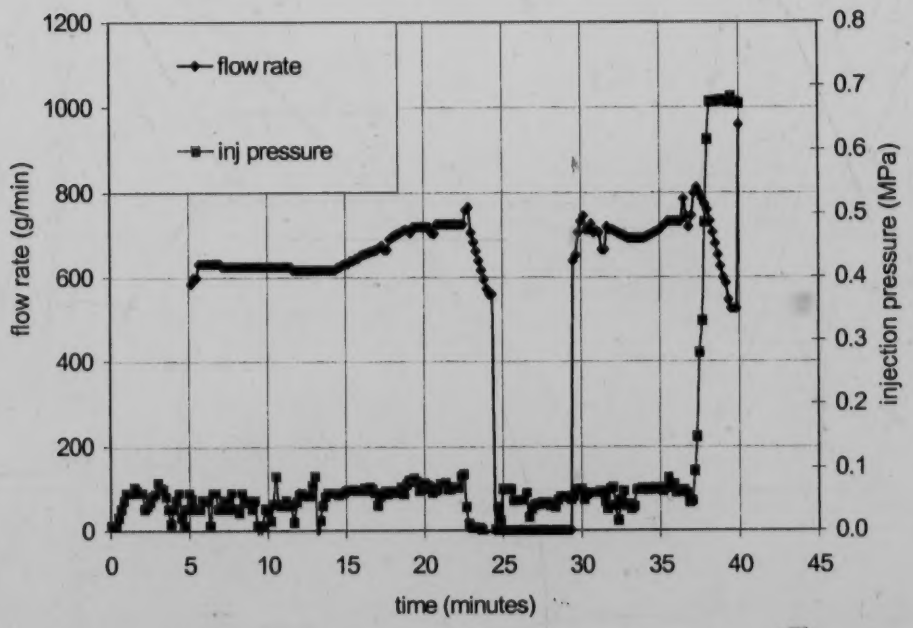

Figure M.2 Flow rate and injection pressure during slurry injection (second water shut-off experiment).

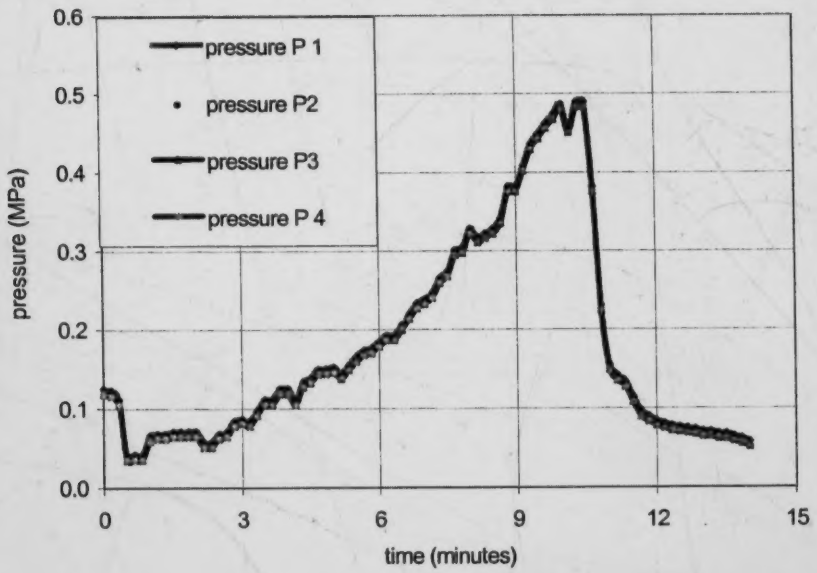

Figure M.3 Pressure inside wormhole during polymer gel squeeze into the annulus (second water shut-off experiment). See Figure 3.3 for pressure port locations.

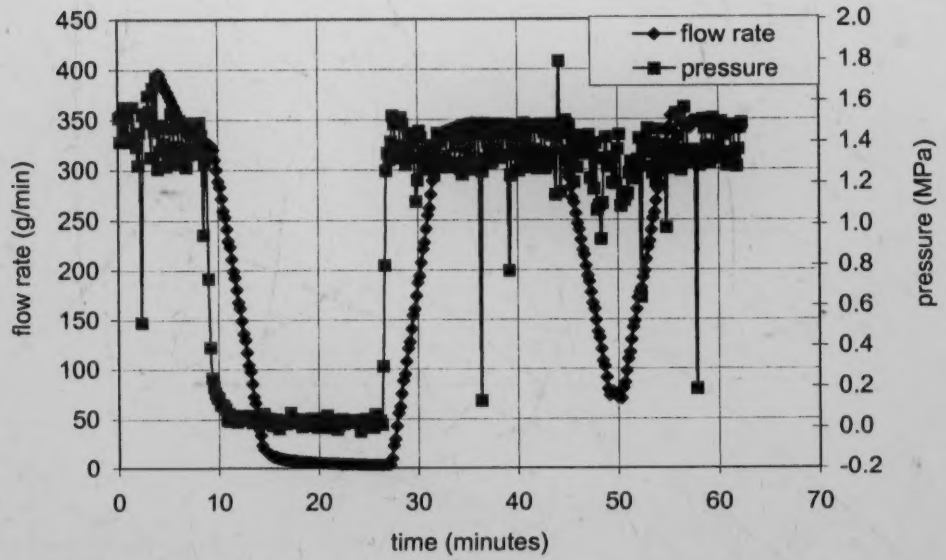

Figure M.4 Polymer gel flooding rate and injection pressure (second water shut-off experiment).

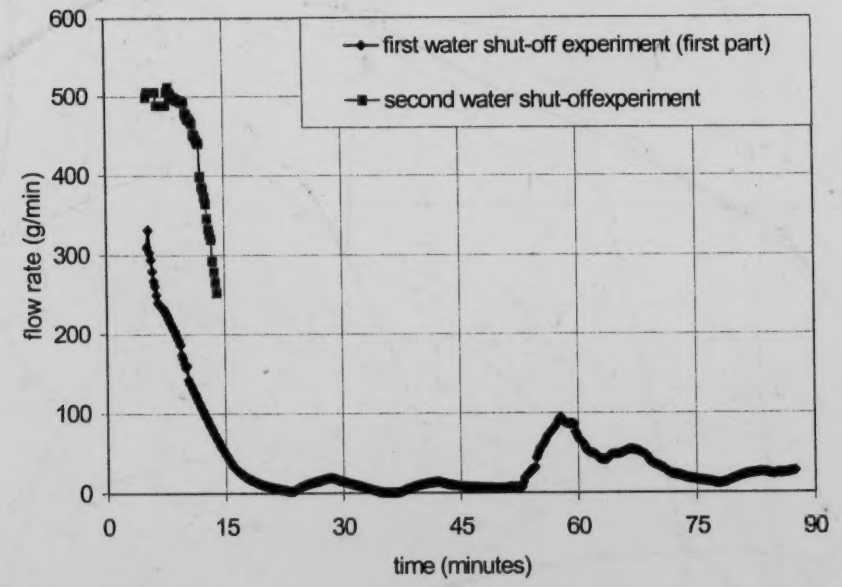

Figure M.5 Flow rate during squeezing of gel for first and second water shut-off experiments.

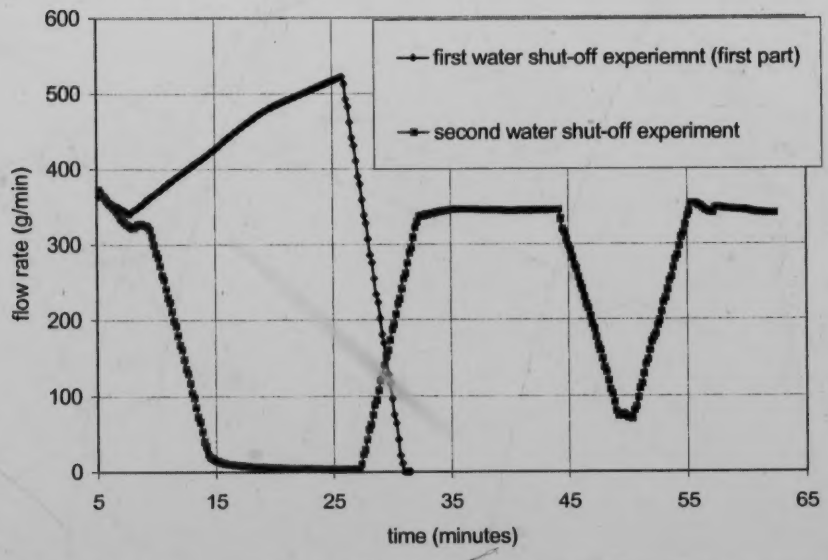

Figure M.6 Polymer gel flooding rate. Comparison for first and second water shut-off experiments.